Source: Document 4-5-6-7/584(Annex 11, Attachment 4)

Annex 19 to
Document 4-5-6-7/715-E
19 August 2014
English only

Annex 19 to Joint Task Group 4-5-6-7 Chairman's Report

DRAFT NEW REPORT ITU-R [FSS-IMT C-BAND UPLINK]

Sharing and compatibility between International Mobile Telecommunication systems and fixed-satellite service networks in 5 850-6 425 MHz frequency range

Scope

This Report describes sharing studies between International Mobile Telecommunication-Advanced systems and satellite networks in the fixed-satellite service in the 5 850-6 425 MHz bands.

1 Introduction

The frequency band 5 850-6 425 MHz has been identified as potentially suitable frequency range for International Mobile Telecommunications (IMT) systems. If deployed in these bands, it is expected IMT stations would be deployed in large numbers as part of dense mobile communication networks.

The 5 850-6 425 MHz frequency range is extensively used by satellites networks in the fixed satellite service (FSS) for Earth-to-space communication. FSS networks typically provide service to large regions encompassing the territory of multiple administrations.

This study defines the technical condition required to protect the Earth-to-space transmissions of satellite systems operating in the FSS in the 5 850-6 425 MHz range from IMT systems.

Additionally, this study investigates the impact of the Earth-to-space transmission of a single FSS earth station into a single IMT receiver in the 5 850-6 425 MHz frequency range. Specifically, it provides the minimum separation distances that would be required to protect a single receiving IMT base station from a single transmitting FSS earth station. Administrations should consider this information in conjunction with information on the deployment of transmitting FSS earth stations in a geographic region in deciding whether any portion of the 5 850-6 425 MHz frequency range may be identified for use by IMT.

2 Technical Studies

Several studies have been conducted to assess potential for sharing and compatibility between IMT systems and FSS networks in the 5 850-6 425 MHz frequency range. Some of the studies are limited only to the 5 925-6 425 MHz frequency band, however, the conclusions of these studies are in general also applicable to the 5 850-5 925 MHz frequency band.

2.1 Interference from FSS earth stations into receiving IMT stations

2.1.1 Study #1

As has been shown in studies #3 and #4 (see below) sharing and compatibility between IMT systems and FSS networks is not feasible in case of IMT outdoor deployment. Accordingly, the focus of study #1 is to assess the impact of FSS earth station transmissions into indoor-only receiving IMT small cells.

For this study, it was assumed that a transmitting FSS earth station and a small cell receiving IMT station were deployed in an urban environment. It was further assumed that the FSS earth station was located on the rooftop of a building and the IMT station was deployed on the last floor of a neighbouring building at approximately the same level.

A worst case assumption was also made that the neighbouring building (in which the IMT station is located) was in the direct path of the FSS earth station antenna's azimuthal pointing direction. Consequently, only the vertical off-axis antenna gain discrimination of the FSS earth stations would provide any reduction in the e.i.r.p. of that station in the direction of the receiving small cell IMT station.

In the study, the efficacy of an IMT network scheduler in mitigating the effect of excess interference (i.e. in excess of the required protection requirement) from a transmitting FSS earth station was examined. This mitigation technique is similar to that currently employed by IMT networks to avoid/reduce intra-network interference, which could be of the same level as that produced by the FSS transmissions illustrated in the study.

2.1.2 Study #2

A sharing analysis was undertaken to ascertain the impact of the Earth-to-space transmissions of a single FSS earth station on a single receiving IMT base station. The focus of the analysis was to determine the separation distances that would have to be maintained between these two stations in order to ensure that the receiving IMT base station would not be subjected to excessive levels of interference from the in-band co-frequency emissions and spurious emissions of the transmitting FSS earth station.

The sharing analysis was conducted for the following IMT base station types and deployments: outdoor macro cell base station (suburban), outdoor macro cell base station (urban), outdoor small cell base station (suburban) and indoor small cell base station (suburban). With the FSS earth station location and antenna pointing fixed, a hypothetical IMT receiving base station was successively placed at many locations around the FSS earth station. At each location, the maximum beam gain lobe of the IMT antenna (with beam-tilt as appropriate) was assumed to be pointed in azimuth towards the FSS earth station. At each location, the I/N at the IMT receiver was calculated taking into account the long-term propagation loss on the interference path and the off-axis antenna gains of the FSS earth station and IMT station. Subsequently, contour lines connecting those points where the I/N was closest to the required single entry protection criterion were computed, resulting in (contour) areas within which the computed I/N would not meet the (I/N) limit required by the protection criterion.

2.2 Interference from IMT stations into receiving FSS space stations

2.2.1 Study #3

The impact of aggregate interference into receiving FSS space stations originating from multiple IMT stations operating in the 5 925-6 425 MHz frequency band and within the satellite's beam (footprint) is the main focus of the study. As the 5 925-6 425 MHz frequency band is used for FSS

GSO networks as well as for FSS NGSO networks this study provides separate analysis for each case. The protection criteria contained in Recommendation ITU-R S.1432 is used in order to assess the impact of interference from a large number of IMT stations in the field-of-view of a satellite's receiving antenna beam. Beams footprints for specific satellites brought into use have been extracted from BR IFIC.

IMT station dissemination and their activity have a significant impact on the results of the study. Accordingly, several values of this parameters and also indoor penetration loss value have been used for sensitivity analysis purposes.

Percentage of indoor IMT systems has been fixed to 95% to account possible indoor installations without or with minimal indoor penetration loss. This is based on the result of preliminary study which has shown that sharing is only feasible for indoor deployment and with establishment of a limit on the maximum allowable e.i.r.p. for IMT stations in this frequency range.

2.2.2 Study #4

This study examines the potential interference from IMT systems to space stations in FSS in the 5 925-6 425 MHz frequency band.

The study provides a calculation of the aggregate interference from the IMT stations and suggests the maximum power of the transmitters that would be required to protect FSS space stations. The results strongly depend on the adoption of the specific parameters for IMT density, building attenuation, propagation model and satellite characteristics (orbital position, footprints and transponder merit of factor G/T).

The methodology used is similar to the one in Study#3 and based on the estimation of the increment of the thermal noise into the wanted satellite receiver (ΔT), due to the aggregate interference created by the IMT stations.

Propagation model used in the study adopts some of the elements related to some sharing studies between radio local area network (RLAN) and EESS satellites in the band 5 350-5 470 MHz discussed under preparation to WRC-15 agenda item 1.1.

3 Technical characteristics

3.1 FSS earth stations parameters

The FSS earth stations parameters used in studies #1 and #2 is provided in Table 1.

TABLE 1

FSS earth station parameters

	Study #1	**Study #2**
Location of earth station	Non-specific FSS earth station location. earth station assumed to be on rooftop	Mississippi, USA
Latitude of earth station (degrees North)		31.3
Longitude of earth station (degrees West)		88.4
Antenna diameter (metres)	1.8	8
Maximum antenna Gain (dBi)	39.9	52.8
Off-axis gain envelope	*Recommends* 2 of Recommendation ITU-R S.465-6	*Recommends* 2 of Recommendation ITU-R S.465-6
Antenna height above ground (metres)	Same level as indoor small cell	10
Antenna elevation angle (degrees above horizon)	5°, 15° and 40°	≈5° see note 1 ≈30° see note 2
Maximum power density into transmitting antenna (dBW/Hz)	–	–36 see note 3
Unwanted emission attenuation (dBc) see note 4	–	53
Transmit power (dBm)	40	–
Feeder loss (dB)	1	–
Occupied bandwidth (MHz)	2	–

NOTES:

1 Assumed that the earth station is pointed to a geostationary satellite located at 14.46° W.L.

2 Assumed that the earth station is pointed to a geostationary satellite located at 43.9° W.L.

3 Value calculated by subtracting the antenna off-axis gain, as specified in *recommends* 2 of Recommendation ITU-R S.465-6, from the maximum e.i.r.p. density limit specified in *recommends* 2 of Recommendation ITU-R S.524-9.

4 Unwanted emission attenuation level was determined using the criteria contained in Table 1 of Appendix **3** of the ITU Radio Regulations for a carrier bandwidth of 40 kHz.

3.2 FSS space stations parameters

3.2.1 Study #3

For study #3, the geostationary orbit (GSO) networks have been selected using the ITU BR data on frequency assignments to space radio services (SRS) with the following basic parameters: spacecraft orbital position, maximum beam gain and receiving system noise temperature. The analysis has been performed for most of the beams recorded in the database with statistical representation of the results, except the beams with antenna gain contours missing or other parameters recorded with errors. This corresponds to more than 90% of beams analysed in the database. Characteristics of receiving antennas (i.e. their gain contours on the Earth surface) for each GSO spacecraft were considered as well.

The non-geostationary orbit (NGSO) networks were also selected using the ITU BR data on frequency assignments to SRS, including the following basic parameters: satellite orbit (apogee, perigee, inclination, perigee argument, ascending node and phase angle of spacecraft), maximum beam gain and receiving system noise temperature.

3.2.2 Study #4

For study #4 uses reference satellite for calculations. The reference satellite is a typical spacecraft with a global C-band payload, mainly used for feeder links and telecommand. The satellite maximum receive gain is assumed to be 22 dBi and the satellite system noise temperature 500 K, equivalent to a G/T of around -5 dB/K on the beam peak. Global footprint is used and therefore quite flat, with a gain range of about 4 dB from the peak to the edge. This antenna roll-off has been included in the model. These characteristics are thought to be common in the FSS in this band. Some satellites using higher gain/regional beam antennas, which might lead to higher interference, have not been modelled in study #4.

Additionally in study #4, since the aggregate interference strongly depends on the cities which are covered by the spacecraft footprint, the orbital position has been changed during the simulations and it was determined that the location 70°E was the worst case location, being the location where the satellite antenna beam is covering the most populated areas as China, India, Indonesia, Pakistan, Bangladesh and Russia.

3.3 IMT stations parameters

The IMT stations parameters used in studies #1 and #2 are provided in Table 2. For study #3 parameters are listed in Table 3.

TABLE 2

IMT characteristics for studies #1 and #2

	Study #1	**Study #2**			
IMT cell base station type	**Small cell base station (indoor)**	**Macro cell base station (suburban)**	**Macro cell base station (urban)**	**Small cell base station (outdoor)**	**Small cell base station (indoor)**
IMT operational environment	N/A	Suburban outdoor	Urban outdoor	Suburban outdoor	Suburban Indoor
Maximum antenna gain (dBi)	0	18	18	5	0
Antenna height above ground (metres)	Same as FSS ES	25	20	6	3
Antenna type	Omni	3-Sector	3-Sector	Omni	Omni
Antenna 3 dB Beam-width in the Horizontal Plane (degrees)	N/A	65°	65°	N/A	N/A
Antenna gain pattern envelope	Recommendation ITU-R F.1336-3	Recommendation ITU-R F.1336-4	Recommendation ITU-R F.1336-4	Recommendation ITU-R F.1336-4	Recommendation ITU-R F.1336-4
Antenna (mechanical) down-tilt (degrees)	N/A	6	10	N/A	N/A
Receiver noise figure (dB)	5	5[see Note]	5[see Note]	5[see Note]	5[see Note]
Noise power density (dBW/Hz)	N/A	–200.6	–200.6	–200.6	–200.6
Aggregate *I/N* requirement (dB)	N/A	–6	–6	–6	–6
Assumed single entry *I/N* requirement (dB)	–6	–9	–9	–9	–9
Maximum permitted single entry interference power density (dBW/Hz)	N/A	–209.6	–209.6	–209.6	–209.6
IMT channel bandwidth, MHz	20	N/A	N/A	N/A	N/A
Maximum permitted single entry interference, dBW	–132	N/A	N/A	N/A	N/A

NOTE - Receiver noise figure assumed to apply at the output port of the receiving (IMT) antenna, i.e. it includes the noise contribution due to feeder losses.

TABLE 3

IMT characteristics for studies #3 and #4

	Study #3	**Study #4**
	Small cell indoor	**Small cell indoor**
Base station characteristics / Cell structure	Not used in the modelling[1]	Not used in the modelling
Cell radius / deployment density	Not used in the modelling[1]	Not used in the modelling
Antenna height	Not used in the modelling[1]	Distribution (1.5 - 28 m)
Sectorization	Single sector	Single sector
Downtilt	n.a.	n.a.
Frequency reuse	1	
Antenna pattern	Recommendation ITU-R F.1336 omni	Omni in both azimuth and elevation
Antenna polarization	linear	linear
Below rooftop base station antenna deployment	n.a.	Clutter model based on ITU-R Rec P.452
Feeder loss	n.a	n.a
Maximum base station output power (5/10/20 MHz)	15 and 24 dBm	5-20 dBm
Maximum base station antenna gain	0 dBi	0 dBi
Maximum base station output power (e.i.r.p.)	15 and 24 dBm	5-20 dBm
Average base station activity	50 %[2]	100 %
Average base station power/sector (to be used in sharing studies)	12 and 21 dBm [2]	5-20 dBm

[1] Due to assessment of aggregate interference into FSS space station receiver those parameters are irrelevant for the calculation.

[2] Typical average activity of a base station and corresponding average output powers during busy hour. For further details see Report ITU-R M.2241, section 2.2.3.2.

3.4 Other study elements

For studies #1 and #2, other major elements of the studies are compiled in Table 4.

TABLE 4

Additional elements considered in studies #1 and #2

	Study #1	**Study #2**
Annex #	1	2
Focus point of the study	In-band (co-channel) interference assessment into indoor IMT small cells from non-specific FSS ES	In-band (co-channel) and unwanted spurious emission interference assessment into different types of IMT base stations for different deployment scenarios
In-band emissions	Yes	Yes
Unwanted emissions	No	Yes
Propagation model	Free space model	Recommendation ITU-R P.452-14
Clutter loss	Without clutter loss and 20 dB fixed value	Clutter loss characteristics for urban and suburban environments as specified in Table 4 of section 4.5.3 of Recommendation ITU-R P.452-14
Indoor building penetration loss	15/25 dB	15/25 dB
Methodology	Separation distances are calculated for the azimuthal direction towards the satellite	Protection zones are calculated using I/N criteria
FSS parameters	VSAT-like FSS earth station is assumed with specific parameters, situated on the rooftop on same level as indoor IMT small cell	Large, high-power FSS earth station is assumed with antenna height of 10 meters above ground
IMT parameters	Indoor IMT small cell	Outdoor macro urban and suburban base station. Outdoor small cell suburban base station. Indoor small cell suburban base station.
Terrain model	N/A	Actual terrain (Mildly hilly terrain)
Protection criteria	I/N= -6 dB (considering specific IMT channel bandwidth) In addition C/(I+N) ratios are assessed for indoor small cell deployment	Single entry: I/N=–9 dB
Mitigation techniques	It has been shown that due to limited coverage area of indoor small cells C/(I+N) ratio is quite high even in case of excessive values of I/N. In cases of narrowband interferers such as most of FSS ES frequency selective scheduler in IMT small cell could allocate interfered spectrum blocks to users with most favourable C/(I+N) conditions. In combination with overall very high values of C/(I+N) within indoor small cell coverage area this could mitigate interference from FSS ES.[3]	No

[3] Frequency selective scheduling designed to mitigate IMT intra-network interference, could be used as a potential mitigation technique to mitigate excessive interference from FSS networks into IMT networks. It should be noted that the effectiveness of such a mitigation technique is expected to be more limited, when the bandwidth of the FSS carrier is larger than the bandwidth of the IMT channel or larger than the aggregate bandwidth of the combined IMT channels.

Other major elements of studies #3 and #4 are contained in Table 5.

TABLE 5

Additional elements considered in studies #3 and #4

	Study #3	**Study #4**
Annex #	3	4
Focus point of the study	Aggregate interference into FSS space station receiver originating from multiple IMT stations within satellite beam footprint. Both GSO and Non-GSO FSS satellite network cases are considered.	Aggregate interference into FSS space station receiver originating from multiple IMT stations within satellite beam footprint. GSO FSS satellite network cases are considered.
In-band emissions	Yes	Yes
Unwanted emissions	No	No
Propagation Model	Free space model	Free space model + Clutter model based on Rec. ITU-R P.452 in relation to antenna height distribution
Indoor building penetration loss	15 dB, 25 dB and 35 dB[4](for scenario considered global average value is used in calculations)	12 dB (Value is based on averaging of Gaussian distribution used to model indoor penetration losses in sharing studies between RLAN and EESS satellites in the band 5 350-5 470 MHz discussed under preparation to WRC-15 agenda item 1.1)
Methodology	ΔT/T coordination criteria in Recommendation ITU-R S.1432 is used in order to assess the impact of interference from a large number of IMT stations in the field-of-view of a satellite antenna beam. Only interference from small cells has been assessed as time division duplex (TDD) frequency arrangement and power control within user terminals make small cell predominant source of interference.	ΔT/T coordination criteria in Recommendation ITU-R S.1432 is used in order to assess the impact of interference from a large number of IMT stations in the field-of-view of a satellite antenna beam. Only interference from small cells base stations has been assessed under an assumption that TDD frequency arrangement is used and interference from user terminals has been assumed to have negligible impact.
FSS parameters	Parameters of GSO satellite networks published in SRS data base for notification and coordination of FSS networks has been used. The NGSO networks were also selected using the ITU BR data on frequency assignments to SRS.	The satellite maximum receive gain is assumed to be 22 dBi and the satellite System Noise Temperature 500 K, equivalent to a G/T of around -5 dB/K on the beam peak. The orbital position has been changed during the simulations and it was determined that the location 70°E was the worst case location
IMT parameters	IMT parameters for small cells in the frequency band 5-6 GHz have been used. E.i.r.p. levels are fixed with values 15 dBm and 24 dBm. 5% of indoor small cells have been modelled without wall penetration loss.	IMT parameters for small cells in the frequency band 5-6 GHz has been used. E.i.r.p. levels are varied in the range 5 - 20 dBm. 5% of indoor small cells have been modelled without wall penetration loss.

[4] Typical value for indoor base station penetration loss is described as 25 dB for horizontal direction in the frequency band 5-6 GHz and for vertical direction based on Recommendation ITU-R P.1238, Table 3. 15 dB and 35 dB values are used for sensitivity analysis. The value 35 dB corresponds well to measurements results provided within Recommendation ITU-R P.2041 and 15 dB is taken as most conservative assumption for global average penetration loss value. See more detailed description in the section 3.1.3 of Study #3.

IMT dissemination parameters:	Some of the parameters relevant to global deployment for small cells have been assumed.	Some of the parameters relevant to global deployment for small cells has been assumed.
a) Population distribution:	Population database for the largest cities of the world is used to model realistic population distribution.	Population database for the largest cities of the world is used to model realistic population distribution.
b) Dissemination rate:	1%, 3% and 6% (The values are based on the assumption that small cells are carrier grade devices and their dissemination rate is not intended to match dissemination rate of unlicensed devices)	3%, 6% and 10%
c) Area activity factor[5]:	20%	20% and 50%
d) Channel activity factor	4% (Twenty five 20 MHz channels are assumed in the 5 925-6 425 MHz frequency band)	4% (Twenty five 20 MHz channels are assumed in the 5 925-6 425 MHz frequency band)
e) Resulting number of active small cells.	Approximately from 0.0001 to 0.0005 active small cells per 20 MHz channel per inhabitant	From 0.00024 to 0.002 active small cells per 20 MHz channel per inhabitant
Protection Criteria	$\Delta T/T$=6% coordination criteria as provided in Recommendation ITU-R S.1432	$\Delta T/T$=6% coordination criteria as provided in Recommendation ITU-R S.1432

[5] As the service areas may cover several time zones, whole countries and continents, simultaneous full loading of millions of such base stations is unrealistic. In this case not loaded small cells transmit only control information with significantly reduced average power or switched off completely for energy savings.

4 Results

The results of Studies #1 and #2 are summarized in Table 6, below.

TABLE 6

Summary of Results of Studies #1 and #2

Study Number	1	2
Information deduced	In the azimuthal direction from the FSS earth station to the satellite, the required separation distances range from hundreds of metres to 6 km for the case of line-of-sight conditions. If obstacles exist between the FSS earth station and the indoor IMT small cell that result in an additional diffraction loss of 20 dB, the separation distance would be several hundred metres. Consideration of operational specifics of indoor small cells has shown that C/(I+N) preserve positive values even in cases of significant interference well beyond I/N threshold. Such conditions combined with frequency selective scheduler could mitigate interference from FSS ES and enable operation with separation distances around 100 m or even smaller.[6]	For protection from co-frequency, in-band interference due to FSS earth station transmission the study showed that depending on the azimuth bearing of the IMT base station relative to the FSS station, the following minimum separation distance should be maintained: 1) 10-78 km to protect outdoor macro cell in a suburban environment, 2) 6- 33 km to protect an outdoor macro cell in an urban environment 3) 4- 33 km to protect an outdoor small-cell in a suburban environment 4) 2.5-13 km to protect an indoor small cell in a suburban environment, depending on the indoor building penetration loss. With regard to spurious FSS transmissions, the study showed that only outdoor IMT base stations would be impacted. Accordingly, depending on the azimuth bearing of the IMT base station relative to the FSS station, the following minimum separation distance should be maintained between an IMT station and an FSS earth station: 1) 4-13 km to protect an outdoor macro cell in a suburban environment, 2) less than 1 km to approximately 7 km to protect an outdoor macro cell in an urban environment 3) 1-6 km to protect an outdoor small-cell in a suburban environment.

[6] Frequency selective scheduling designed to mitigate IMT intra-network interference could be used as a potential mitigation technique to mitigate excessive interference from FSS networks into IMT networks. It should be noted that the effectiveness of such a mitigation technique is expected to be more limited, when the bandwidth of the FSS carrier is larger than the bandwidth of the IMT channel or larger than the aggregate bandwidth of the combined IMT channels.

The results of Study #3 is summarized in Table 7, below.

TABLE 7

Summary of Results of Study #3 and #4

Study Number	3	4
Information deduced	For 15 dBm e.i.r.p. per 20 MHz case for 95% of indoor small cells the coordination criteria ΔT/T=6% is fulfilled for 90-99% satellite beams in the database depending on the assumptions. 90% corresponds to the most conservative and pessimistic assumptions. Under the assumption of dissemination of 3% and indoor penetration of 25 dB there are only limited number of cases when it is not fulfilled. For approximately 1% of beams analysed such excess equals to 3-6 dBs and up to 9 dBs in single instances. In such cases usually only one of multiple beams of a satellite is is identified as possible affected. Other beams of the satellite covering same region will have smaller ΔT/T increase. Based on the aforementioned results of the study 15 dBm e.i.r.p. per 20 MHz limit and indoor only deployment are suggested as a requirement to ensure long term protection of FSS space stations receivers.	Based on this study, if this band were to be used for IMT system, the e.i.r.p. should be limited to a maximum value of 10 dBm and devices would need to be limited to indoor only operation. The limitation may be placed on the e.i.r.p in the total bandwidth of the emission, rather than on the power spectral density, on the assumption that a use of emissions with a narrow bandwidth (that would leave to higher e.i.r.p spectral density) is balanced by a lower probability of the emission coinciding with the FSS receiver bandwidth (i.e. a lower band usage factor). It has to be noted that these values have been estimated basing the calculation on the hypothesis that the IMT transmitters will use frequencies uniformly distributed over the entire available spectrum of 500 MHz. If a smaller bandwidth were to be made available for IMT devices, this would increase the band usage factor, leading to increased interference to the FSS in that part of the band in which IMT devices operate, and increased interference to FSS space stations operating in that part of the band.

5 Summary

Several studies have been conducted to assess sharing and compatibility between IMT systems and FSS networks in 5 850-6 425 MHz frequency range. These studies considered the technical conditions required to protect the Earth-to-space transmissions received by an FSS satellite system operating in the geostationary orbit from potential aggregate interference from transmitting IMT stations, as well as the technical conditions required to protect a single IMT receiving station from the emissions of an FSS transmitting earth station.

Concerning the protection of a receiving geostationary FSS space network, the studies showed that GSO FSS space networks would be subjected to excessive levels of interference from the aggregate operation of IMT (small cell) base stations, irrespective of whether they are deployed outdoors or indoors.

The e.i.r.p. limit of an IMT station to protect FSS satellites is dependent on dissemination of IMT stations, activity factors, actual channelization scheme and building penetration losses. The studies show that for case when IMT stations are limited only to indoor use (deployed 95% indoors and 5% without building attenuation) the e.i.r.p. of IMT station should be limited to 10-15 dBm. Under certain conditions for the 15 dBm e.i.r.p. limit, interference above the 6% ΔT/T criterion equal to several dBs could be observed for some beams with high gain antennas. For approximately 1% of beams analysed such excess equals to 3-6 dBs and up to 9 dBs in single instances. In such cases usually only one of multiple beams of a satellite is identified as possibly affected. Other beams of the satellite covering same region will have smaller ΔT/T increase. The limitation may be placed on the e.i.r.p. in the total bandwidth of the emission, rather than on the power spectral density.

The above limits are based on the assumption that the whole of the band 5 925-6 425 MHz is identifiedfor IMT stations. If a narrower or wider band is identified for IMT (or used in a particular country), the power limits should be adjusted according to the following formula:

Adjustment (dB) = 10×log(500/B)

Where B is the available bandwidth for IMT systems, in MHz.

With regard to interference resulting from FSS transmissions into IMT, a separation distance is required between an FSS earth station and an IMT base station in order to protect the IMT station from interference from FSS transmissions. Concerning the protection of a single receiving IMT base station, the studies concluded that separation distances up to many tens of kilometres would be required between a single transmitting FSS earth station and a single outdoor IMT receiving base station, in order to protect the IMT station from co-frequency interference. For indoor deployed IMT stations, a separation distance ranging from several hundred meters up to several kilometres would be required.

The effectiveness of frequency selective scheduling (described in Annex 1, section 4.3) as a method to mitigate interference from a transmitting FSS earth station into IMT system has been studied. For the specific case studied, the entirety of the interfering FSS carrier was contained within the bandwidth of the IMT channel. The results indicated that the use of this mitigation technique could reduce the separation distance to around 100 meters– even with the IMT protection criteria being exceeded. It should be noted that the effectiveness of such a mitigation technique is expected to be more limited, relative to the specific case studied, when the bandwidth of the FSS carrier is larger than the bandwidth of the IMT channel or larger than the aggregate bandwidth of the combined IMT channels.

Thus it is generally concluded that no specific separation distance is required between FSS transmitting station and indoor IMT small cell.

Summarizing the above mentioned results it is concluded that sharing and compatibility between IMT systems and FSS networks in 5 850-6 425 MHz frequency range is feasible under certain conditions. These conditions include deployment of IMT systems only indoor and establishment of limit on maximum allowable e.i.r.p. for IMT stations in this frequency range.

ANNEX 1

Interference assessment into indoor IMT small cells from fixed-satellite service earth stations in the 5 925-6 425 MHz frequency band

1 Introduction

The frequency band 5 925-6 425 MHz has been proposed as a possible candidate band for IMT identification, which most likely will result in MS stations deployment in large quantities as part of dense mobile communication networks. As it has been shown in the other study to ensure coexistence with FSS space stations receivers IMT deployment should be limited to indoor operation with limited e.i.r.p. However for successful IMT deployment in the 5 925-6 425 MHz frequency band the impact of interference from FSS earth station into IMT indoor small cells should be tolerable.

2 Background

The frequency band 5 925-6 425 MHz is already allocated to mobile service on the primary basis worldwide. However identification of this band for IMT will significantly change the usage of the frequency band which requires the coexistence studies with other incumbent services. The main services deployed in this band are FS and FSS (Earth-to-space).

There are no specific studies describing typical deployment of FSS ES in the 5 925-6 425 MHz frequency band to be used for assessment of interference into MS systems, however there are several ITU-R deliverables relevant for interference assessment from such ES:

– Report ITU-R F.2240 “Interference analysis modelling for sharing between HAPS gateway links in the fixed service and other systems/services in the range 5 850-7 075 MHz”.

– Recommendation ITU-R S.524 “Maximum permissible levels of off-axis e.i.r.p. density from earth stations in geostationary-satellite orbit networks operating in the fixed-satellite service transmitting in the 6 GHz, 13 GHz, 14 GHz and 30 GHz frequency bands.”

– Recommendation ITU-R S.1587 “Technical characteristics of earth stations on board vessels communicating with FSS satellites in the frequency bands 5 925-6 425 MHz and 14-14.5 GHz which are allocated to the fixed-satellite service.”

3 Technical characteristics

3.1 IMT systems characteristics and assumptions

Considering rather high frequency of the frequency band 5 925-6 425 MHz, it was assumed that the IMT systems would be most likely deployed in dense urban areas and mainly indoor as pico and femto cells with wideband channels and high data rate. It was also assumed that the frequency band 5 925-6 425 MHz would be used as a separate level of coverage without macro cells, making the time division duplex more advantageous for such IMT systems. Only indoor deployment is considered.

TABLE 1
IMT-Advanced specification related parameters

Duplex mode	**TDD**	
Parameter	**Base station**	**Mobile station**
Channel bandwidth (MHz)	20 MHz	
Signal bandwidth (MHz)	20 MHz	
Transmitter characteristics		
Polarization discrimination (dB)	3	0
Receiver characteristics		
Noise Figure	5 dB	9 dB

TABLE 2
Deployment-related parameters

	Small cell indoor
Base station characteristics / Cell structure	
Cell radius / Deployment density	Depending on indoor coverage/capacity demand
Antenna height	3 m
Sectorization	Single sector
Downtilt	n/a
Frequency reuse	1
Antenna pattern	Recommendation ITU-R F.1336 omni
Antenna polarization	linear
Indoor base station deployment	100 %
Indoor base station penetration loss	25 dB (5-6 GHz) (horizontal direction) P.1238, Table 3 (vertical direction)
Below rooftop base station antenna deployment	n.a.
Feeder loss	n.a
Maximum base station output power (5/10/20 MHz)	24 dBm
Maximum base station antenna gain	0 dBi
Maximum base station output power (e.i.r.p.)	24 dBm
Average base station activity	50 %
Average base station power/sector (to be used in sharing studies)	21 dBm
User terminal characteristics	
Indoor user terminal usage	100%
Indoor user terminal penetration loss	25 dB (5-6 GHz) (horizontal direction) P.1238, Table 3 (vertical direction)
User terminal density in active mode to be used in sharing studies	depending on indoor coverage/capacity demand
Maximum user terminal output power	23 dBm
Average user terminal output power	–9 dBm
Typical antenna gain for user terminals	–4 dBi
Body loss	4 dB

Protection criteria for IMT systems usually used for macro and micro cells is the following:

I/N = –6 dB for co-existence cases where interference effects a limited number of cells

I/N = –10 dB for co-existence cases where interference effects a large number of cells

The same interference criteria could be used for small cells as well, however small cells and especially indoor small cells a used with very limited coverage area and could tolerate relatively high levels intra network interference from other small cells, thus the C/I criteria is also used in a mitigation section to asses impact of FSS ES into such IMT deployment.

3.2 FSS ES characteristics and assumptions

There is a large number of transmitting FSS earth station in the frequency band 5 925-6 425 MHz varying in antenna sizing personal use. However the deployment of indoor small cell is anticipated mostly in highly populated areas where ES using high power or large antennas are unlikely.

Based on Report ITU-R F.2240 and Recommendation ITU-R S.1587 characteristics of representative VSAT have been compiled and presented in the Table 3. Recommendation ITU-R S.524 has not been used as it describes maximum permissible levels more relevant for very specific high power ES, which will be usually used outside large cities and with significant distance separations from IMT indoor small cells.

TABLE 3

FSS earth station parameters

Frequency (MHz)	5 850-6 725
Transmit power (dBm)	40
Feeder loss (dB)	1
Occupied bandwidth (MHz)	2
Polarization	Circular
Earth station antenna diameter (metres)	1.8
Earth station antenna maximum gain, GES, (dBi)	39.9
Earth station antenna off-axis gain, GES(θ), (dBi)	Recommendation ITU-R S.465
Minimum earth station antenna elevation angle, h, (degrees)	5, 15 and 40

4 Analysis

4.1 Assumptions and methodology

Interference scenario considered in this study is depicted in Fig. 1. Urban deployment is assumed both for FSS ES located on the rooftop of the building and IMT small cell deployed on the last floor of the neighbouring building practically on the same level. The worst case is assumed when the neighbouring building is in the same direction as the serving satellite and only vertical elevation provides off-axis angle required to reduce e.i.r.p. in the direction of the small cell.

For the simplicity only interference into IMT small cell receiver is calculated, but due to similar characteristics between user terminals and small cells the results are applicable to user terminals as well. For calculation of signals levels the free space propagation model is used. All interfering signals are additionally attenuated by 25 dB due to wall or ceiling penetration loss.

FIGURE 1

Interference scenario description

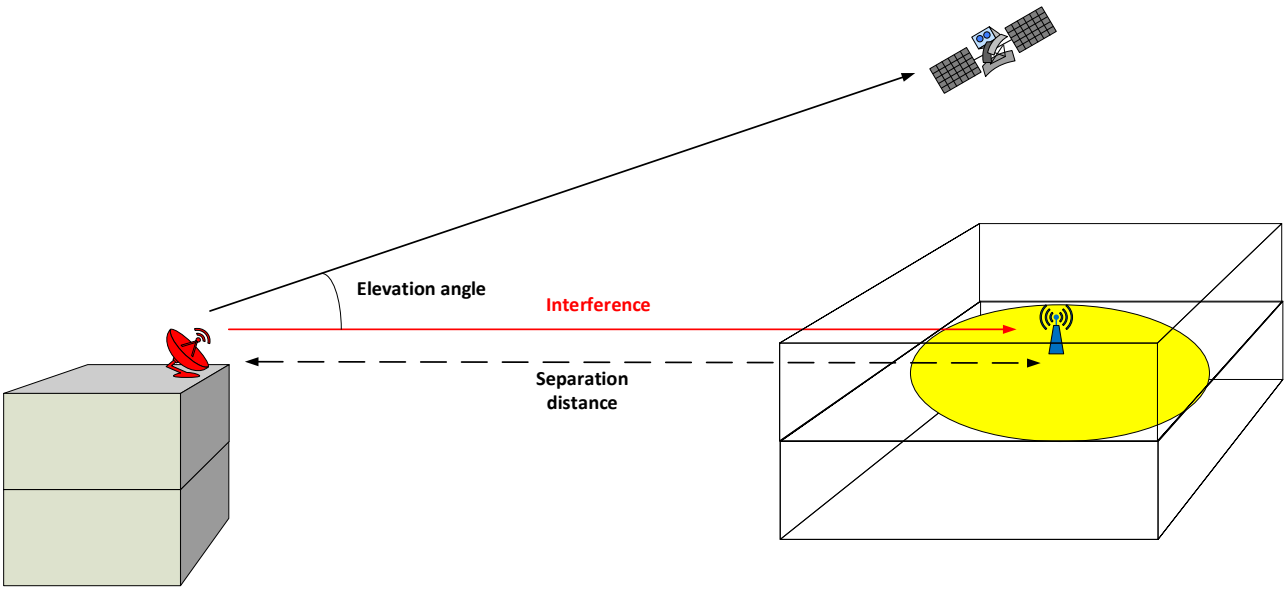

4.2 Calculations and results

The results of the calculation are presented on fig.2. As could be seen from the figure in the case of large off-axis angles, which also corresponds to sidelobes and backlobes of antenna at small elevation angles, separation distances are relatively small up to few hundred metres. In the case of small off-axis angles separation distances increase up to 6 kilometres. It should be noted that free space model is very pessimistic assumption at such long distances especially in urban environments and in practice separation distances would be much smaller. As an illustration of such case blue curve represents separation distance calculation with e.i.r.p. based on 5º off-axis angle and additional 20 dB diffraction loss due to obstacles. In this case separation distance even with worst case will be not higher than 500 metres.

FIGURE 2

Separation distances calculation

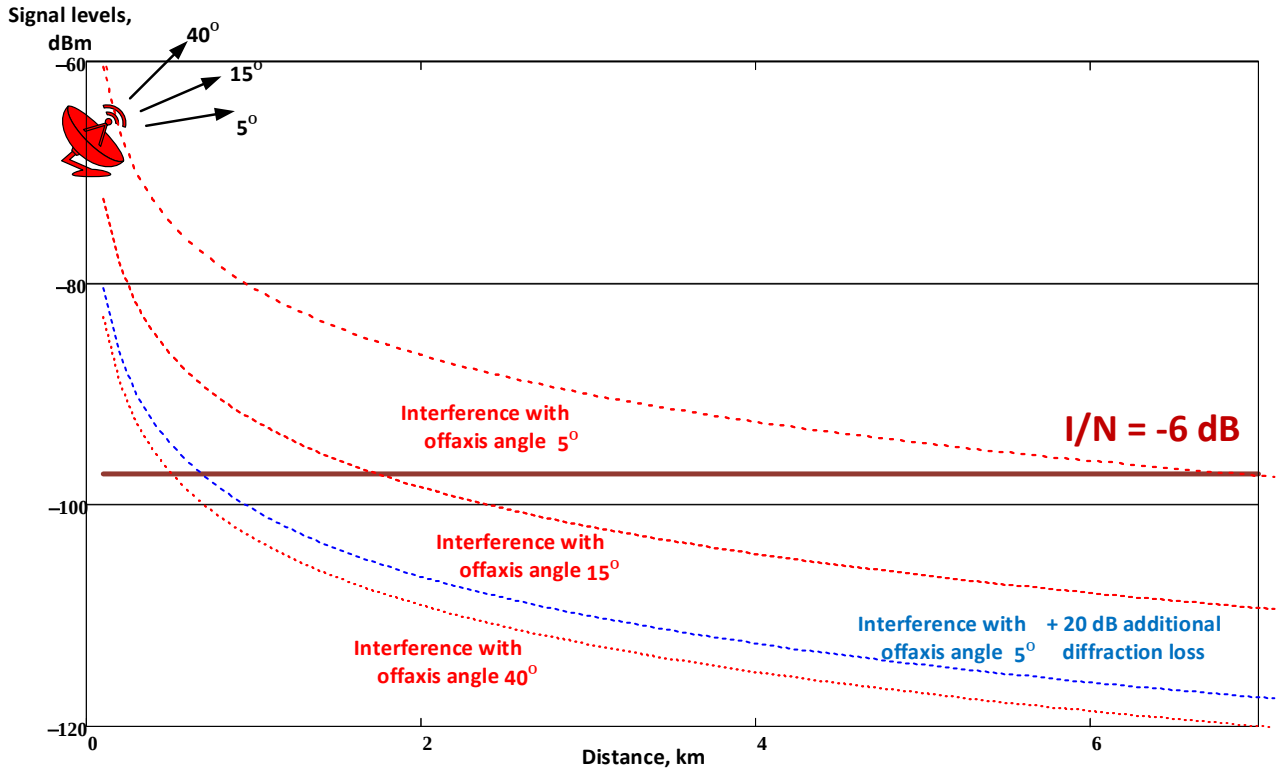

4.3 Mitigation techniques

In addition to calculating interference levels from ES also wanted signal levels from user terminals are calculated to illustrate IMT indoor small cells capabilities to minimize the impact of interference. In addition possible intra-network interference is assessed from another unsynchronized small cell (TDD frequency arrangement is assumed for this band) to illustrate operational conditions in which small cells would be operating. Calculations details are depicted in Figure 3.

For calculation of signals levels the free space propagation model is used. All interfering signals are additionally attenuated by 25 dB due to wall or ceiling penetration loss. In case of more complex model is used for indoor radiowave propagation, modelling of any additional attenuation will be also applicable to interfering signals as well, thus power levels relationships won't change significantly.

The results of the calculations are presented on Figure 4, including interference signal levels for different off-axis angles of ES, wanted signals for user terminals located in the cell assuming maximum e.i.r.p. and also intranetwork interference example.

FIGURE 3

Excessive interference impact assessment on IMT small cells operation

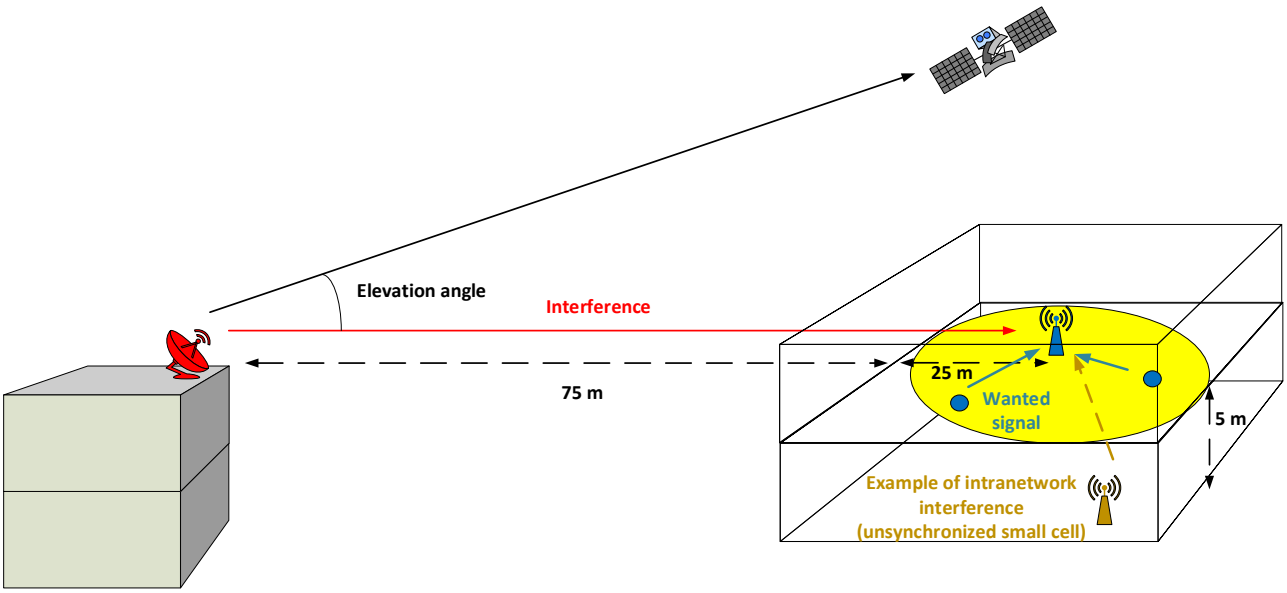

FIGURE 4

Signal levels calculation results

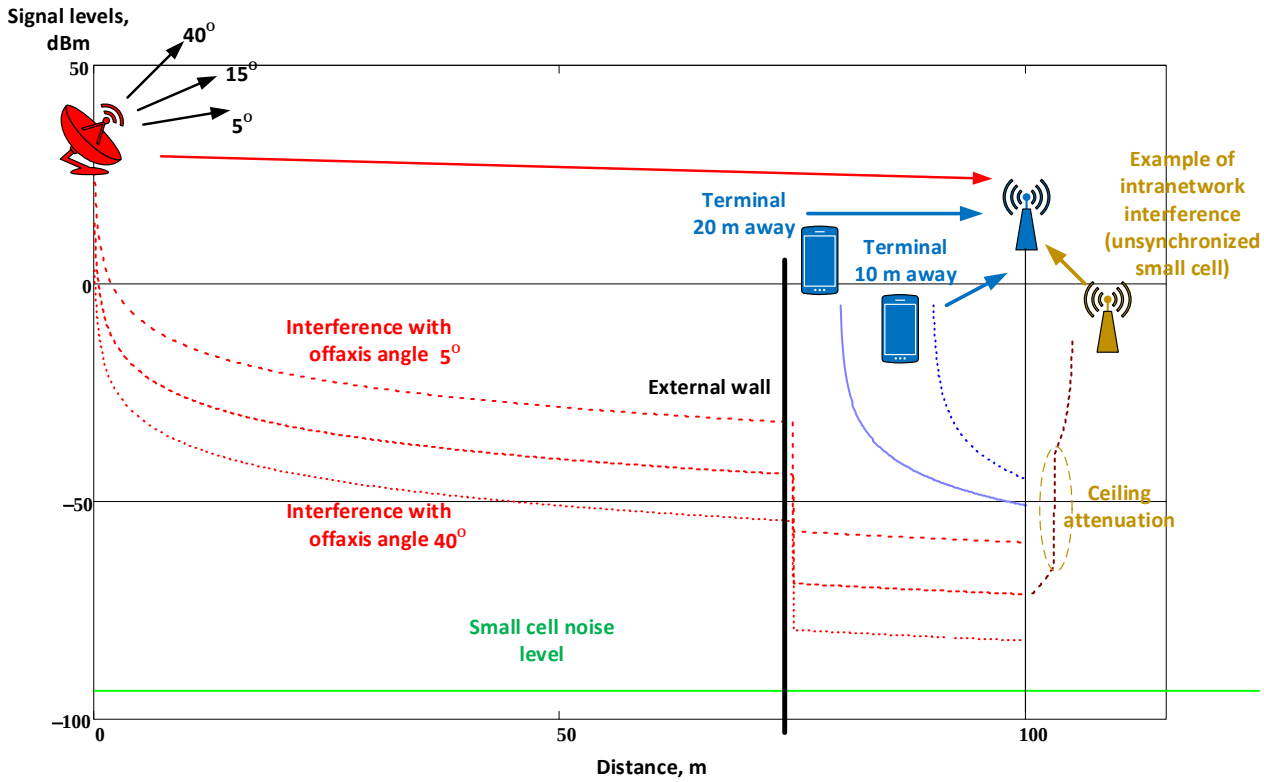

As could be seen from this analysis power levels of interference from FSS ES will usually be above noise levels of small cells. In the worst case of only 5º off-axis angle I/N might reach few tenths of dB above noise. However wanted signals levels in small cells will be usually even higher. For larger off-axis angles C/(I+N) will become few tenths dB, thus rendering even such strong interference tolerable.

It should be noted that interference levels from FSS ES are of the same magnitude as possible intra-network interference calculated as an example. IMT-Advanced radio interfaces optimized for small cell operation will be able tolerate such interference by design.

For example, IMT-Advanced small cells will be capable to further mitigate such interference even in the worst cases by radio resource management algorithms. In the analysed example VSAT station has used 2 MHz channel which is much smaller than IMT systems channel bandwidth of 20 MHz (even wider channels are anticipated in future). If several MHz of bandwidth in such wide channel are interfered by continuous FSS ES transmission the frequency selective scheduler could allocate such interfered resources to user terminals operating in the vicinity of small cell, which will result in a very high C/(I+N) ration.

To assess the effectiveness of such ability of modern IMT systems simple Monte-Carlo simulation had been performed. Specifically small cell inside the building depicted on figure 5 have been simulated with the assumptions previously considered for minimum coupling loss calculation. The only difference in the simulation was the use of propagation models:

– wanted signal was simulated with the indoor model in accordance with Recommendation ITU-R P.1238 with standard deviation of 17 dB;

– interfering signal was modelled by free space propagation model with additional losses within building modelled as sum of entry loss 25 dB and 0.5·d, where d is the distance of the signal travelled inside the building (similar to 3GPP TR36.814, WINNER model etc.).

Four user terminals were modelled operating within the cell simultaneously with 5 MHz block allocated to each user. It is assumed that only first block of 5 MHz within 20 MHz channel is interfered with FSS ES signal. The Fig. 5 illustrates scenario considered.

FIGURE 5

Simulation scenario representation

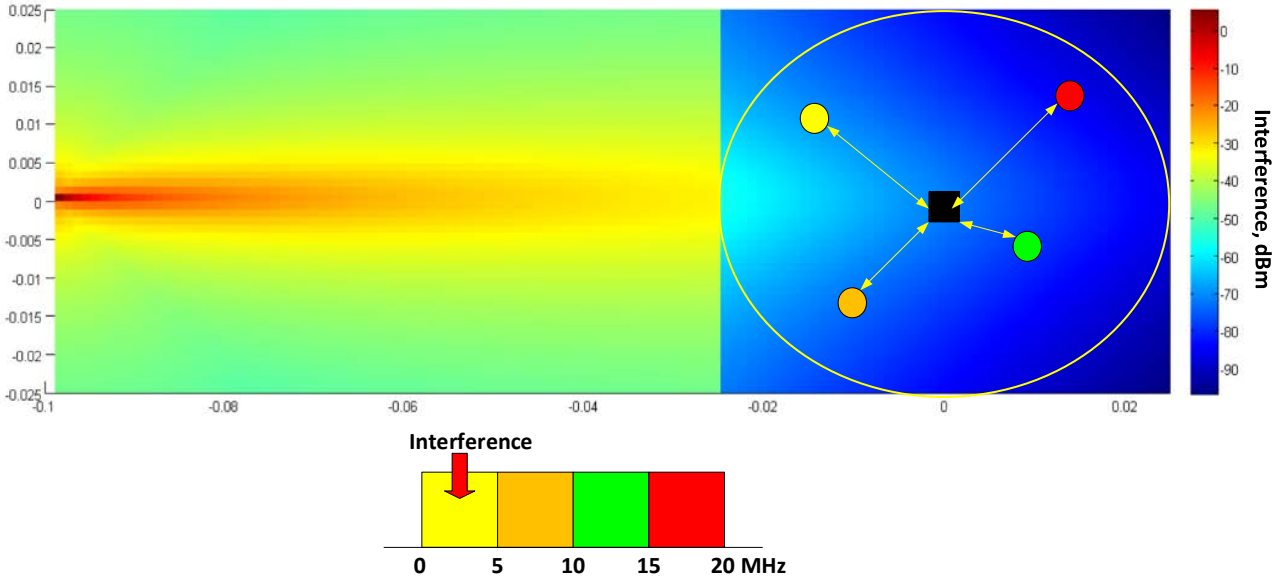

Based on the large number of simulation snapshots the capacity of the cell and of the interfered block were calculated based on achieved C/(I+N) and Shannon-modified curves as presented in 3GPP 36.942. The capacity is calculated for three different cases:

– without interference from FSS ES (base line);

– with interference from FSS ES;

– with interference from FSS ES with scheduling of interfered block to the user with best C/(I+N) conditions.

The results of the simulation are captured in table 4 for the case of 25 dB value for indoor penetration loss, which is representative for most of buildings. For the purpose of sensitivity analysis the value 15 dB was also used, which could occur for some buildings. The result of simulation for this case is shown in table 5.

TABLE 4

Capacity loss in the presence of FSS ES interference (25 dB wall loss)

Scenario	FSS ES elevation 5 deg		FSS ES elevation 15 deg		FSS ES elevation 40 deg	
	20 MHz capacity,%	Interfered block capacity,%	20 MHz capacity,%	Interfered block capacity,%	20 MHz capacity,%	Interfered block capacity,%
Downlink						
No inter.	100.00	100.00	100.00	100.00	100.00	100.00
With inter.	92.03	68.06	95.80	83.18	98.47	93.91
With mitig.	99.02	102.02	99.83	105.30	99.99	106.23
Uplink						
No inter.	100.00	100.00	100.00	100.00	100.00	100.00
With inter.	95.38	81.53	98.54	94.14	99.70	98.89
With mitig.	99.92	100.61	100.00	101.01	100.00	100.91

TABLE 5

Capacity loss in the presence of FSS ES interference (15 dB wall loss)

Scenario	FSS ES elevation 5 deg		FSS ES elevation 15 deg		FSS ES elevation 40 deg	
	20 MHz capacity,%	**Interfered block capacity,%**	**20 MHz capacity,%**	**Interfered block capacity,%**	**20 MHz capacity,%**	**Interfered block capacity,%**
Downlink						
No inter.	100.00	100.00	100.00	100.00	100.00	100.00
With inter.	85.60	42.42	90.68	62.71	95.57	82.30
With mitig.	93.54	80.26	98.41	99.71	99.80	105.21
Uplink						
No inter.	100.00	100.00	100.00	100.00	100.00	100.00
With inter.	90.50	62.00	96.06	84.26	98.70	94.81
With mitig.	98.78	96.06	99.95	100.78	100.00	100.95

As could be seen from the table the capacity loss is more severe in the downlink where user terminals may be close to the outer wall in front of FSS ES. However even in this case the capacity loss is limited only to one block of 5 MHz within 20 MHz channel, which doesn't degrade the overall cell capacity significantly. If frequency selective scheduling is applied (leading to the situation when interfered block is usually allocated to the user with best C/(I+N) within the cell) than overall capacity loss could be almost avoided completely. The effectiveness of the mitigation technique is still valid even in the rare cases of excessive interference in buildings with lower indoor penetration loss values.

5 Summary

The analysis provided in the document has shown that FSS ES interference may easily reach positive I/N ratio values and violate traditional interference criteria. The separation distances to fulfill I/N criteria may vary from hundreds of metres up to few kilometres in rare cases. Few hundred metres separation distance could be used as general assumption.

However due to specifics of small cells operation even interference with smaller separation distances won't degrade C/(I+N) ratio within IMT small cell, which provides intrinsic mitigation technique. Furthermore narrowband operation of FSS ES (with channels up to few MHz) compared to wideband channel of IMT systems (20 MHz or even wider in the future) could be mitigated by small cell radio resource management algorithms by allocating interfered blocks of spectrum to user terminals having best C/(I+N) ratios. Simulation results have shown the effectiveness of such mitigation technique.

ANNEX 2

Compatibility study between IMT and FSS transmit earth stations operating in the 5 850-6 425 MHz frequency band

1 Introduction

The study in this annex investigates the impact of the Earth-to-space transmission of a single FSS earth station into a single IMT receiver in the 5 850-6 425 MHz frequency band. Specifically, it provides the minimum separation distances that would be required to protect a single receiving IMT base station from a single transmitting FSS earth station at a specific geographic location. Administrations should consider this information in conjunction with information on the deployment of transmitting FSS earth stations in a geographic region in deciding whether any portion of the 5 850-6 425 MHz frequency band may be identified for use by IMT.

2 Background

Utilizing the information on typical FSS earth stations parameters in the 5 850-6 700 MHz frequency band and IMT systems parameters and the protection criteria to be applied to IMT receivers provided in ITU-R Report M.2292-0, a sharing analysis was undertaken to ascertain the impact of the Earth-to-space transmissions of a single FSS earth station on a single receiving IMT base station. The focus of the analysis was to determine the separation distances that would have to be maintained between these two stations in order to ensure that the receiving IMT base station would not be subjected to excessive levels of interference from the in-band co-frequency and spurious emissions of the transmitting FSS earth station.

3 Technical characteristics

The technical characteristics of the IMT and FSS systems and any related assumptions are summarized in Tables 1 and 2 in this Report. The signal propagation model used for the study was that contained in Recommendation ITU-R P.452-14 for overland interference paths.

4 Analysis

4.1 Assumptions

The aggregate protection criterion to be applied to IMT receivers is expressed as an interference-to-noise (“I/N”) ratio of no greater than –6 dB. This criterion could be applied in conjunction with the receiver noise figures provided in Report ITU-R M.2292-0 to derive the maximum permissible power level of the interfering signal at the IMT receiver. However, there is no guidance as to the single entry protection criterion to be applied with respect to an IMT receiver. In this regard, noting that the 5 850-6 425 MHz frequency band is allocated on a primary basis to the fixed satellite service, the fixed service and the mobile service (the service under which IMT would potentially operate); it was assumed that the aggregate I/N of –6 dB criterion was divided equally between the fixed service and the fixed satellite service, thus resulting in an assumed IMT single entry protection criterion of I/N of –9 dB.

Concerning the FSS earth-to-space transmissions, e.i.r.p density levels to be used in direction of the horizon are contained in Recommendation ITU-R S.524-9. For the sharing analysis, the e.i.r.p density levels specified in *recommends* 2 of the Recommendation ITU-R S.524-9 were used.

With regard to the transmitting antenna of an FSS earth station, the off-axis gain of such antennas should be compliant with the antenna reference pattern specified in Recommendation ITU-R S.465.

Accordingly, for the analysis, it was assumed that the maximum power density of the FSS earth-to-space transmission was limited to –36 dBW/Hz[7] at the input to the antenna of the FSS earth station.

Concerning the unwanted spurious emissions of the transmitting FSS earth station, it was assumed that the applicable attenuation values that should be used to calculate the maximum spurious domain emission power levels are those specified in Table 1 of Appendix **3** of the Radio Regulations. Applying this methodology to an assumed 40 kHz wide FSS carrier, leads to an applicable attenuation level of 53 dBc[8]. Using this attenuation level, the power density level of the FSS carrier's unwanted emission was calculated to be -89 dBW/Hz.

4.2 Methodology

A sharing analysis was conducted for the IMT base stations and associated deployment scenarios indicated in Table 1. The analysis considered the impact upon a single receiving IMT base station from both in-band co-frequency emissions and spurious emissions of a single transmitting FSS earth station in the 5 850-6 425 MHz frequency band. For each IMT base station scenario studied, the interference into the IMT base station was calculated for two FSS earth station antenna elevation angles: 5° and 30° above horizon. A geographic area exhibiting mildly hilly terrain features was chosen for the study.

With the FSS earth station location and antenna pointing fixed, a hypothetical IMT receiving base station was successively placed at many locations around the FSS earth station. At each location, the maximum beam gain lobe of the IMT antenna (with beam-tilt as appropriate) was assumed pointed in azimuth towards the FSS earth station. At each location, the I/N at the IMT receiver was calculated taking into account the long-term propagation loss on the interference path and the off-axis antenna gains of the FSS earth station and IMT station. Subsequently, contour lines connecting those points where the I/N was closest to the required single entry protection criterion were computed, resulting in (contour) areas within which the computed I/N would not meet the (I/N) limit required by the protection criterion.

4.3 Results

The results of the study are provided in Figures 1a, 1b, 2a, 2b, 3a, 3b, 4a and 4b. The approximate range of separation distances are summarized in Table 3.

Noting that the contours produced by this study enclose areas of considerable size, as quantified in the lower left-hand corner of each figure, and given the considerable numbers of FSS earth stations that operate within the 5 850-6 425 MHz frequency band in many countries, it may be concluded from the results of the study that IMT deployment in this band would face many sharing problems.

Additionally, with regard to the indoor small cells, it is unclear as to how indoor only operation can be practically enforced, as no regulatory enforcement mechanism exists on an international basis. Therefore, the indoor case should not be used as a basis for decision making under this (WRC-15) agenda item.

---

[7] It is noted that the application of the off-axis gain limits of Recommendation ITU-R S.465-6 to the e.i.r.p. limits of *recommends* 1.1 and 1.3 of Recommendation ITU-R S.524-9 would permit the use of emissions with a power density level that is 3 dB higher than that assumed for this analysis, i.e. –33 dBW/Hz.

[8] Typical value for the minimum FSS emission bandwidth is 40 kHz.

5 Summary

A sharing study was conducted in the 5 850-6 425 MHz frequency band to determine the impact of interference from a single transmitting FSS earth station upon a single outdoor macro cell receive IMT base station deployed in a suburban environment and in an urban environment, a single outdoor small-cell IMT receiving base station deployed in a suburban environment, and a single indoor small-cell IMT receiving base station deployed in a suburban environment. The study was conducted for a geographic area exhibiting mildly hilly terrain features and considered two FSS earth station antenna elevation angles: 5° and 30° above horizon. It was assumed that at each location the maximum gain lobe of the IMT base station (with down-tilt as appropriate) was facing in azimuth towards the transmitting FSS earth station.

The analysis was conducted for an assumed IMT single entry I/N protection criteria of -9 dB; whereby the IMT aggregate I/N protection criterion of -6 dB was assumed to be divided equally among two other services – fixed satellite service and fixed service – that are allocated on a primary basis, along with the mobile service, in the 5 850-6 425 MHz frequency band. The results of the study showed a minimum separation distance should be maintained between an FSS earth station and an IMT base station in order to protect the IMT station from excessive interference from FSS transmissions. Specifically, for protection from co-frequency, in-band FSS transmissions, the study showed that depending on the azimuth bearing of the IMT base station relative to the FSS station 1) a minimum separation distance of approximately 10 to 78 kilometres should be maintained to protect an outdoor macro cell IMT base station deployed in a suburban environment, 2) a minimum separation distance of approximately 6 to 33 kilometres should be maintained to protect an outdoor macro cell IMT deployed in an urban environment, 3) a minimum separation distance of approximately 4 to 33 kilometres should be maintained to protect an outdoor small-cell IMT station deployed in a suburban environment and 4) depending on the indoor building penetration loss, a minimum separation distance of approximately 2.5 to 13 kilometres should be maintained to protect an indoor small cell base station deployed in a suburban environment.

Similarly, for protection from spurious FSS transmissions, the study showed that only outdoor IMT base stations would be impacted and that 1) a minimum separation distance of approximately 4 to 13 kilometres should be maintained to protect an outdoor macro cell IMT base station deployed in a suburban environment, 2) a minimum separation distance of less than 1 kilometre to approximately 7 kilometres should be maintained to protect an outdoor macro cell IMT deployed in an urban environment and 3) a minimum separation distance of approximately 1 to 6 kilometres should be maintained to protect an outdoor small-cell IMT station deployed in a suburban environment.

Noting that the contours produced by this study enclose areas of considerable size and given the considerable numbers of FSS earth stations that operate within the 5 850-6 425 MHz frequency band in many countries, it may be concluded from the results of the study that IMT deployment in this band would face many sharing problems.

Additionally, with regard to the indoor small cells, it is unclear as to how indoor only operation can be practically enforced, as no regulatory enforcement mechanism exists on an international basis. Therefore, the indoor case should not be used as a basis for decision making under this (WRC-15) agenda item.

APPENDIX 1 TO ANNEX 2

TABLE 1

IMT characteristics

IMT cell base station type	**Macro cell base station (Suburban)**	**Macro cell base station (Urban)**	**Small cell base station (Outdoor)**	**Small cell base station (Indoor)**
IMT operational environment	Suburban outdoor	Urban outdoor	Suburban outdoor	Suburban Indoor
Maximum antenna gain (dBi)	18	18	5	0
Antenna height above ground (metres)	25	20	6	3
Antenna type	3-Sector	3-Sector	Omni	Omni
Antenna 3 dB Beam-width in the Horizontal Plane (degrees)	65°	65°	N/A	N/A
Antenna gain pattern envelope	Recommendation ITU-R F.1336-4	Recommendation ITU-R F.1336-4	Recommendation ITU-R F.1336-4	Recommendation ITU-R F.1336-4
Antenna (mechanical) down-tilt (degrees)	6	10	N/A	N/A
Clutter loss at the IMT receiving base station site (dB)	Clutter loss characteristics for suburban environment as specified in Table 4 of section 4.5.3 of Recommendation ITU-R P.452-14	Clutter loss characteristics for urban environment as specified in Table 4 of section 4.5.3 of Recommendation ITU-R P.452-14	Clutter loss characteristics for suburban environment as specified in Table 4 of section 4.5.3 of Recommendation ITU-R P.452-14	Clutter loss characteristics for suburban environment as specified in Table 4 of section 4.5.3 of Recommendation ITU-R P.452-14
Building penetration loss (dB)	0	0	0	15 / 25 dB
Receiver noise figure (dB)	5[see Note]	5[see Note]	5[see Note]	5[see Note]
Noise power density (dBW/Hz)	–200.6	–200.6	–200.6	–200.6
Aggregate *I/N* requirement (dB)	–6	-6	–6	-6
Assumed single entry *I/N* requirement (dB)	–9	–9	–9	–9
Maximum permitted single entry interference power density (dBW/Hz)	–209.6	–209.6	–209.6	–209.6

NOTE - Receiver noise figure assumed to apply at the output port of the receiving (IMT) antenna, i.e. it includes the noise contribution due to feeder losses.

TABLE 2

FSS characteristics

Location of earth station	Mississippi, USA
Latitude of earth station (degrees North)	31.3
Longitude of earth station (degrees West)	88.4
Antenna diametre (metres)	8
Maximum antenna Gain (dBi)	52.8
Off-axis gain envelope	*Recommends* 2 of Recommendation ITU-R S.465-6
Antenna height above ground (metres)	10
Antenna elevation angle (degrees above horizon)	≈5° see note 1 ≈30° see note 2
Maximum power density into transmitting antenna (dBW/Hz)	–36 see note 3
Unwanted emission attenuation (dBc) see note 4	53

NOTES:

1 Assumed that the earth station is pointed to a geostationary satellite located at 14.46° W.L.

2 Assumed that the earth station is pointed to a geostationary satellite located at 43.9° W.L.

3 Value calculated by subtracting the antenna off-axis gain, as specified in *recommends* 2 of Recommendation ITU-R S.465-6, from the maximum e.i.r.p. density limit specified in *recommends* 2 of Recommendation ITU-R S.524-9.

4 Unwanted emission attenuation level was determined using the criteria contained in Table 1 of Appendix **3** of the ITU Radio Regulations for a carrier bandwidth of 40 kHz.

FIGURE 1a

Distance separation contours for a single outdoor IMT macro base station located in a suburban environment (Single entry IMT protection criterion: *I/N* ≤ -9 dB) (FSS earth station antenna elevation angle above the horizon: 5°)

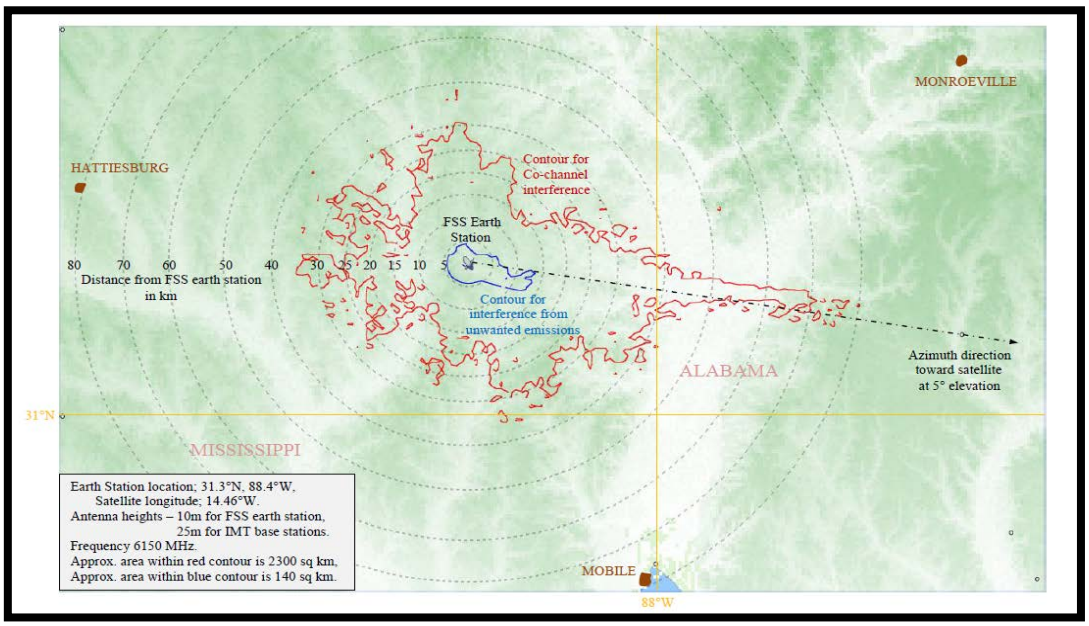

FIGURE 1b

Distance separation contours for a single outdoor IMT macro base station located in a suburban environment (Single entry IMT protection criterion: *I/N* ≤ -9 dB) (FSS earth station antenna elevation angle above the horizon: 30°)

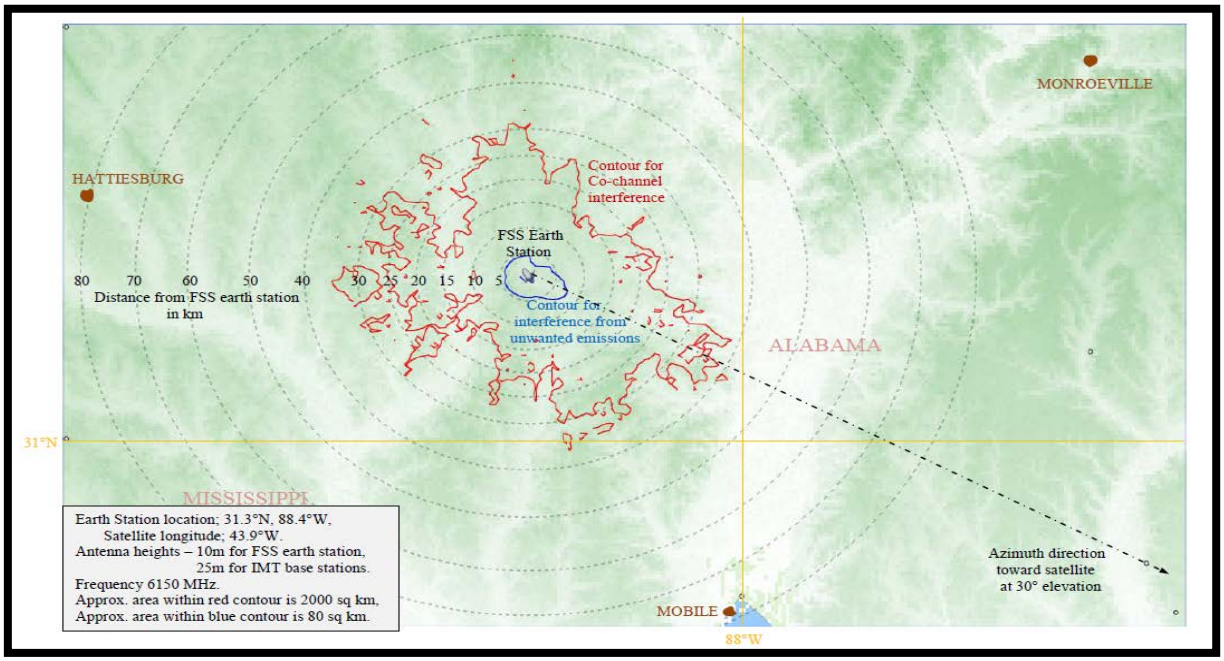

FIGURE 2a

Distance separation contours for a single outdoor IMT macro base station located in an urban environment (Single entry IMT protection criterion: *I/N* ≤ -9 dB) (FSS earth station antenna elevation angle above the horizon: 5°)

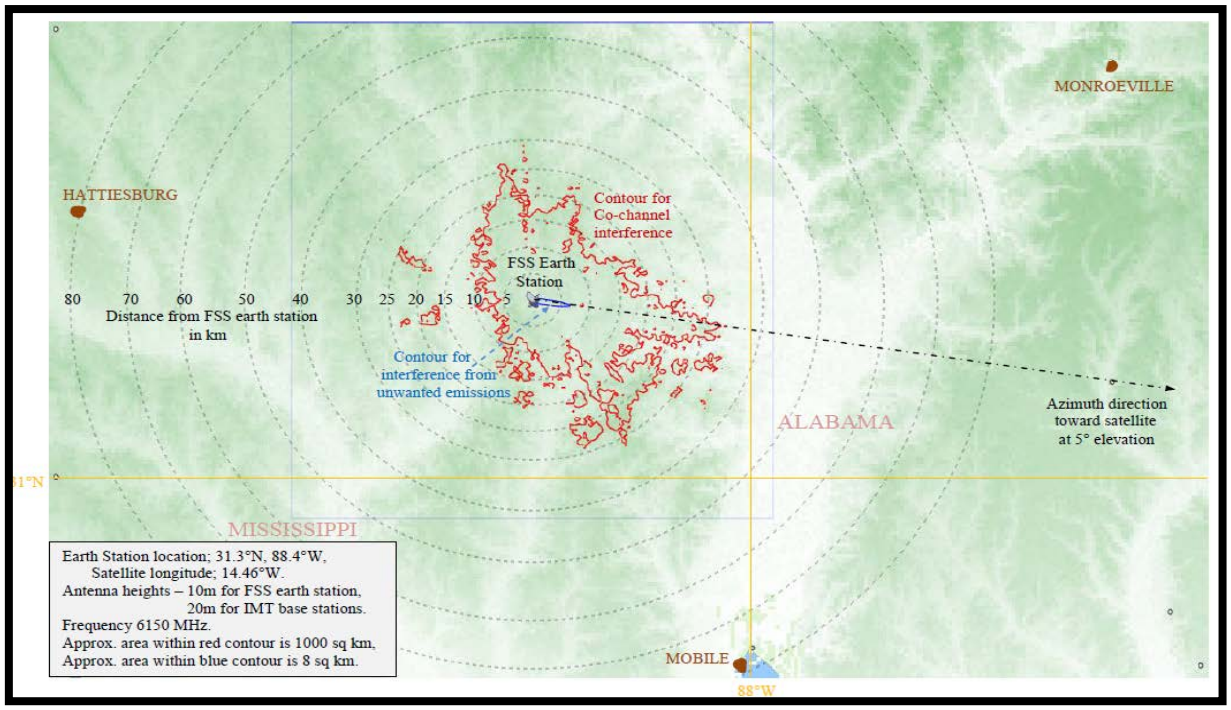

FIGURE 2b

Distance separation contours for a single outdoor IMT macro base station located in an urban environment (Single entry IMT protection criterion: *I/N* ≤ -9 dB) (FSS earth station antenna elevation angle above the horizon: 5°)

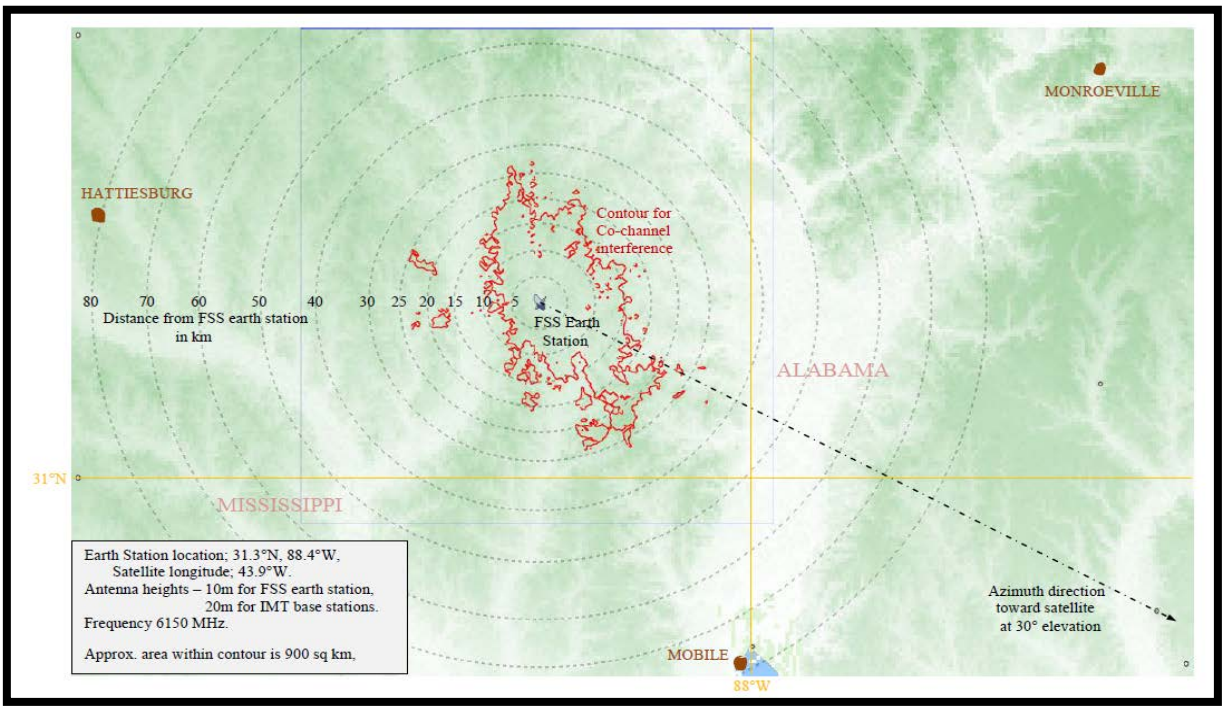

FIGURE 3a

Distance separation contours for a single outdoor IMT small cell base station located in a suburban environment (Single entry IMT protection criterion: *I/N* ≤ -9 dB) (FSS earth station antenna elevation angle above the horizon: 5°)

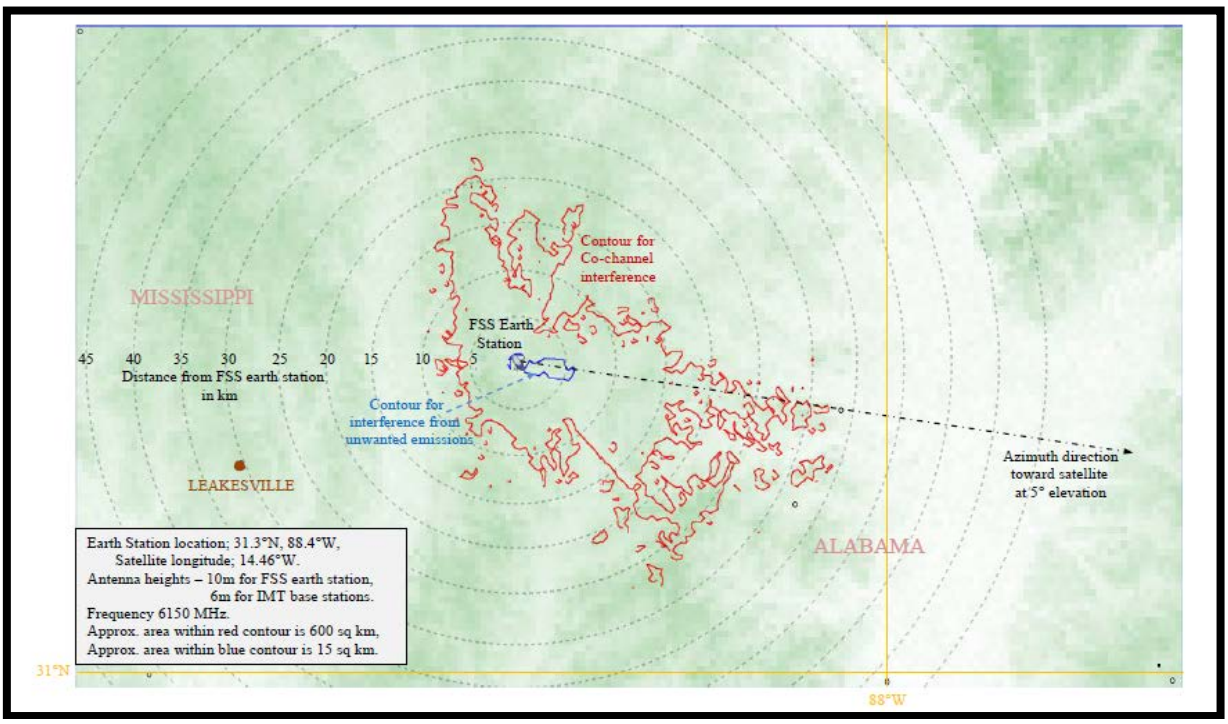

FIGURE 3b

Distance separation contours for a single outdoor IMT small cell base station located in a suburban environment (Single entry IMT protection criterion: *I/N* ≤ -9 dB) (FSS earth station antenna elevation angle above the horizon: 30°)

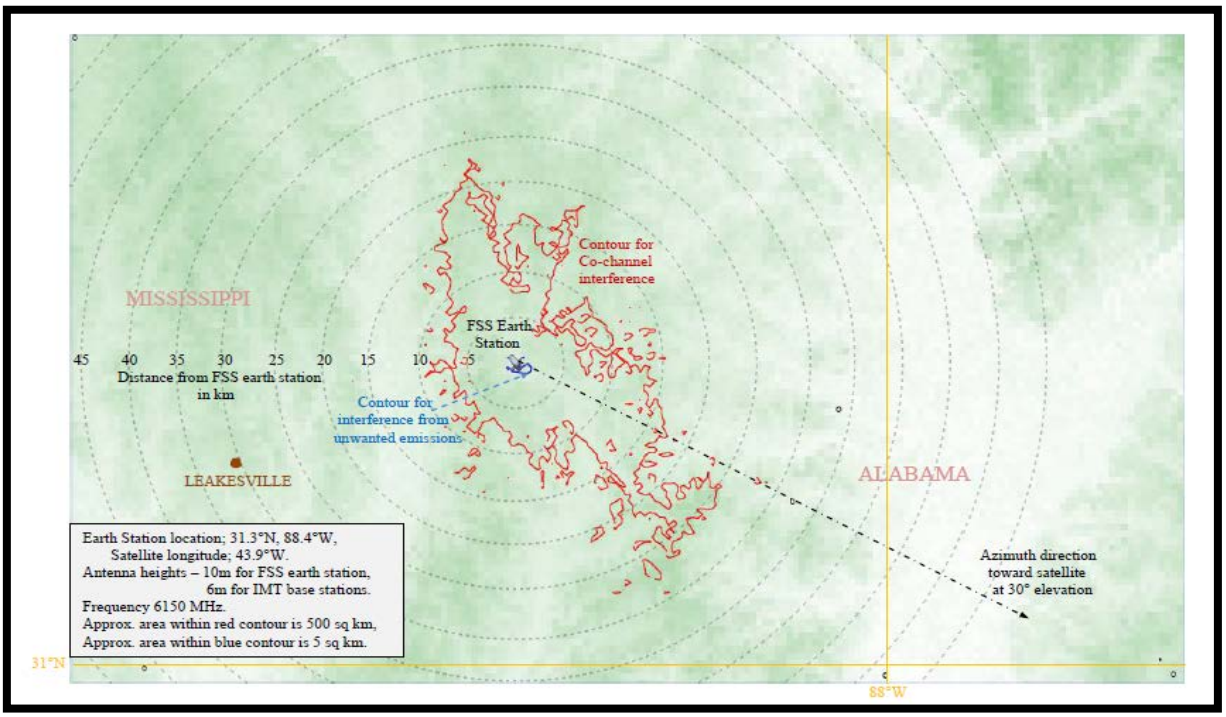

FIGURE 4a

Distance separation contours for a single indoor IMT small cell base station located in a suburban environment (Single entry IMT protection criterion: *I/N* ≤ -9 dB) (FSS earth station antenna elevation angle above the horizon: 5°)

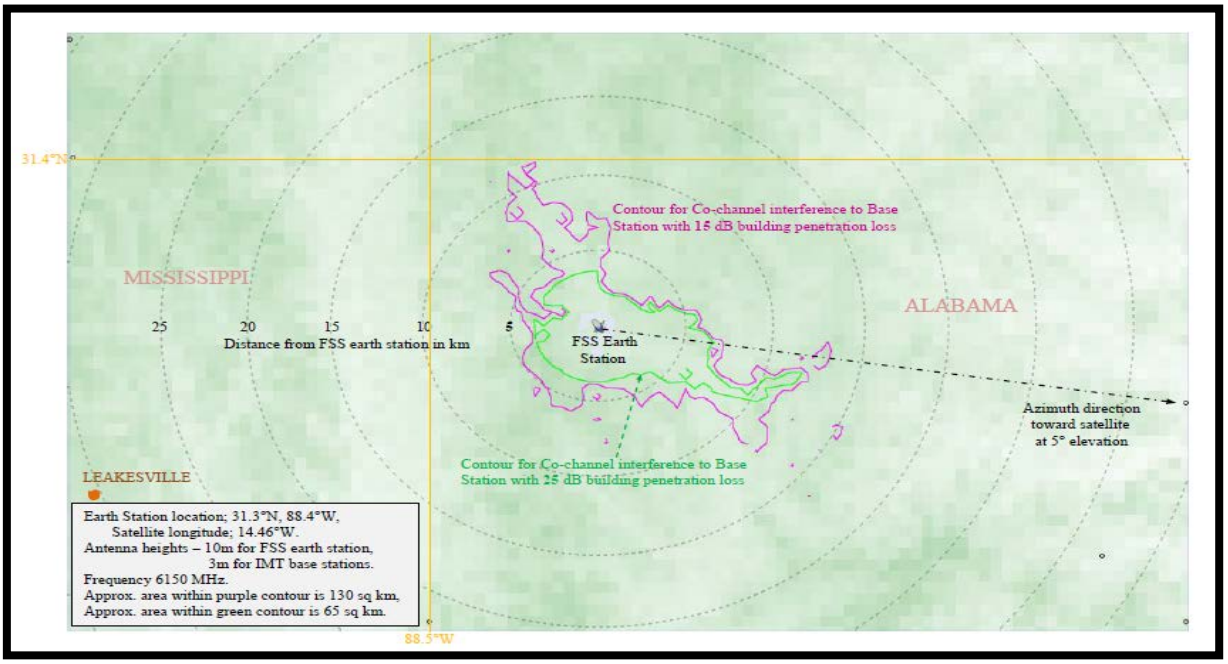

FIGURE 4b

Distance separation contours for a single indoor IMT small cell base station located in a suburban environment (Single entry IMT protection criterion: *I/N* = ≤ -9 dB) (FSS earth station antenna elevation angle above the horizon: 30°)

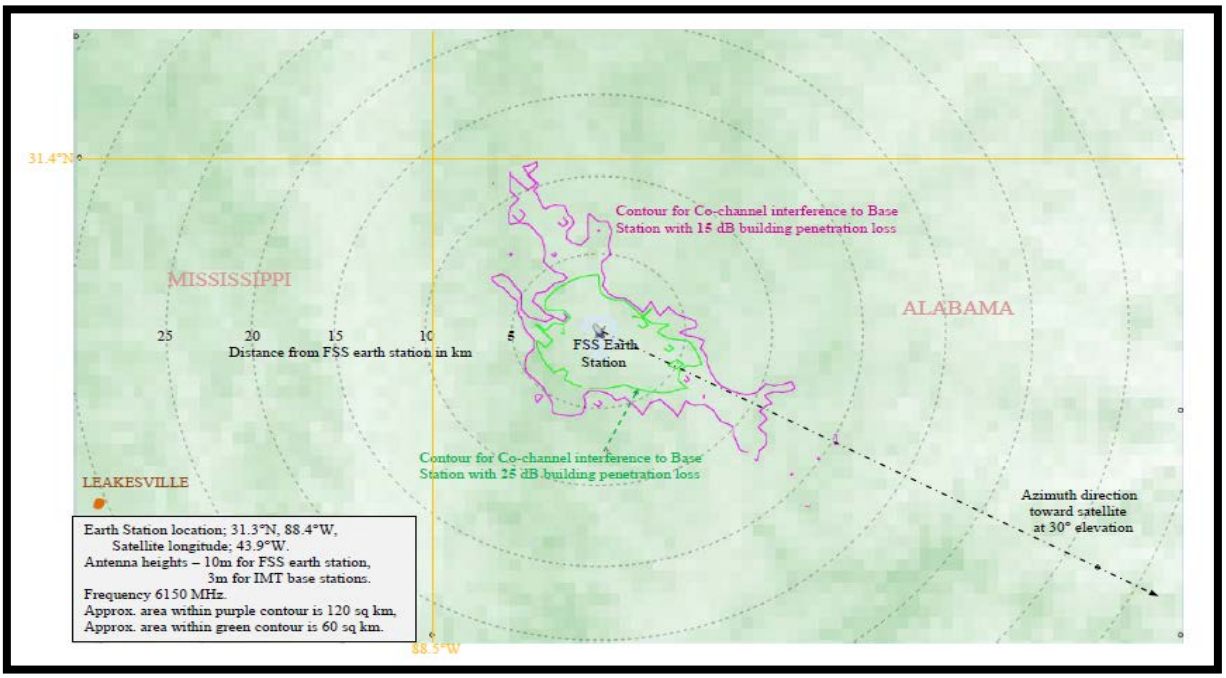

TABLE 3

Minimum required separation distance between a single transmitting FSS earth station and a single receiving IMT base station (Single entry IMT I/N protection criterion: *I/N*≤ -9 dB)

IMT base station type	Interference type	FSS antenna elevation (° above horizon)	Approximate required separation distance (km)	Approximate size of area within which the IMT protection criterion is not met (sq. km)
Outdoor macro, suburban	Co-frequency	5	10 – 78	2 300
		30	10 – 40	2 000
	Spurious	5	4 – 13	140
		30	4 – 7.5	80
Outdoor macro, urban	Co-frequency	5	6 – 33	1 000
		30	6 – 30	900
	Spurious	5	<1 – 7	8
		30	Protection criterion met	N/A
Outdoor small cell, suburban	Co-frequency	5	4 – 33	600
		30	4 – 27	500
	Spurious	5	1 – 6	15
		30	1 – 2	5
Indoor small cell, suburban (Building loss: 15 dB)	Co-frequency	5	2.5 – 13	130
		30	2.5 – 12.5	120
	Spurious	5	Protection criterion met	N/A
		30		N/A
Indoor small cell, suburban (Building loss: 25 dB)	Co-frequency	5	2.5 – 12	65
		30	2.5 – 6	60
	Spurious	5	Protection criterion met	N/A
		30		N/A

ANNEX 3

Sharing and compatibility between IMT systems and FSS receiving space stations in the 5 925-6 425 MHz frequency band

1 Introduction

The frequency band 5 925-6 425 MHz has been proposed as a possible candidate band for IMT identification, which most likely will result in MS stations deployment in large quantities as part of dense mobile communication networks.

However this band is extensively used for FSS networks as satellites reception band across the world. As aggregate interference from MS stations could affect all of the satellites irrelatively to specific administration deploying IMT systems, consideration of the 5 925-6 425 MHz frequency band as a candidate band should be based only on technical conditions ensuring protection of FSS in the long term.

The goal of this study is to define technical condition for IMT systems deployment which will facilitate sharing of the 5 925-6 425 MHz frequency band with FSS space stations. Comparing such technical conditions with actual requirements of IMT systems networks could be used to define potential of the 5 925-6 425 MHz frequency band as a candidate one. Technical conditions could be also incorporated into regulatory requirements associated with IMT identification.

As the 5 925-6 425 MHz frequency band is used for FSS GSO networks as well as for FSS NGSO networks this study provides separate analysis for each case. As aggregate interference into satellite receiver is the focus of the study, the assumptions about MS stations dissemination and their activity are part of the study and have a significant impact on the results of the study.

It should be noted that studies are focused only on assessment of interference into FSS satellite receivers and don’t cover interference from FSS earth stations into IMT receivers.

2 Background

The frequency band 5 925-6 425 MHz is already allocated to mobile service on the primary basis worldwide. However identification of this band for IMT will significantly change the usage of the frequency band which requires the coexistence studies with other incumbent services. The main services deployed in this band are FS and FSS (Earth-to-space). Of the two the most tremendous impact could be on FSS (Earth-to-space) because the impact from IMT systems can’t be localized within administrations deploying IMT systems and it is impossible to pinpoint the source of aggregate interference. Figure 1 illustrates aggregate interference mechanism affecting FSS GSO satellite, where interference originates from multiple sources and locations within beam footprint. For FSS NGSO satellite aggregate interference could be calculated in the same way, however due to the movement of the satellite its footprint is not constant.

FIGURE 1

Aggregation of the interference from IMT transmitters within satellite footprint

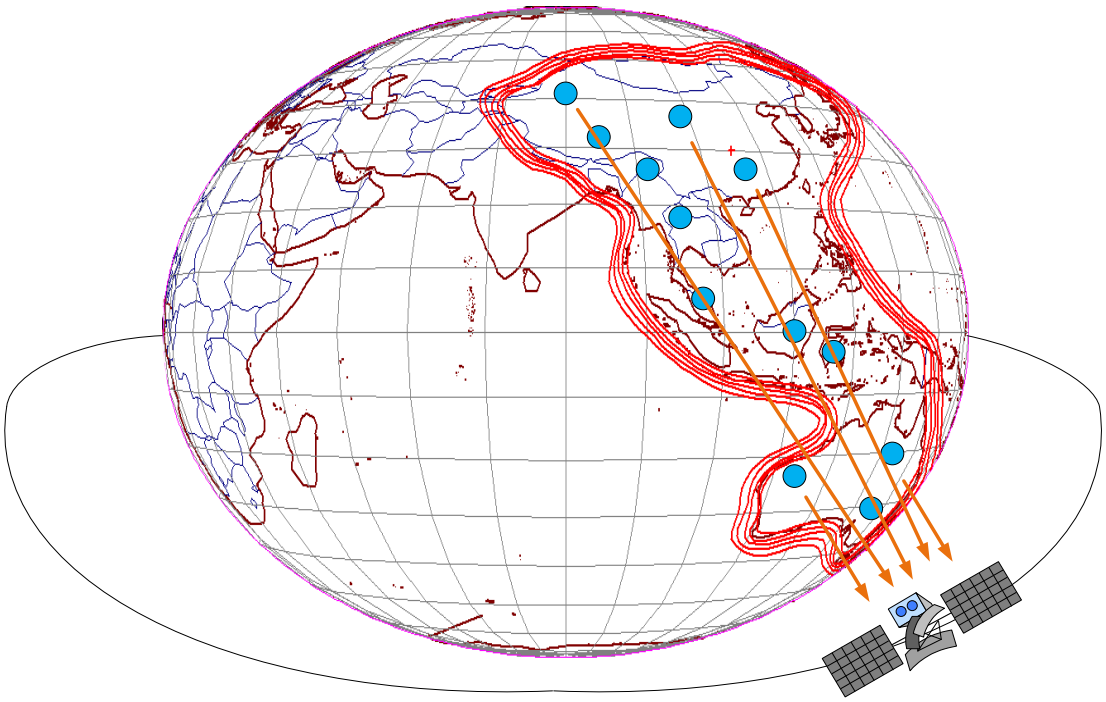

There are no specific ITU-R Recommendations or ITU-R Reports describing in detail the interference calculation for such a case, however the study is based on ΔT/T approach in Appendix 8 of the ITU Radio Regulations in order to assess the impact of interference from a large number of IMT stations in the field-of-view of a satellite antenna beam. Although not strictly for use in the case of inter-service sharing, it does provide a very simple method of analysing the impact without much knowledge of the characteristics of the carriers used on the satellite network requiring protection. In this technique, the interference from the IMT networks into the satellite receivers is treated as an increase in thermal noise in the wanted FSS network and hence is converted to a noise temperature (by considering the interference power per Hz) and compared with tolerable percentage increase in noise temperature. This approach has the advantage in that very few satellite parameters are required to be known and a detailed link budget for every type of carrier (especially those most sensitive to interference) is not required for the satellite network requiring protection. Recommendation ITU-R S.1432 “Apportionment of the allowable error performance degradations to FSS hypothetical reference digital paths arising from time invariant interference for systems operating below 30 GHz” provides appropriate ΔT/T criterion both for GSO and NGSO cases.

3 Technical characteristics

3.1 IMT systems characteristics and assumptions

3.1.1 IMT stations parameters

Considering rather high frequency of the frequency band 5 925-6 425 MHz, it was assumed that the IMT systems would be most likely deployed in dense urban areas and mainly indoor as pico and femto cells with wideband channels and high data rate. It was also assumed that the frequency band 5 925-6 425 MHz would be used as a separate level of coverage without macro cells, making the time division duplex more advantageous for such IMT systems. Taking this into account the calculations consider only small base stations emitting up to 100% of time. Subscriber stations, which are generally low power and power controlled, were not considered (justification for such assumption is provided in the section 3.1.4). Parameters for small base stations used in the calculations are given in Table 1 below. Footnotes in the table are used to highlight differences between parameters used in the modelling and typical values established for IMT systems.

TABLE 1

IMT stations parameters

	Small cell indoor
Base station characteristics / Cell structure	Not used in the modelling[9]
Cell radius / Deployment density	Not used in the modelling[11]
Antenna height	Not used in the modelling[11]
Sectorization	Single sector
Downtilt	n.a.
Frequency reuse	1
Antenna pattern	Recommendation ITU-R F.1336 omni
Antenna polarization	linear
Indoor base station deployment	100 %
Indoor base station penetration loss	15 dB, 25 dB and 35 dB[10]
Below rooftop base station antenna deployment	n.a.
Feeder loss	n.a
Maximum base station output power (5/10/20 MHz)	15 dBm and 24 dBm
Maximum base station antenna gain	0 dBi
Maximum base station output power (e.i.r.p.)	15 dBm and 24 dBm
Average base station activity	50 %

9 Due to assessment of aggregate interference into FSS space station receiver those parameters are irrelevant for the calculation.

10 Typical value for Indoor base station penetration loss is described as 25 dB for horizontal direction in the frequency band 5-6 GHz and for vertical direction based on Recommendation ITU-R P.1238, Table 3. 15 dB and 35 dB values are used for sensitivity analysis. The value 35 dB corresponds well to measurements results provided within Recommendation ITU-R P.2041 and 15 dB is taken as most conservative assumption for global average penetration loss value.

Average base station power/sector (to be used in sharing studies)	12 dBm and 21 dBm

3.1.2 IMT base stations density assumptions

The number of simultaneously emitting IMT base stations is proposed to be calculated considering the world population density and predicted dissemination factor $K_{\text{DISSEMINATION}}$ of small cells expressed in % relative to the population. The area activity factor K_{ACTIVE} of base stations serving small cells, which reflects the average loading of such stations (in percentage) within FSS satellite coverage footprint, should also be taken into account, as well as band usage factor $K_{\Delta f}$ of the frequency band 5 925-6 425 MHz by a single IMT base station with equi-probable selection of a carrier frequency with 20 MHz frequency bandwidth. The population density is modelled by distribution of the world population between major cities to obtain a representative distribution for FSS spacecraft service areas.

In the calculations the $K_{\text{DISSEMINATION}}$ of IMT base stations is assumed to be 1%, 3% and 6% of the population. Considering the availability of other IMT bands and alternative RLAN solutions for home use, the usage of higher bands for IMT will be demanded in densely populated areas only, making unlikely the dissemination factor more than 6%. The number of small base stations in all bands is predicted to reach 70 million by 2017[11]. Being only one of several bands used for IMT small cells and RLAN hotspots the number of small cell being deployed in the frequency band 5 925-6 425 MHz would be only a fraction of all small cells in the future. Furthermore small cells deployment involving multiple IMT bands, including 5 925-6 425 MHz frequency band, and RLAN bands in one device would be mostly driven by carrier grade small cells due to the fact that consumer grade devices (installed by consumers in their premises) will be using mostly RLAN spectrum for capacity. Thus the dissemination factor of 6% in the frequency band 5 925-6 425 MHz which corresponds to 400 million base stations is a pessimistic assessment from the compatibility point of view with the FSS.

The areal activity factor for IMT base stations is assumed to be 20%. As the service areas may cover several time zones, whole countries and continents, simultaneous full loading of millions of such base stations is unrealistic. Moreover, on the way of improving emission efficiency, the standardization agencies consider a possibility of designing new type of base station capable to entirely cease emission when traffic is zero.

It is assumed that each single base station will use only one 20 MHz channel, so for the entire 5 925-6 425 MHz frequency band the usage factor $K_{\Delta f}$ may be assumed to be 4%.

The above factors and assumed values will result in around 0.0001 to 0.0005 active small cell per 20 MHz per inhabitant, which is around one tenth of penetration of RLAN access points predicted in developed countries, which still is a very high penetration value for carrier grade small cells. The above factors are applied to a city population M_{CITY} to obtain the number of actively emitting IMT base stations associated with the coordinates of the specific city. To obtain the representative distribution of the world population between major cities, a world country database has been used including data on the population of countries and geographical location (latitude, longitude, height above sea level) of the cities (see Fig. 2) with their population.

To simplify calculations, prior to the calculation for each separate country, a list of major cities has been defined with their population in descending order, and then a list of the cities has been chosen,

[11] Small Cell Market Status. Informa Telecoms & Media, February 2013.

mostly representing land settlement density (see Fig. 3). This is especially important for the countries with vast territories.

After the list of the cities is determined, all population of the country is distributed to the selected cities (see Appendix 1) in accordance with the percentage of the population in the cities. Further calculations are conducted based only on the selected cites of each country (with the total number of their population equalled to the population of the country) and with the precise reference to their geographical locations.

FIGURE 2

World location of major cities (population of at least 10/50 thousand people depending on the country)

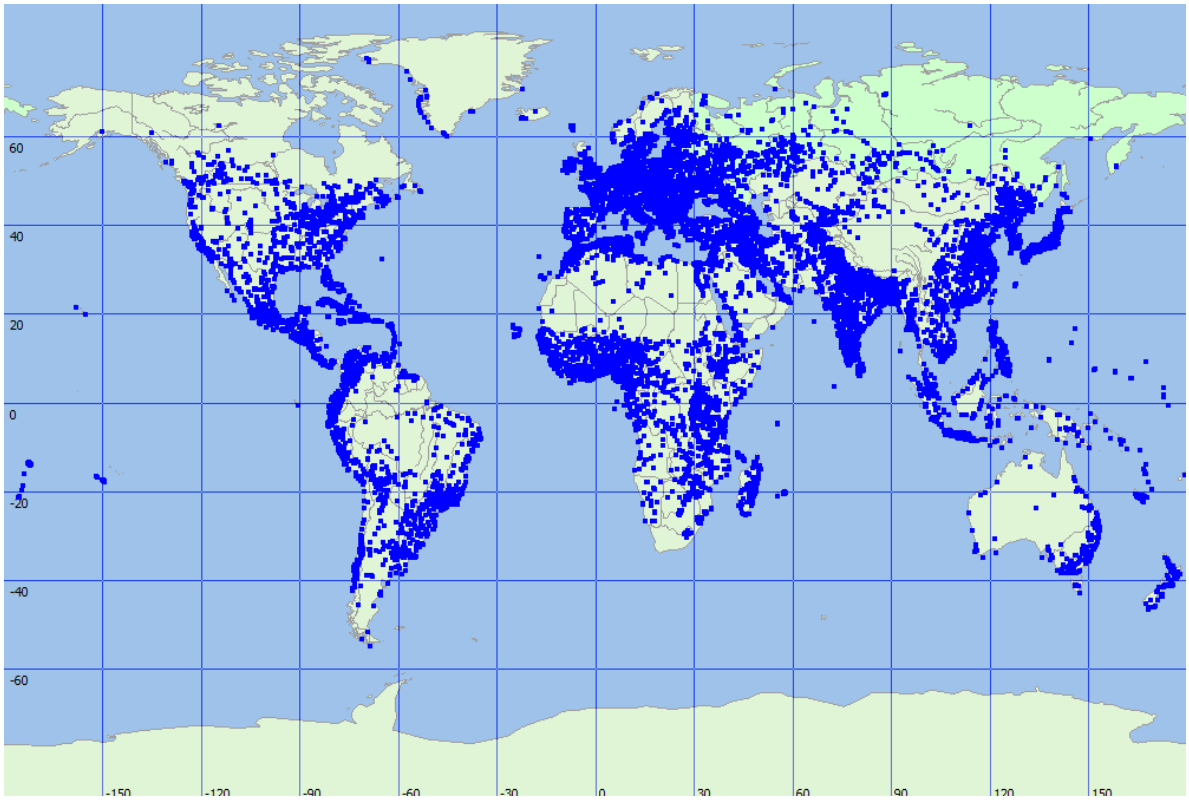

FIGURE 3

World location of the selected cities mostly representing land settlement density of the countries

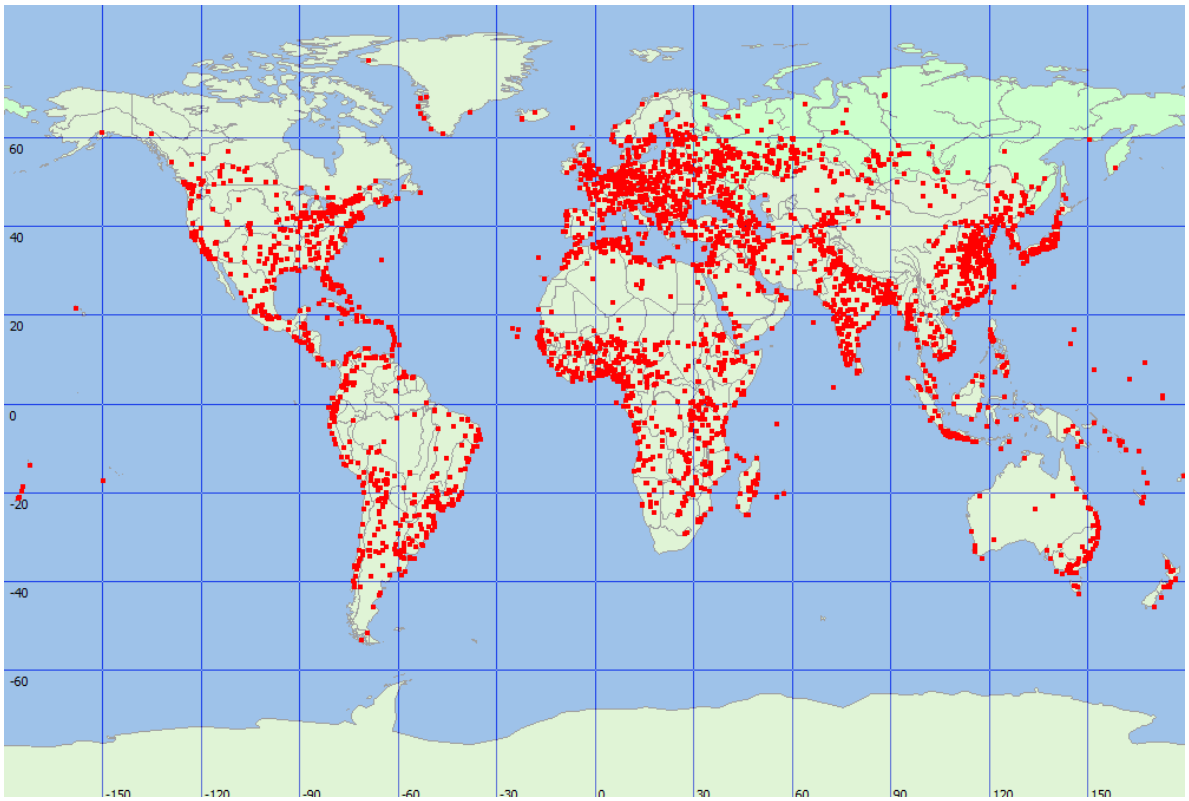

3.1.3 Indoor penetration loss values

Typical values for indoor base station penetration loss is described as 25 dB for the horizontal direction in the frequency band 5-6 GHz and for the vertical direction based on from Table 3 Recommendation ITU-R P.1238. Values for indoor penetration loss reflect values used for network planning based on practical experience.

In accordance with from Table 3 Recommendation ITU-R P.1238, the following values are relevant for vertical direction.

TABLE 2

Floor penetration loss factors, L_f (dB) with n being the number of floors penetrated, for indoor transmission loss calculation ($n \geq 1$)

Frequency	Residential	Office	Commercial
5.2 GHz	13[(1)] (apartment) 7[(2)] (house)	16 (1 floor)	–
5.8 GHz		22 (1 floor) 28 (2 floors)	

(1) Per concrete wall.

(2) Wooden mortar.

In addition Recommendation ITU-R P.1238 states that when the external paths are excluded, measurements at 5.2 GHz have shown that at normal incidence the mean additional loss due to a typical reinforced concrete floor with a suspended false ceiling is 20 dB, with a standard deviation of 1.5 dB. Lighting fixtures increased the mean loss to 30 dB, with a standard deviation of 3 dB, and air ducts under the floor increased the mean loss to 36 dB, with a standard deviation of 5 dB.

Another recommendation which is relevant for indoor penetration loss is Recommendation ITU-R P.1411 dealing with horizontal direction propagation. The experimental results provided in the recommendation and in shown in Table 3 were obtained at 5.2 GHz through an external building wall made of brick and concrete with glass windows. The wall thickness was 60 cm and the window-to-wall ratio was about 2:1.

TABLE 3

Example of building entry loss

Frequency	**Residential**		**Office**		**Commercial**	
	Mean	Standard deviation	Mean	Standard deviation	Mean	Standard deviation
5.2 GHz			12 dB	5 dB		

Table 4 copied from Recommendation ITU-R P.1411 shows the results of measurements at 5.2 GHz through an external wall made of stone blocks, at incident angles from 0° to 75°. The wall was 400 mm thick, with two layers of 100 mm thick blocks and loose fill between. Particularly at larger incident angles, the loss due to the wall was extremely sensitive to the position of the receiver, as evidenced by the large standard deviation.

TABLE 4

Loss due to stone block wall at various incident angles

Incident angle (degrees)	0	15	30	45	60	75
Loss due to wall (dB)	28	32	32	38	45	50
Standard deviation (dB)	4	3	3	5	6	5

In addition Recommendation ITU-R P.2041 suggests even higher value for indoor penetration loss for the frequency ranges above 5 GHz. Specifically most of the measurements results show that indoor penetration loss is usually in excess of 25 dB.

Taking into account that it is anticipated that the significant mobile data traffic demand will originate in dense urban areas indoors, most of small cells in the 5 925-6 425 MHz will be deployed in multi-storey buildings. In addition to significant vertical direction penetration loss due to several floors above majority of small cells, there would be additional clutter losses present outside the buildings in the case of vertical direction propagation of at least around 10-20 dBs.

As a result it is assumed that the 25 dB indoor penetration loss value provides a conservative value which could be used as a baseline for sharing and compatibility studies. The values 15 dB and 35 dB are used for a sensitivity analysis. The value 35 dB corresponds well to measurements results provided within Recommendation ITU-R P.2041 and 15 dB is taken as most conservative assumption for global average penetration loss value.

3.1.4 Omission of user terminals in interference calculation

It is assumed that the frequency band 5 925-6 425 MHz would be used as a separate level of coverage without macro cells, making the time division duplex more advantageous for such IMT systems. In this case in any moment of time either small cells or connected terminals will be transmitting. The Monte-Carlo based simulation with SEAMCAT[12] software showed that in case of isolated indoor cell with maximum e.i.r.p. of 23 dBm serving 3-6 mobile terminals also with maximum e.i.r.p. of 23 dBm the total interference from downlink (DL) and uplink (UL) observed in significant distance from this cell is practically the same with DL interference being higher for few dBs. The simulation scenario is illustrated in Fig. 4.

FIGURE 4

Simulation scenario description

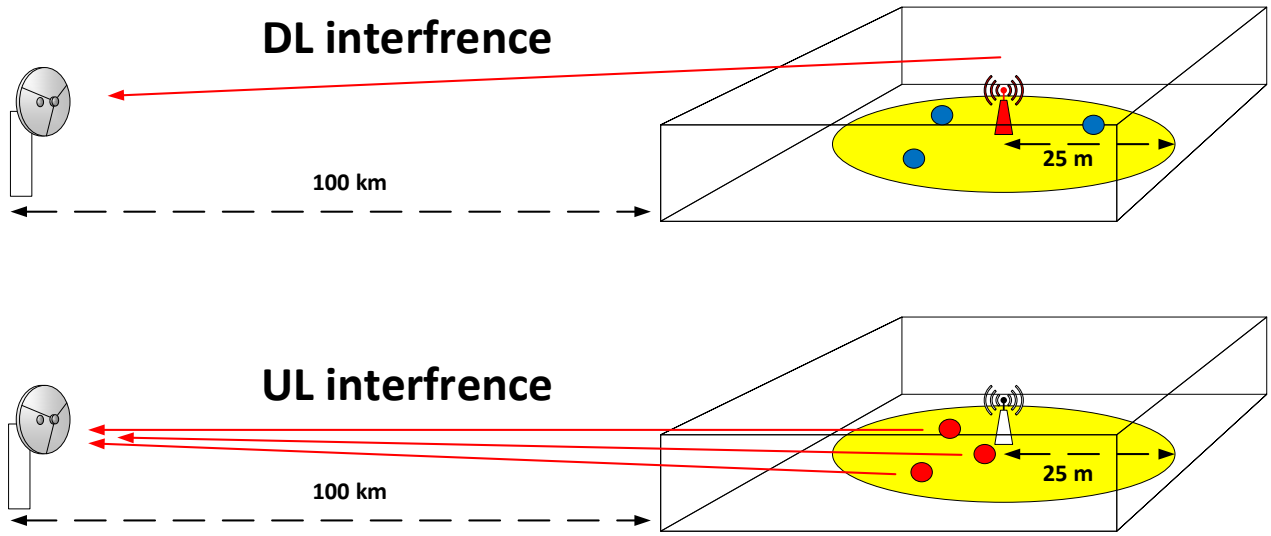

Such result is observed due to power control algorithm implemented in modern IMT systems in the uplink. In case of higher e.i.r.p. of small cell the difference between DL and UL interference will be only higher. Thus consideration of small cells transmitting 100% of time corresponds to worst case scenario.

3.2 FSS GSO networks characteristics

The GSO networks have been selected using the ITU BR data on frequency assignments to space radio services (SRS) with the following basic parameters: spacecraft orbital position, maximum beam gain and receiving system noise temperature. In particular, parameters of GSO satellite networks published in SRS data base in the IFIC No. 2734 of 11.12.2012 have been used.
The analysis has been performed for most of the beams recorded in the database with statistical representation of the results except the beams with antenna gain contours missing or other parameters recorded with errors. Characteristics of receiving antennas (gain contours on the Earth's surface) for GSO spacecraft, also published by ITU BR in SRS No. 2734, have been considered as well. Statistical data on satellite beams is provided in Figures 5-8.

[12] Spectrum Engineering Advanced Monte Carlo Analysis Tool (SEAMCAT) is a specialized software used for interference assessments which includes capability to model LTE cells based on the methodology very similar to 3GPP TR 36.942.

FIGURE 5

Satellite orbital position

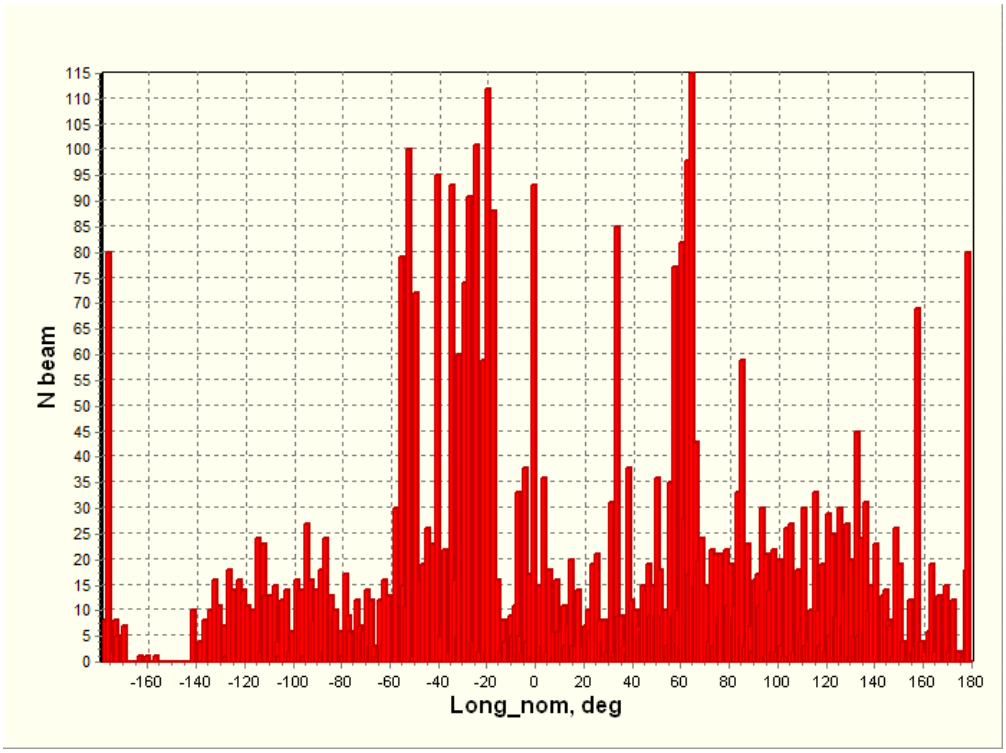

FIGURE 6

Satellite maximum receive gain

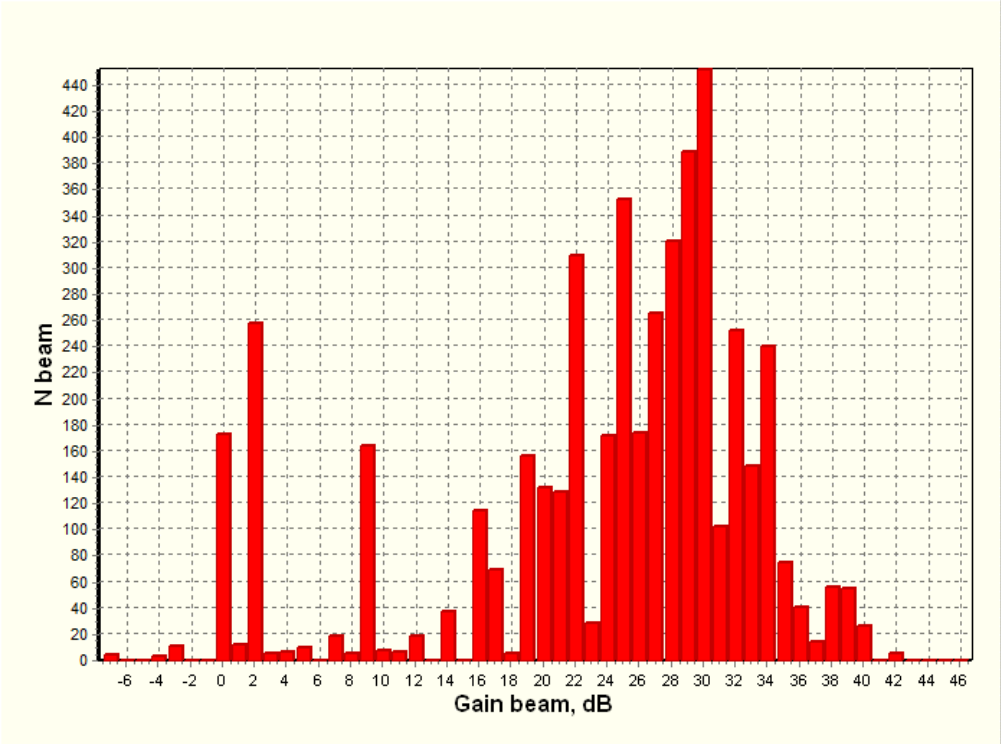

FIGURE 7

Satellite receiving system noise temperature

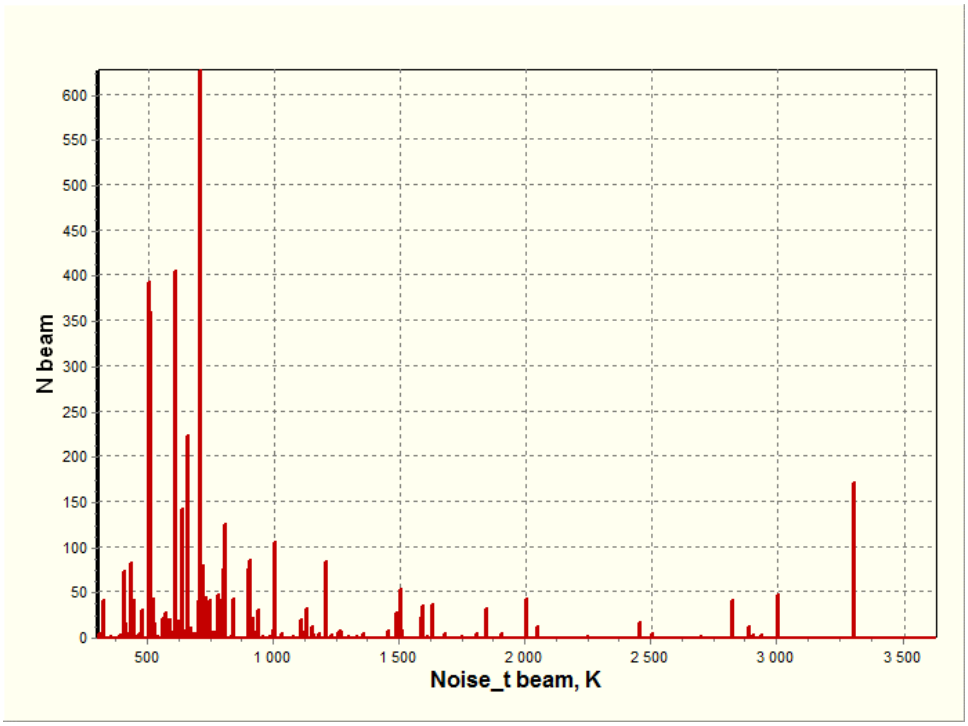

FIGURE 8

Satellite coverage area (approximate)

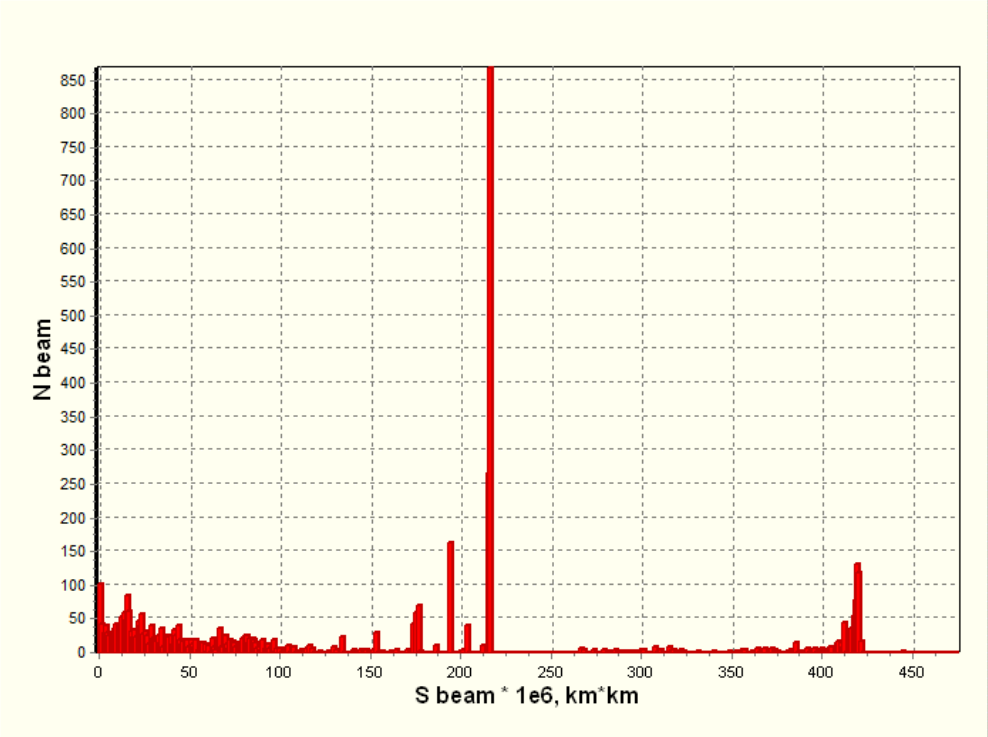

As a criterion of noise impact on the GSO FSS space stations, Recommendation ITU-R S.1432-1 specifies the threshold for allowable increase in noise temperature, ΔT/T, for FSS systems operating below 30 GHz, that accounts for 6%, in the case of interference caused by systems operating in the same band on a primary basis. The criterion perfectly suits to assess the aggregate impact of the IMT base stations on the GSO spacecraft receivers.

3.3 FSS NGSO networks characteristics

The NGSO networks were also selected using the ITU BR data on frequency assignments to SRS, including the following basic parameters: satellite orbit (apogee, perigee, inclination, perigee argument, ascending node and phase angle of spacecraft), maximum beam gain and receiving system noise temperature. In particular, data on the NGSO satellite networks published in SRS No. 2734 of 11.12.2012 were used.

List of selected NGSO satellite networks and their basic characteristics are given in Table 5 NGSO satellite trajectory footprint on the Earth's surface and an instant service area footprint are shown in Appendix 2.

TABLE 5

List of 5/6 GHz NGSO satellite networks and their basic characteristics

Satellite	Satellite orbital position						Beam	Satellite Maximum Receive Gain (dBi)	Satellite Receiving System Noise Temperature (K)
	Apogee (km)	Perigee (km)	Inclination (deg)	Perigee argument (deg)	Longitude (deg)	Phase (deg)			
MOLNIA-1	40000	500	65	–	–	–	R1	18	2500
MOLNIA-2	40000	500	63	–	–	–	R1	17	3000
MOLNIA-3	40000	500	63	–	–	–	R1	17.3	3000
USASAT-28C	47103	24469	63.4	270	–	0	OM1	3	630
OSAT	49278	22294	52	–	–	–	CRR	30	494
INSAT-NAV-A-GS	35790	35790	29	–	–	–	RTC	–3	1000
INSAT-NAVR-GS	35786	35786	29	–	–	–	RTC	–3	1000

In the case of NGSO spacecraft, the Recommendation ITU-R S.1432-1 specifies that the permissible long-term total noise temperature increase of 6% shall not be exceeded more than 20% of any month. Moreover, short-term total noise temperature increase due to impact of IMT devices on NGSO spacecraft receiver shall not exceed 57.5% (I/N = –2.4 dB) for 0.03% of any month, and 100% (I/N = 0 dB) for 0.005% of any month. These ΔT/T limits are shown as a diagram in Figure 9.

FIGURE 9

Threshold values for permissible increase of noise temperature for FSS NGSO SC due to interference effect

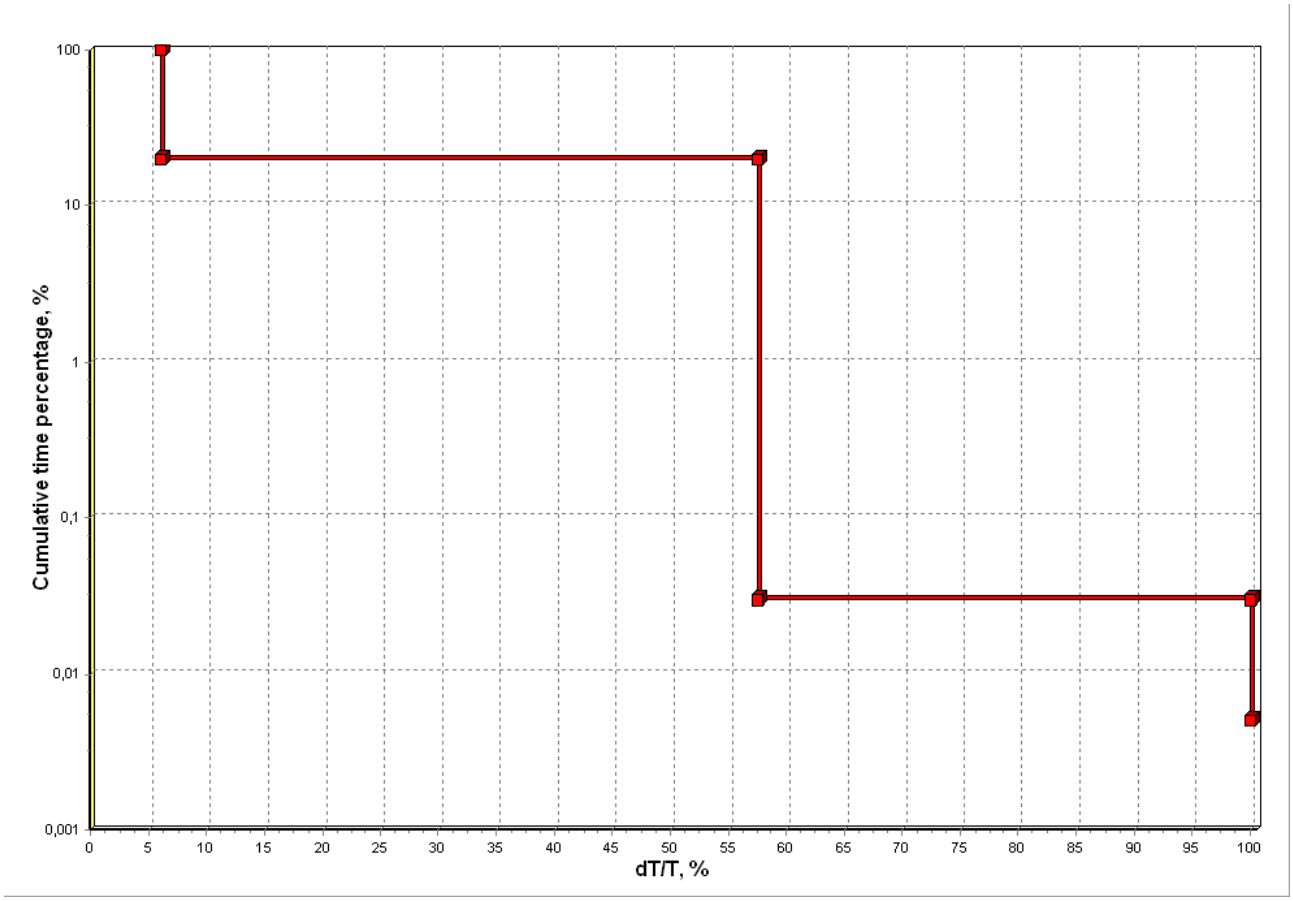

4 Analysis

4.1 Impact on FSS GSO networks

4.1.1 Assumptions

Basic assumptions refer to a number and density of IMT base stations. These assumptions are described in detail in Section 3.1. IMT base stations are assumed to be operating with omnidirectional antennae which have e.i.r.p. 15 dBm or 24 dBm with channel bandwidth of 20 MHz. For indoor signal attenuation three values are considered 15 dB, 25 dB and 35 dB. The percentage of indoor IMT systems has been fixed to 95% to account possible indoor installations without or with minimal indoor penetration loss. This is based on the result of preliminary study which has shown that sharing is only feasible for indoor deployment with limited e.i.r.p. It should be noted that results obtained with such percentage are somewhat conservative and will provide substantial margin in case of other assumptions such as small cell dissemination rate had been underestimated.

A total number of IMT base stations will supposedly be proportional to the world population and a number of IMT base stations for each city will be determined by dissemination factor $K_{\text{DISSEMINATION}}$ of IMT base stations as a percentage of the city population M_{CITY}, IMT base station activity factor K_{ACTIVE} and usage factor $K_{\Delta f}$ of the frequency band 5 925-6 425 MHz use by IMT base stations.

The dissemination factor for IMT base stations servicing small cells in the 5 925-6 425 MHz frequency band, expressed as percentage of the population, is specified to be 1%, 3% or 6%, activity factor for IMT base stations will be 20%, and 5 925-6 425 MHz frequency band usage factor will be 4%, with 20 MHz channel bandwidth.

4.1.2 Methodology

4.1.2.1 Interference from single source

Taking into account that interference from IMT systems is equivalent to thermal noise, the equation to calculate increase ΔT_{SAT1} from single IMT station will be as follows:

$$\Delta T_{SAT1} = \frac{\frac{e.i.r.p._{IMT} \cdot G_{INDOOR}}{\Delta f_{IMT}} \cdot G_{SAT}}{k \cdot 10^{\frac{L_{fsl}+L_{amm}}{10}}}, \quad (1)$$

where:

$e.i.r.p._{IMT}$ – e.i.r.p. of IMT transmitter located within the FSS spacecraft service area, W;

G_{INDOOR} – indoor attenuation factor at the IMT base station location;

Δf_{IMT} – IMT channel bandwidth, Hz;

G_{SAT} – receive satellite antenna gain towards interfering IMT transmitter;

k – Boltzmann constant ($k = 1.38 \cdot 10^{-23} J/K$);

$L_{fsl} = 32.4 + 20\lg(R \cdot f)$ – free-space loss determined according to the Rec. ITU-R P.525-2, dB;

R – Distance between IMT station and GSO (NGSO) spacecraft, km;

f – Operational frequency of IMT transmitter, MHz;

L_{atm} – Atmospheric loss, dB:

$$L_{atm} = \begin{cases} \frac{\left(\gamma_0 \sqrt{H_0} F\left(tg(\beta)\sqrt{R_e/H_0}\right) + \gamma_w \sqrt{H_w} F\left(tg(\beta)\sqrt{R_e/H_w}\right)\right)\sqrt{R_e}}{\cos(\beta)} & for \quad \beta \le 10^\circ \\ \frac{H_0 \cdot \gamma_0 + H_w \cdot \gamma_w}{\sin(\beta)} & for \quad \beta > 10^\circ \end{cases};$$

$\gamma_0 = \left(\frac{7.27}{f^2 + 0.351} + \frac{7.5}{(f-57)^2 + 2.44} \right) \cdot f^2 \cdot 10^{-3}$ – attenuation due to absorption by oxygen;

H_0 – Height for oxygen (H_0 =6 km);

β – Elevation angle of IMT transmitter towards SC, deg;

R_e – Earth radius, taking into account atmospheric refraction (R_e =8 500 km);

$\gamma_w = \gamma_{w1} + \gamma_{w2}$ – Attenuation due to absorption by hydrogen;

$$\gamma_{w1} = 3.27 \cdot 10^{-2} + 1.67 \cdot 10^{-3} \rho + 7.7 \cdot 10^{-4} \sqrt{f} + \frac{3.79}{(f-22.235)^2 + 9.81};$$

$$\gamma_{w2} = \left(\frac{11.73}{(f-183.31)^2 + 11{,}85} + \frac{4.01}{(f-325.153)^2 + 10.44} \right) \cdot \rho \cdot 10^{-4};$$

ρ – atmospheric density (ρ =7.5 g/m^3);

$$H_w = H_{w0}\left(1+\frac{3}{(f-22.2)^2+5}+\frac{5}{(f-183.3)^2+6}+\frac{2.5}{(f-325.4)^2+4}\right)$$ – height for hydrogen (H_{w0} =1.6 km);

f – Operational frequency of IMT transmitter, GHz;

$$F(x)=\frac{1}{0.661\cdot x+0.339\sqrt{x^2+5.51}}.$$

4.1.2.2 Aggregated interference

In the case under consideration, ΔT_{SAT} is a total interference impact on the FSS satellite link from IMT base stations deployed worldwide. Therefore to calculate increase in noise temperature, one must know the number of IMT base stations simultaneously interfering with GSO (NGSO) spacecraft, and take into account their localization.

The calculation is initiated by deriving the satellite position at GSO from the longitude of its sub-satellite point. For each city, according to its geographical coordinates, the following parameters are calculated: elevation angle towards the satellite, satellite receiving antenna gain G_{SAT} towards interfering IMT transmitter and signal propagation losses L_{fsl} and L_{atm}. The G_{SAT} value for GSO spacecraft is determined based on the performance of its receiving antenna (gain contours on the Earth's surface) published by the ITU in the BR IFIC on satellite networks, taking into account geographical coordinates of interfering IMT transmitter.

Next, the number of IMT transmitters is predicted for each city using the following equation:

$$N_{IMT} = M_{CITY} K_{\text{DISSEMINATION}} K_{\text{ACTIVE}} K_{\Delta f} \tag{2}$$

and having calculated ΔT_{SAT1} from one IMT transmitter using equation (1), the increase in noise temperature from each city is determined by the formula $\Delta T_{CITY} = N_{IMT}\Delta T_{SAT1}$. For more accurate calculation of ΔT_{CITY} it is assumed that some of IMT base stations may be located outdoor (K_{INDOOR} – percentage of indoor IMT base stations). Taking into account (1), equations for increase in noise temperature due to a single IMT transmitter and from one city take the following forms:

$$\Delta T_{SAT1} = \frac{e.i.r.p._{IMT}\left(G_{INDOOR}\,K_{INDOOR}/100+(1-K_{INDOOR}/100)\right)\cdot G_{SAT}/\Delta f_{IMT}}{k\cdot 10^{\frac{L_{fsl}+L_{atm}}{10}}}; \tag{3}$$

$$\Delta T_{CITY} = N_{IMT}\,\frac{e.i.r.p._{IMT}\left(G_{INDOOR}\,K_{INDOOR}/100+(1-K_{INDOOR}/100)\right)\cdot G_{SAT}/\Delta f_{IMT}}{k\cdot 10^{\frac{L_{fsl}+L_{atm}}{10}}}. \tag{4}$$

Values obtained for each city using equation (4) are added together and resulted in relative increase in noise temperature as follows:

$$\Delta T/T = {\sum_{N_{CITY}} \Delta T_{CITY}} \Big/ T_{NOISE}, \tag{5}$$

where:

N_{CITY} - Number of selected cities in the world;

T_{NOISE} - Noise temperature of the spacecraft receiving system, *K*.

4.1.3 Example of calculations

As an example let us consider the interference impact from IMT systems towards Statsionar–20 geostationary network (№90500256, SRS No. 2734 of 11.12.2012) with the longitude of the sub-satellite point 70° East. Initial data for the calculations are shown in Table 6.

TABLE 6

Initial data for IMT system and GSO network

Parameter		Value
IMT		
Maximum e.i.r.p., dBm	$EIRP_{IMT}$	24
Channel bandwidth, MHz	Δf_{IMT}	20 MHz
Antenna		Isotropic
Percent of indoor cells, %	K_{INDOOR}	95
Indoor-to-outdoor penetration losses, dB	G_{INDOOR}	15
IMT base station dissemination factor	$K_{\mathrm{DISSEMINATION}}$	0.06
IMT base station activity factor	K_{ACTIVE}	0.04
Usage factor for 5 925-6 425 MHz frequency band	$K_{\Delta \mathrm{f}}$	0.2
STATSIONAR-20		
Noise temperature, *K*	T_{NOISE}	3 000

Figure 10 shows visibility area of the STATSIONAR-20 geostationary network and cities covered by this visibility area. As the Figure 10 shows, significant number of cities (more than 3 700) in different countries is in the visibility area of this GSO spacecraft. In order to demonstrate operational capability of the proposed methodology, it was assumed to consider only one largest city of each country, but its population is assumed to be equal to the population of the whole country. Under such approach, there will be inaccuracy in calculation of ΔT/T, however its order of magnitude will remain the same, as calculation showed.

FIGURE 10

Visibility area of the STATSIONAR-20 geostationary network

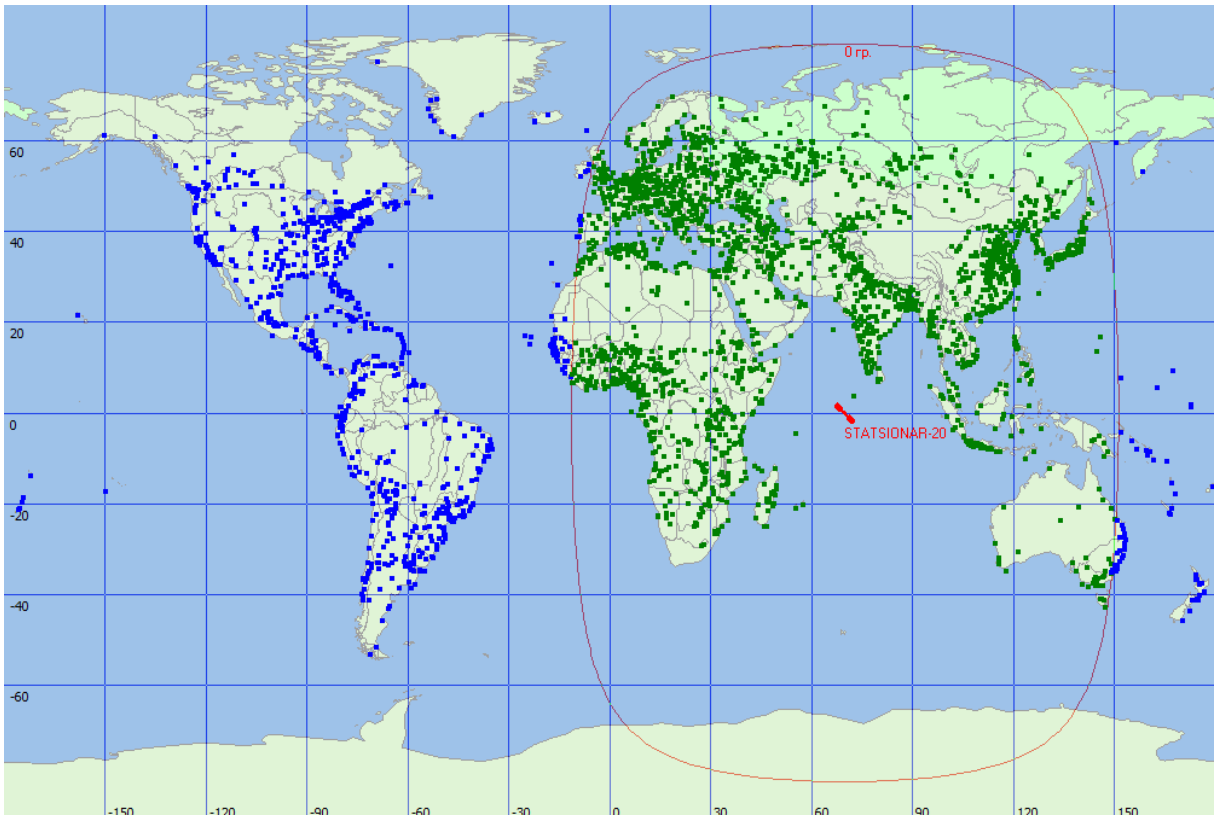

According to the methodology in section 4.1.2.2, the calculation is initiated by deriving the satellite position at GSO from the longitude of its sub-satellite point, and after that for each city, according to its geographical coordinates (geographical latitude φ_{IMT} and longitude λ_{IMT}, and height above sea level), the following parameters are calculated: elevation angle β_{SAT} and distance D_{SAT} towards the satellite, satellite receiving antenna gain G_{SAT} towards interfering IMT transmitter and signal propagation losses L_{fsl} and L_{atm}. The G_{SAT} value for GSO spacecraft is determined based on the performance of the STATSIONAR-20 receiving antenna, published in SRS No. 2734 of 11.12.2012 (Figure 11).

FIGURE 11

Gain contours of the STATSIONAR-20 geostationary network on the Earth's surface

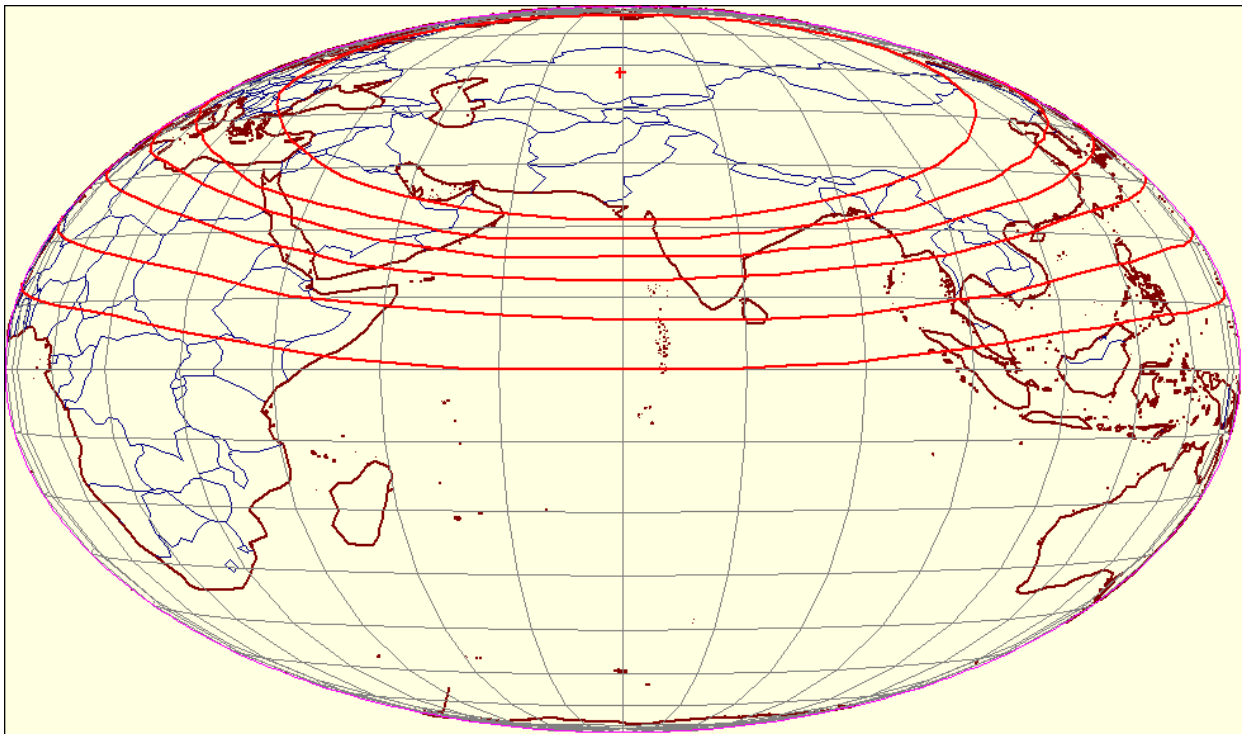

The number of IMT transmitters is predicted for each city using the equation (2):

$$N_{IMT} = M_{CITY} K_{\text{DISSEMINATION}} K_{\text{ACTIVE}} K_{\Delta f} = M_{CITY} \cdot 0.06 \cdot 0.2 \cdot 0.04 = 0.00048 \cdot M_{CITY},$$

then ΔT_{SAT1} from a single IMT transmitter and ΔT_{CITY} from each city are calculated using equations (3) and (4) accordingly. A list of modelled cities and results for increase in noise temperature ΔT_{CITY} from them towards the STATSIONAR-20 geostationary network are summarized in Table 7.

Table 7 shows that the total increase in noise temperature from all the cities is $\sum_{N_{CITY}} \Delta T_{CITY} = 50.71513436\ K.$

Relative increase in noise temperature is calculated using the equation (5):

$$\Delta T / T = \sum_{N_{CITY}} \Delta T_{CITY} \Big/ T_{NOISE} = \frac{50.71513436\ \text{K}}{3000\ \text{K}} \cdot 100\% = 1.690504479\ \%,$$

that is practically the same as the value 1.659751% for the STATSIONAR-20 geostationary network, accurately calculated for all modelled cities within the visibility area of the network as per Figure 11.

TABLE 7

Calculation of increase in noise temperature due to IMT operation towards STATSIONAR-20 network

Country	**City**	**Population**	N_{IMT}	φ_{IMT}, **deg**	λ_{IMT}, **deg**	D_{SAT}, **km**	β_{SAT}, **deg**	L_{fsl}, **dB**	L_{atm}, **dB**	G_{SAT}, **dB**	ΔT_{SAT1}, ***K***	ΔT_{CITY}, ***K***
Austria	Wien	8452835	10143	48.2	16.4	40068.9	14.9	200.17	0.18	-0.23	3.0445E-05	0.123515201
Azerbaijan	Baku	9235100	11082	40.5	50	37867.5	38.9	199.68	0.07	-1.57	3.34069E-05	0.148092964
Albania	Tirana	2831741	3398	41.4	19.8	39494.1	20.6	200.04	0.13	-0.44	2.88397E-05	0.039193212
Algeria	Algiers	36485828	43783	36.9	3.1	40614.6	9.8	200.28	0.27	-0.1	1.98445E-05	0.347536715
Angola	Luanda	20162516	24195	–8.9	13.2	39075.2	24.9	199.95	0.11	-0.64	4.91781E-07	0.004759458
Andorra	Andorra La Vella	78115	94	42.5	1.5	40896.8	7.2	200.34	0.36	-0.05	2.22022E-05	0.000821483
Armenia	Yerevan	3277500	3933	40.3	44.6	38047.9	36.6	199.72	0.08	-1.39	3.25744E-05	0.051239495
Afghanistan	Kabul	33397058	40076	34.5	69.3	37082.9	49.9	199.49	0.06	-2.58	2.89307E-05	0.463787367
Bangladesh	Dhaka	152518016	183022	23.8	90.5	36842.2	53.9	199.44	0.06	-3.01	1.89859E-05	1.389939913
Bahrain	Al Manamah	1234571	1481	26.3	50.7	36919.9	52.6	199.46	0.06	-2.86	2.17226E-05	0.012881525
Belarus	Minsk	9460000	11352	54	27.6	39812.8	17.4	200.11	0.16	-0.31	3.33515E-05	0.151449187
Belgium	Brussels	11041266	13250	51	4.5	40959.4	6.6	200.36	0.39	-0.05	2.74923E-05	0.145709089
Benin	Cotonou	9351838	11222	6.5	2.6	40160.4	14.1	200.19	0.19	-0.2	5.05644E-07	0.002269836
Burma	Dagon	50020000	60024	16.9	96.2	36832.1	54.1	199.44	0.06	-3.03	9.5012E-06	0.22812386
Bulgaria	Sofia	7364570	8837	42.8	23.3	39339	22.2	200.01	0.12	-0.51	3.09382E-05	0.109366514
Bosnia and Herzegovina	Bosna-sarai	3839737	4608	43.8	18.5	39704.9	18.5	200.09	0.15	-0.35	2.97063E-05	0.054748789
Botswana	Gaborone	2053237	2464	–24.8	26	38298.7	33.6	199.77	0.08	-1.17	4.56534E-07	0.000450143
Brunei	Bandar Seri Begawan	412892	495	5	115.1	37947	37.9	199.69	0.08	-1.49	4.33111E-07	8.5756E-05
Burkina Faso	Ouagadouga	17481984	20978	12.4	358.4	40647.2	9.5	200.29	0.28	-0.09	5.9097E-07	0.004958833
Burundi	Cibitoke	8749387	10499	–3.4	29.4	37558.4	42.9	199.61	0.07	-1.91	4.01569E-07	0.001686588
Bhutan	Thimphu	750443	901	27.6	89.8	37010	51	199.48	0.06	-2.7	2.29704E-05	0.008269343
Hungary	Budapest	9962000	11954	47.5	19.2	39853.3	17	200.12	0.16	-0.3	3.19306E-05	0.152691899
East Timor	Dili	1066409	1280	–8.8	126.2	39018.1	25.5	199.94	0.11	-0.68	4.89907E-07	0.000250832
Vietnam	Ho Chi Minh City	90549392	108659	10.8	106.7	37343.3	46	199.56	0.06	-2.19	2.89444E-06	0.125803988

Country	**City**	**Population**	N_{IMT}	φ_{IMT}, **deg**	λ_{IMT}, **deg**	D_{SAT}, **km**	β_{SAT}, **deg**	L_{fsl}, **dB**	L_{atm}, **dB**	G_{SAT}, **dB**	ΔT_{SAT1}, ***K***	ΔT_{CITY}, ***K***
Gabon	Libreville	1563873	1877	0.5	9.6	39401.8	21.5	200.02	0.13	-0.48	5.00334E-07	0.000375751
Ghana	Accra	25545940	30655	5.7	359.8	40458.7	11.2	200.25	0.24	-0.13	9.21587E-07	0.011300504
Germany	Berlin	81843808	98213	52.5	13.4	40470.7	11.1	200.25	0.24	-0.13	3.02837E-05	1.189693432
Guernsey	St.Peter Port	61811	74	49.5	357.3	41399.5	2.8	200.45	0.8	-0.01	2.118E-05	0.000635399
Gibraltar	Gibraltar	29441	35	36.1	354.6	41329	3.4	200.44	0.69	-0.01	1.49196E-05	0.000208874
Hong Kong	Hong Kong	7136300	8564	22.4	114.2	38230.3	34.4	199.76	0.08	-1.23	1.19374E-05	0.040885629
Greece	Athens	11290785	13549	38.1	23.9	39050.3	25.2	199.94	0.11	-0.66	2.79537E-05	0.151509289
Georgia	Tbilisi	4497600	5397	41.8	44.9	38148.3	35.4	199.74	0.08	-1.3	3.35376E-05	0.072407606
Guam	Hagatha	184334	221	13.5	144.8	40998.2	6.3	200.37	0.41	-0.04	7.46823E-07	6.57204E-05
Denmark	Copenhagen	5580516	6697	55.7	12.7	40669.4	9.3	200.3	0.28	-0.09	3.05594E-05	0.081868559
Djibouti	Jibuti	922708	1107	11.7	43.3	36714.8	56.2	199.41	0.06	-3.27	4.08964E-06	0.001811712
Egypt	Al Qahirah	83063000	99676	30	31.2	38147.1	35.4	199.74	0.08	-1.3	2.35621E-05	0.93942079
Zambia	Lusaka	13883577	16660	–15.4	28.4	37819.6	39.5	199.67	0.07	-1.61	4.23558E-07	0.002822593
Zimbabwe	Harare	13013678	15616	–17.8	31.1	37676.4	41.3	199.63	0.07	-1.77	4.11912E-07	0.002573213
Yemen	Sanaa	25569264	30683	15.4	44.3	36758.1	55.4	199.42	0.06	-3.18	7.89068E-06	0.096842255
Israel	Jerusalem	7836000	9403	31.9	35.3	37982	37.4	199.7	0.08	-1.45	2.62153E-05	0.09859566
India	Bombay	1229582976	1475500	19	72.9	36203.9	67.4	199.29	0.05	-4.71	1.2182E-05	7.189806958
Indonesia	Medan	245641328	294770	3.7	98.7	36708.2	56.3	199.41	0.06	-3.29	4.21781E-07	0.049731384
Jordan	Amman	6390500	7669	32.1	36.1	37949.5	37.8	199.7	0.08	-1.48	2.66119E-05	0.081618692
Iraq	Baghdad	33703068	40444	33.4	44.5	37590.2	42.5	199.61	0.07	-1.87	2.7758E-05	0.449040503
Iran	Tehran	77002704	92403	35.7	51.5	37472.5	44.1	199.59	0.07	-2.02	2.97196E-05	1.098465649
Spain	Madrid	46163116	55396	40.5	356.2	41281.6	3.8	200.43	0.63	-0.01	1.79821E-05	0.398448066
Italy	Rome	60820764	72985	42	12.6	40034	15.3	200.16	0.18	-0.24	2.68832E-05	0.784828385
Kazakhstan	Almaty	16856000	20227	43.2	76.9	37807.3	39.6	199.66	0.07	-1.63	3.8338E-05	0.310192549
Cambodia	Phnom Penh	14478320	17374	11.6	104.9	37232.9	47.6	199.53	0.06	-2.35	3.9229E-06	0.027264161
Cameroon	Douala	20468944	24563	4.1	9.9	39384.3	21.7	200.02	0.13	-0.49	4.99969E-07	0.004912193
Qatar	Doha	1699435	2039	25.3	51.7	36835.4	54	199.44	0.06	-3.02	2.0804E-05	0.016976105
Kenia	Nairobi	42749416	51299	–1.4	36.8	36990.4	51.4	199.47	0.06	-2.74	3.43042E-07	0.007039231
Cyprus	Lemesos	862011	1034	34.8	33.2	38268.6	33.9	199.77	0.08	-1.19	2.86859E-05	0.011875943
China	Beijing Shi	1355719936	1626864	40	116.4	39170.9	23.9	199.97	0.11	-0.59	2.97557E-05	19.36342634
Comoro Islands	Moroni	753943	905	–11.7	43.3	36714.5	56.2	199.41	0.06	-3.27	3.08006E-07	0.000111498

Country	**City**	**Population**	N_{IMT}	φ_{IMT} , **deg**	λ_{IMT} , **deg**	D_{SAT} , **km**	β_{SAT} , **deg**	L_{fsl} , **dB**	L_{atm} , **dB**	G_{SAT} , **dB**	ΔT_{SAT1} ,***K***	ΔT_{CITY} ,***K***
DRC	Kinshasa	69575392	83490	–4.4	15.3	38837.4	27.5	199.9	0.1	-0.78	4.83248E-07	0.016138558
The Republic of Congo	Brazzaville	4233063	5080	–4.3	15.3	38837.1	27.5	199.9	0.1	-0.78	4.83236E-07	0.000981935
North Korea	Pyongyang	0	0	39	125.8	39790.9	17.6	200.11	0.15	-0.32	2.5712E-05	0.303041845
South Korea	Seoul	48580000	58296	37.7	127	39829.4	17.3	200.11	0.16	-0.31	2.40905E-05	0.561741779
Cote-d'Ivoire	Abidjan	20594616	24714	5.4	355.9	40885	7.3	200.34	0.35	-0.06	9.21E-07	0.009104086
Kuwait	Al Kuwait	2891553	3470	29.4	48.1	37197.3	48.1	199.52	0.06	-2.4	2.45345E-05	0.034053875
Kirgizstan	Bishkek	5477600	6573	42.9	74.6	37759.1	40.3	199.65	0.07	-1.68	3.84924E-05	0.101196445
Laos	Nakhon Viangchan	6348800	7619	18	102.8	37256.7	47.3	199.54	0.06	-2.31	9.76414E-06	0.029751346
Latvia	Riga	2049500	2459	57	24.1	40174	13.9	200.19	0.19	-0.2	3.24542E-05	0.03193494
Lesoto	Maseru	2216850	2660	–29.3	27.6	38362.8	32.8	199.79	0.09	-1.12	4.60312E-07	0.000489772
Liberia	Monrovia	3476608	4172	6.4	349.2	41628.2	0.9	200.5	1.48	0	6.72836E-07	0.001122963
Lebanon	Beirut	4291719	5150	33.9	35.6	38079.3	36.2	199.72	0.08	-1.36	2.80768E-05	0.057838299
Libya	Tripoli	6469497	7763	33	13.3	39628.4	19.3	200.07	0.14	-0.38	2.00947E-05	0.062394097
Lithuania	Vilnius	2988400	3586	54.8	25.3	39973	15.9	200.15	0.17	-0.26	3.29151E-05	0.047200185
Liechtenstein	Vaduz	36476	44	47.2	9.5	40469.1	11.1	200.25	0.24	-0.13	2.76654E-05	0.000497978
Luxemburg	Luxemburg	524853	630	49.7	6.2	40794.7	8.1	200.32	0.32	-0.07	2.7624E-05	0.006961249
Mauritius	Port Louis	1280294	1536	–20.3	57.6	36408.6	62.4	199.34	0.05	-4.03	2.63081E-07	0.000161795
Madagaskar	Antananarivo	21928518	26314	–18.9	47.5	36718	56.1	199.41	0.06	-3.26	3.08653E-07	0.003248882
Mayotte	Mamoudzou	217172	261	–12.9	45.3	36633.2	57.7	199.39	0.06	-3.45	2.9685E-07	3.08724E-05
Macao	Macau	542200	651	22.3	113.6	38183.9	35	199.75	0.08	-1.27	1.18797E-05	0.003088733
Macedonia	Skopje	2057284	2469	42	21.6	39406.4	21.5	200.02	0.13	-0.48	2.97951E-05	0.029407773
Malawi	Lilongwe	15882815	19059	–14.1	33.9	37372.3	45.5	199.56	0.07	-2.15	3.8413E-07	0.002928607
Malaysia	Kuala Lumpur	29562236	35475	3.2	101.7	36898.3	52.9	199.45	0.06	-2.9	3.31725E-07	0.004707173
Mali	Bamako	14517176	17421	12.6	352	41338.2	3.3	200.44	0.71	-0.01	4.43389E-07	0.003089535
Maldives	Male	324313	389	3.6	72.9	35810.1	84.6	199.19	0.05	-7.42	4.17527E-07	6.51343E-05
Malta	Birkirkara	420085	504	36	14.6	39640.4	19.1	200.07	0.14	-0.38	2.34172E-05	0.004730268
Marocco	Casablanca	32783000	39340	33.7	352.2	41510	1.9	200.47	1.05	0	1.02295E-05	0.160971151
Mozambique	Maputo	23700716	28441	–26.1	32.6	37873.4	38.8	199.68	0.07	-1.56	4.27608E-07	0.004864466
Moldova	Chisinau	3559500	4271	47.1	28.9	39267.5	22.9	199.99	0.12	-0.54	3.32861E-05	0.056885914

Country	**City**	**Population**	N_{IMT}	φ_{IMT}, **deg**	λ_{IMT}, **deg**	D_{SAT}, **km**	β_{SAT}, **deg**	L_{fsl}, **dB**	L_{atm}, **dB**	G_{SAT}, **dB**	ΔT_{SAT1}, ***K***	ΔT_{CITY}, ***K***
Monaco	Monaco	35444	43	43.7	7.4	40485.4	11	200.26	0.24	-0.13	2.58484E-05	0.000439423
Mongolia	Da Huryee	2736800	3284	47.9	106.9	39114.6	24.5	199.96	0.11	-0.62	3.39836E-05	0.044654403
Namibia	Windhoek	2364433	2837	–22.6	17.1	38970.7	26	199.93	0.11	-0.7	4.88369E-07	0.000554299
Nepal	Katmandu	31011136	37213	27.7	85.3	36866	53.5	199.44	0.06	-2.96	2.24387E-05	0.333999907
Niger	Niamey	16644339	19973	13.7	1.9	40284.6	12.9	200.21	0.21	-0.17	9.64053E-07	0.007701823
Nigeria	Lagos	166629376	199955	6.5	3.5	40061.5	15	200.17	0.18	-0.23	5.0619E-07	0.040486096
The Netherlands	Amsterdam	16804900	20166	52.3	4.9	40982.7	6.4	200.36	0.4	-0.04	2.82564E-05	0.227916173
Norway	Oslo	5049100	6059	59.9	10.8	40989.6	6.4	200.36	0.4	-0.04	2.98171E-05	0.072276672
UAE	Dubayy	4800250	5760	25.3	55.4	36711.6	56.2	199.41	0.06	-3.28	2.01982E-05	0.046536687
Oman	As Sib	2773479	3328	23.8	58.3	36558.3	59.2	199.37	0.05	-3.63	1.85913E-05	0.024745058
Isle of Man	Doolish	83739	100	54.3	355.4	41646.3	0.8	200.5	1.56	0	1.67971E-05	0.000671883
Pakistan	Karachi	177791008	213349	24.9	67.2	36483.4	60.8	199.35	0.05	-3.83	1.8736E-05	1.598932339
Papua New Guinea	Port Moresby	7170112	8604	–9.6	147.3	41245.6	4.1	200.42	0.59	-0.02	4.56663E-07	0.001571834
Poland	Warsaw	38208616	45850	52.2	21	40025.8	15.4	200.16	0.18	-0.24	3.23287E-05	0.592909075
Puerto Rico	San Juan	3725789	4471	18.2	66.6	36173.5	68.3	199.28	0.05	-4.83	1.11282E-05	0.019897281
Reunion	Saint-Denis	816364	980	–21.2	55.7	36506.7	60.3	199.36	0.05	-3.76	2.78326E-07	0.000109104
Russian Federation	Moscow	143302400	171963	55.8	37.8	39525.4	20.3	200.05	0.13	-0.43	3.46433E-05	2.382937342
Rwanda	Kigali	10718379	12862	–2	30.2	37490.5	43.9	199.59	0.07	-1.99	3.95477E-07	0.002034727
Romania	Bucuresti	21355848	25627	44.6	26.1	39270.1	22.9	199.99	0.12	-0.54	3.21841E-05	0.329919245
San Marino	San Marino	31945	38	44	12.6	40121.2	14.4	200.18	0.19	-0.22	2.76689E-05	0.000415034
Sao Tome and Principe	Sao Tome	171878	206	0.2	6.7	39701.5	18.5	200.09	0.15	-0.36	5.04949E-07	4.19108E-05
Saudi Arabia	Riyadh	28705132	34446	24.7	46.8	37002.2	51.2	199.48	0.06	-2.72	2.0009E-05	0.27568413
Swaziland	Manzini	1220408	1464	–26.6	31.4	37983	37.4	199.7	0.08	-1.45	4.35759E-07	0.000255355
North Mariana Islands	Saipan	62152	75	16.8	145.9	41139.1	5	200.4	0.5	-0.03	1.5758E-06	4.7274E-05
Seychelles	Victoria	87169	105	–4.6	55.5	36049.5	72.1	199.25	0.05	-5.39	1.96681E-07	8.26058E-06
The Gaza Strip	Khan Yunis	4168858	5003	31.4	34.3	38019.9	37	199.71	0.08	-1.42	2.5513E-05	0.051051454

Country	**City**	**Population**	N_{IMT}	φ_{IMT}, **deg**	λ_{IMT}, **deg**	D_{SAT}, **km**	β_{SAT}, **deg**	L_{fsl}, **dB**	L_{atm}, **dB**	G_{SAT}, **dB**	ΔT_{SAT1}, ***K***	ΔT_{CITY}, ***K***
Serbia	Kosovo	9846582	11816	42.7	21.2	39467.5	20.9	200.04	0.13	-0.45	3.00913E-05	0.142211605
Singapore	Singapore	5183700	6220	1.4	103.8	37038.2	50.6	199.48	0.06	-2.66	3.4839E-07	0.000866794
Syria	Aleppo	21117690	25341	36.2	37.2	38123.8	35.7	199.73	0.08	-1.32	2.9481E-05	0.298819784
Slovakia	Bratislava	5404322	6485	48.3	17.1	40027.3	15.3	200.16	0.18	-0.24	3.07693E-05	0.079815543
Slovenia	Ljubljana	2062650	2475	46.1	14.6	40076	14.9	200.17	0.18	-0.23	2.92849E-05	0.028992036
United Kingdom	London	62989552	75587	51.5	359.9	41280.6	3.8	200.43	0.63	-0.01	2.14285E-05	0.647890105
Somali	Mogadishu	9797445	11757	2.1	45.4	36467.1	61.1	199.35	0.05	-3.87	2.9555E-07	0.001389972
Sudan	Umm Durman	30894000	37073	15.7	32.5	37518.4	43.5	199.6	0.07	-1.96	5.6791E-06	0.084215398
Tajikistan	Djuschambe	7800000	9360	38.7	68.8	37394.5	45.2	199.57	0.07	-2.12	3.38046E-05	0.126564406
Taiwan	Taipei	23282670	27939	25.1	121.6	38931.3	26.5	199.92	0.1	-0.73	1.31674E-05	0.147159403
Thailand	Bangkok	65479452	78575	13.8	100.5	36991	51.4	199.47	0.06	-2.74	5.76218E-06	0.181105419
Tanzania	Dar Es Salaam	47656368	57188	–6.9	39.4	36860.5	53.6	199.44	0.06	-2.98	3.27013E-07	0.007480426
Togo	Lome	5753324	6904	6.3	1.3	40299.5	12.7	200.22	0.21	-0.17	5.04152E-07	0.001392469
Tunisia	Tunes	10673800	12809	36.8	10.3	40011.3	15.5	200.15	0.17	-0.25	2.24525E-05	0.115024043
Turkmenistan	Asgabat	5169660	6204	38	58.5	37452.5	44.4	199.58	0.07	-2.05	3.2319E-05	0.080183327
Turkey	Constantinople	74724272	89669	41	29.1	38878.9	27	199.91	0.1	-0.76	3.11873E-05	1.11862449
Uganda	Kampala	35620976	42745	0.5	32.7	37288.5	46.8	199.54	0.06	-2.27	3.75728E-07	0.006424193
Uzbekistan	Tashkent	29874600	35850	41.3	69.2	37608.2	42.3	199.62	0.07	-1.85	3.7029E-05	0.530995793
Ukraine	Kiev	45560256	54672	50.6	30.5	39428	21.3	200.03	0.13	-0.47	3.39783E-05	0.743070721
Philippines	Manila	103775000	124530	14.6	121.1	38621.1	29.9	199.85	0.09	-0.93	3.51724E-06	0.175200936
Finland	Helsinki	5426300	6512	60.3	24.9	40367.9	12.1	200.23	0.22	-0.15	3.19582E-05	0.08325117
France	Paris	63468168	76162	48.9	2.5	41020.6	6.1	200.37	0.42	-0.04	2.51115E-05	0.765022942
Croatia	Zagreb	4398150	5278	46	16	39978.6	15.8	200.15	0.17	-0.26	2.97506E-05	0.062803619
Central African Republic	Bangui	4575586	5491	4.4	18.7	38505.6	31.2	199.82	0.09	-1.01	4.68013E-07	0.001027758
Chad	Tandjile	11274106	13529	9.3	16.1	38800.6	27.9	199.89	0.1	-0.81	5.75155E-07	0.003112738
Montenegro	Podgorica	632796	759	42.5	19.4	39579.7	19.7	200.06	0.14	-0.4	2.93525E-05	0.008923164
Czech	Praha	10507566	12609	50.2	14.5	40290.9	12.8	200.22	0.21	-0.17	3.06852E-05	0.154776025

Country	**City**	**Population**	N_{IMT}	φ_{IMT} , **deg**	λ_{IMT} , **deg**	D_{SAT} , **km**	β_{SAT} , **deg**	L_{fsl} , **dB**	L_{atm} , **dB**	G_{SAT} , **dB**	ΔT_{SAT1} ,***K***	ΔT_{CITY} ,***K***
Republic												
Switzerland	Geneve	7952600	9543	46.2	6.2	40667.6	9.3	200.3	0.28	-0.09	2.62859E-05	0.10033344
Sweden	Stockholm	9540065	11448	59.5	18	40616.5	9.8	200.28	0.27	-0.1	3.07848E-05	0.140963732
Sri Lanka	Colombo	21223550	25468	7.1	80	35955.5	75.6	199.23	0.05	-5.93	1.7993E-06	0.018329513
Equatorial Guinea	Bata	740471	889	1.9	9.8	39387.9	21.7	200.02	0.13	-0.49	5.00045E-07	0.000177516
Eritrea	Asmara	5580862	6697	15.5	39.1	37061.6	50.2	199.49	0.06	-2.61	6.61746E-06	0.017728168
Estonia	Tallinn	1339662	1608	59.4	24.8	40314.5	12.6	200.22	0.21	-0.16	3.21331E-05	0.020661555
Ethiopia	Addis Abeba	91195672	109435	9.2	38.7	36940.2	52.2	199.46	0.06	-2.82	1.92144E-06	0.08410925
South Sudan	Djuba	8260490	9913	4.8	31.6	37394.5	45.2	199.57	0.07	-2.12	3.86171E-07	0.001531166
Japan	Tokyo	127561000	153073	35.7	139.8	40827.7	7.8	200.33	0.33	-0.06	1.77717E-05	1.088142665
											$\sum_{N_{CITY}} \Delta T_{CITY} =$	**50.71513436**

4.1.4 Results

Calculations of the noise temperature increase ΔT/T at the GSO SC receiver input with global deployment of advanced IMT systems were performed for beams described in Section 3.2 The results are represented in statistical form in figures below for different combinations of assumed parameters.

FIGURE 12

ΔT/T increase distribution for e.i.r.p. 15 dBm and dissemination 1%

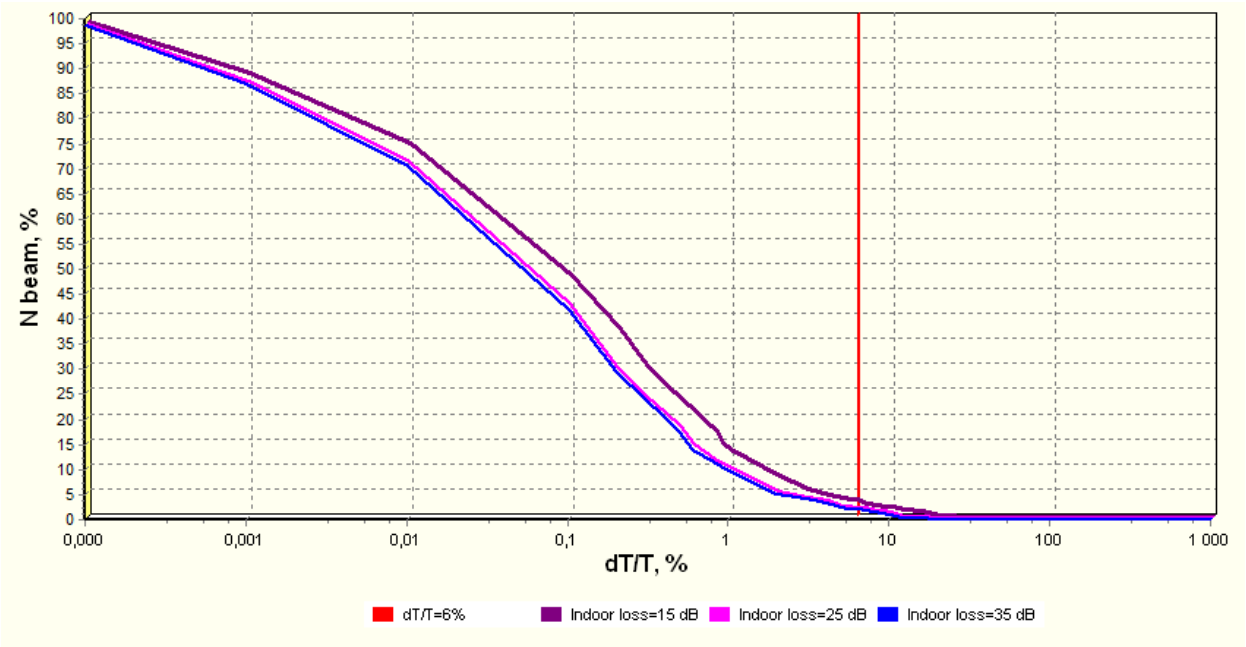

FIGURE 13

ΔT/T increase distribution for e.i.r.p. 15 dBm and dissemination 3%

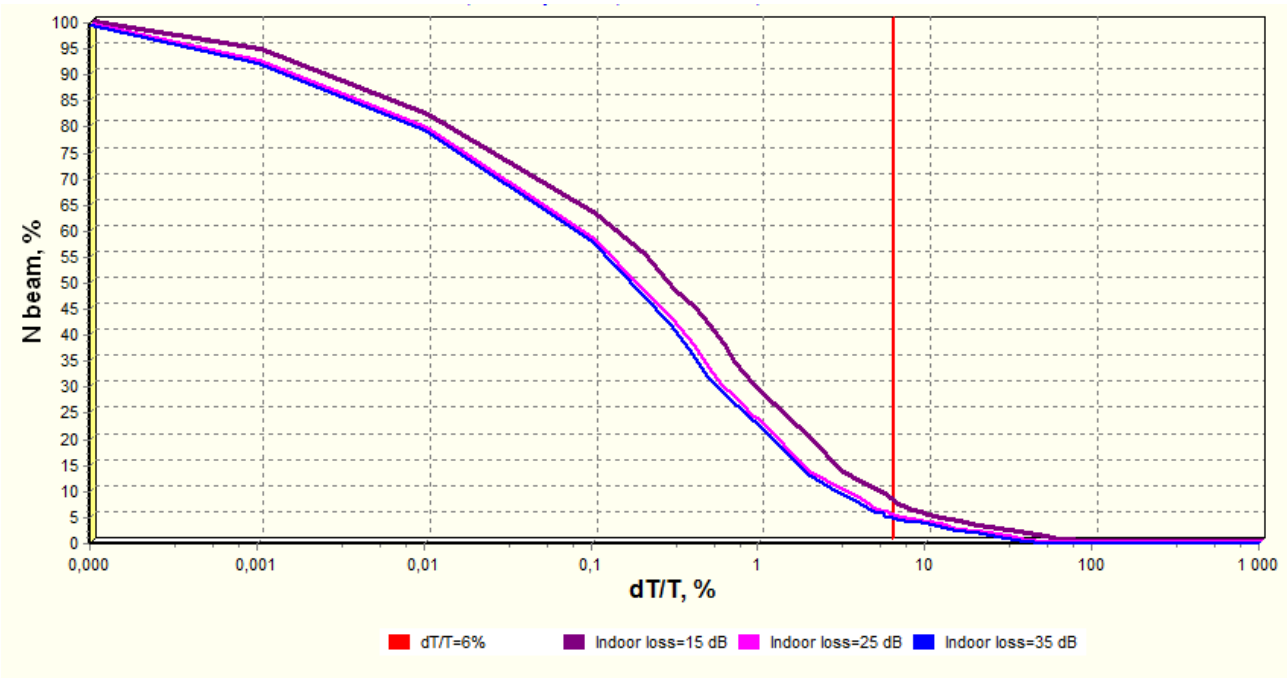

FIGURE 14

ΔT/T increase distribution for e.i.r.p. 15 dBm and dissemination 6%

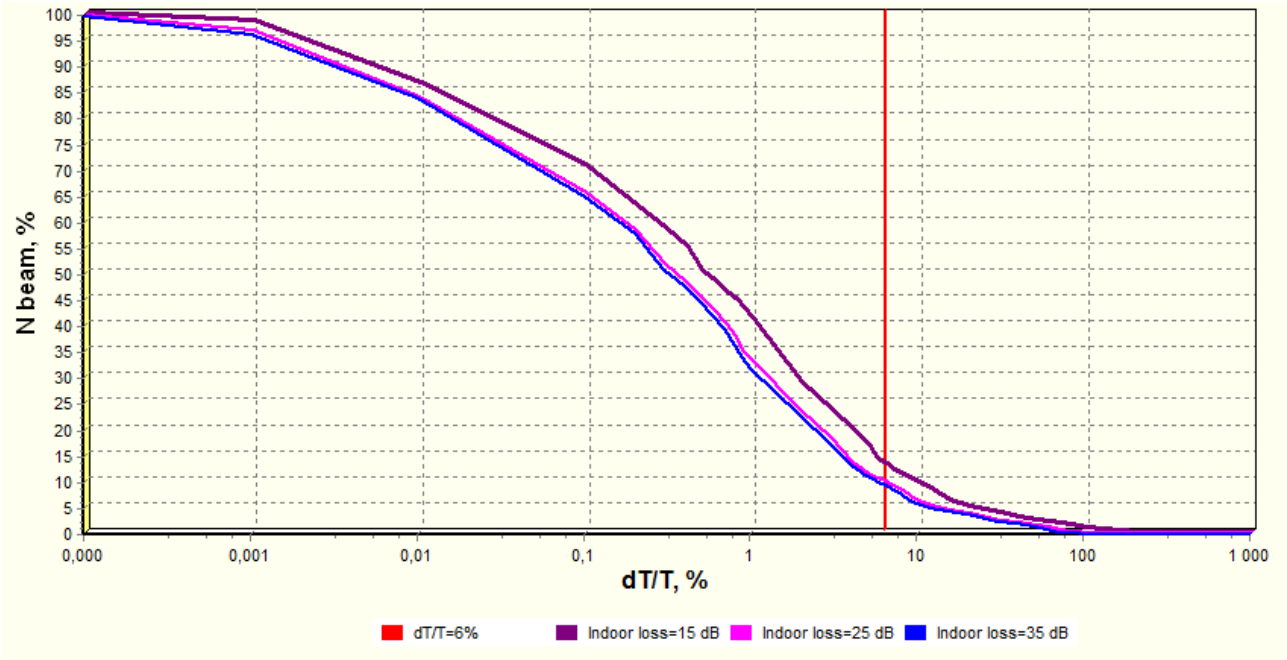

FIGURE 15

ΔT/T increase distribution for e.i.r.p. 24 dBm and dissemination 1%

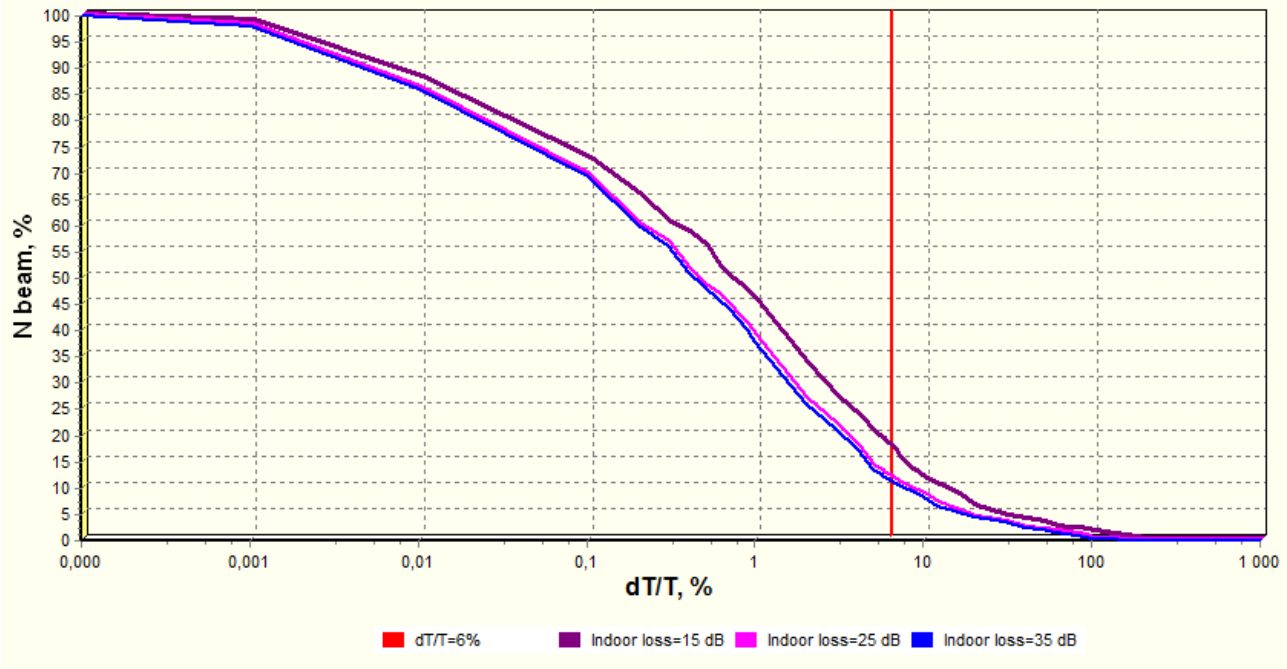

FIGURE 16

ΔT/T increase distribution for e.i.r.p.24 dBm and dissemination 3%

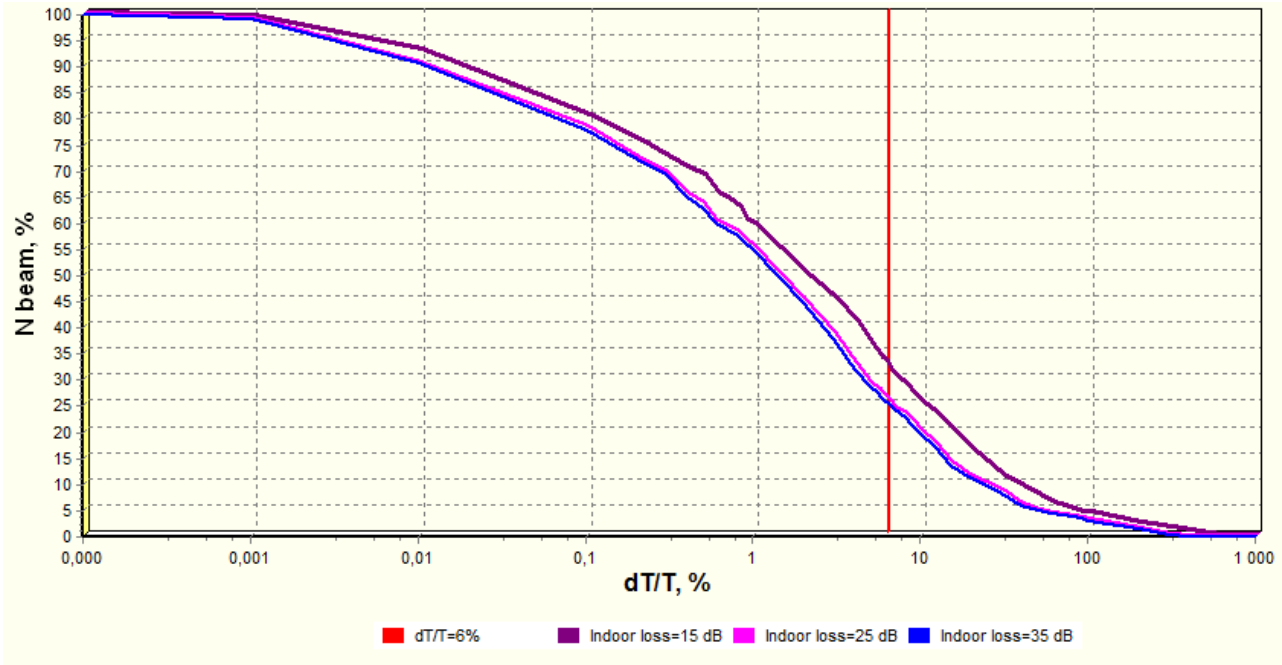

FIGURE 17

ΔT/T increase distribution for e.i.r.p. 24 dBm and dissemination 6%

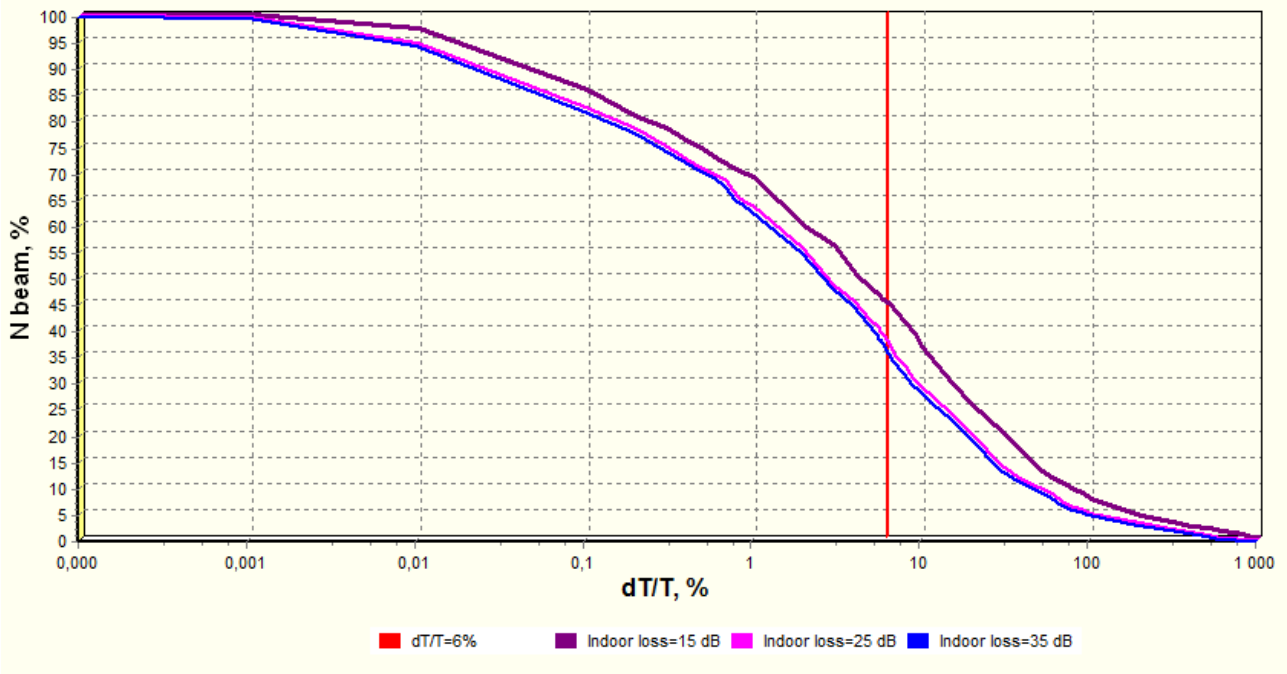

It could be concluded that 15 dBm per 20 MHz provides sufficient protection for FSS SC receivers in which case only a small number of beams will experience ΔT/T increase above 6%. And even in such cases the ΔT/T increase won't be excessive. Furthermore the mode detailed analysis of the results in figure 18 has shown that ΔT/T excessive values correspond to a beam with a very large global footprint but with a very high antenna gain. As BR database is used for coordination purposes such beam usually represents small footprints. However such beams (or satellites) may be redirected several times to different parts of the globe during the lifecycle of the satellite, thus coordination footprint is notified with such artificial parameters. If a real footprint is considered for such cases, the ΔT/T increase may be lower.

FIGURE 18

ΔT/T increase results for e.i.r.p. 15 dBm, indoor penetration loss 15 dB and dissemination 6% as a function of antenna gain and beam coverage area

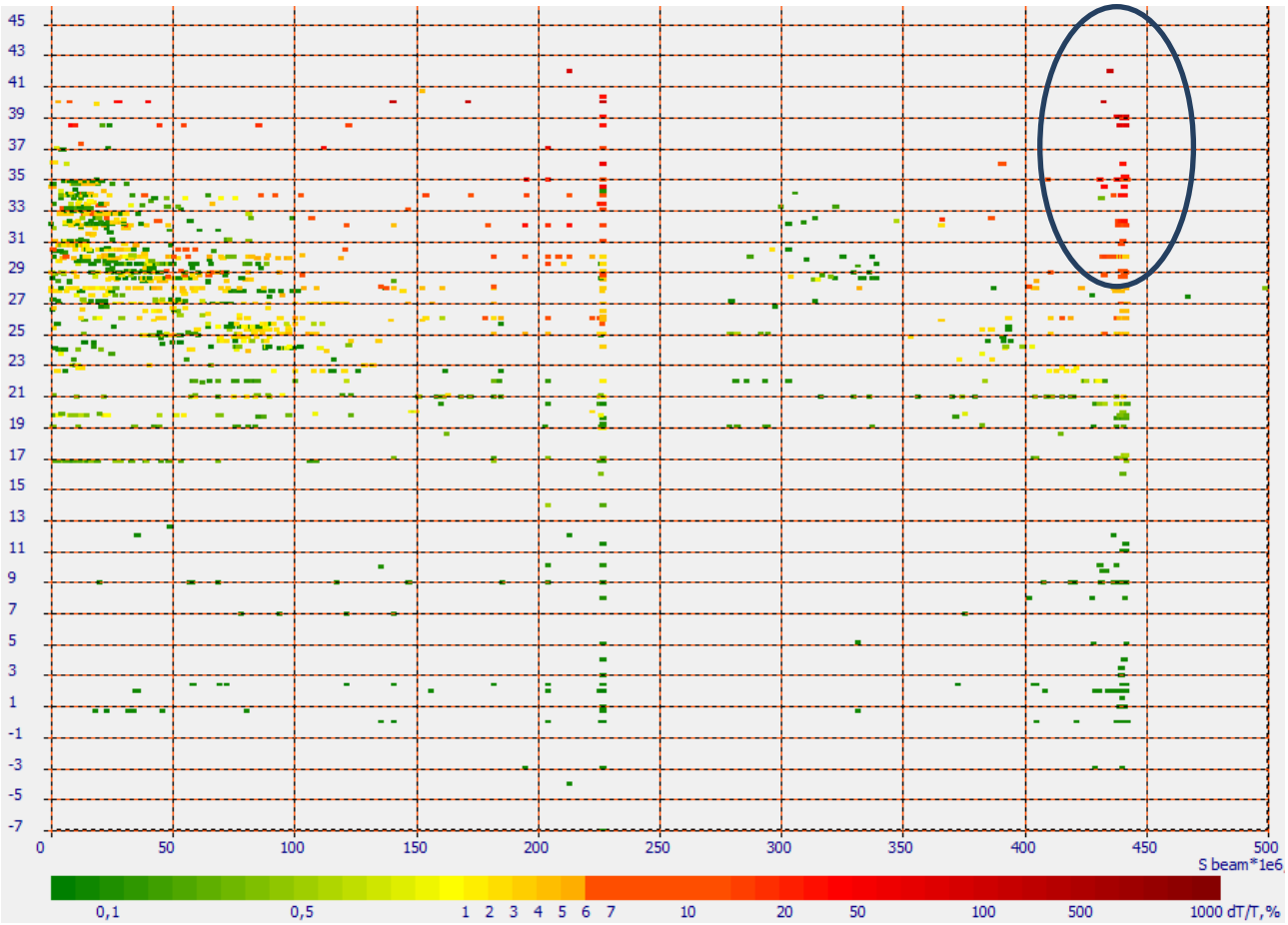

Based on such assumption beams with antenna gain exceeding 29 dBi and with estimated coverage area more than 400*1 000 000 square km have been excluded and above listed calculation have been repeated. The results of such calculation for 15 dBm case are listed in figures 19-21.

FIGURE 19

ΔT/T increase distribution for e.i.r.p. 15 dBm and dissemination 1% with beams filtered by gain and coverage footprint

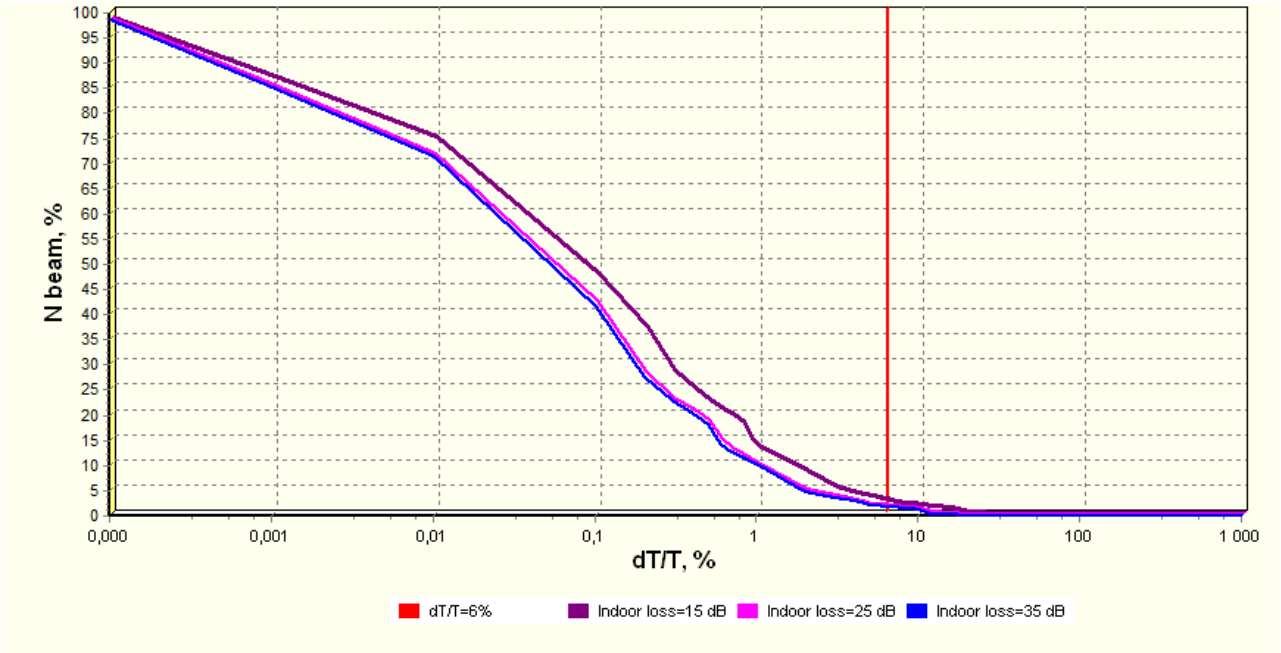

FIGURE 20

ΔT/T increase distribution for e.i.r.p. 15 dBm and dissemination 3% with beams filtered by gain and coverage footprint

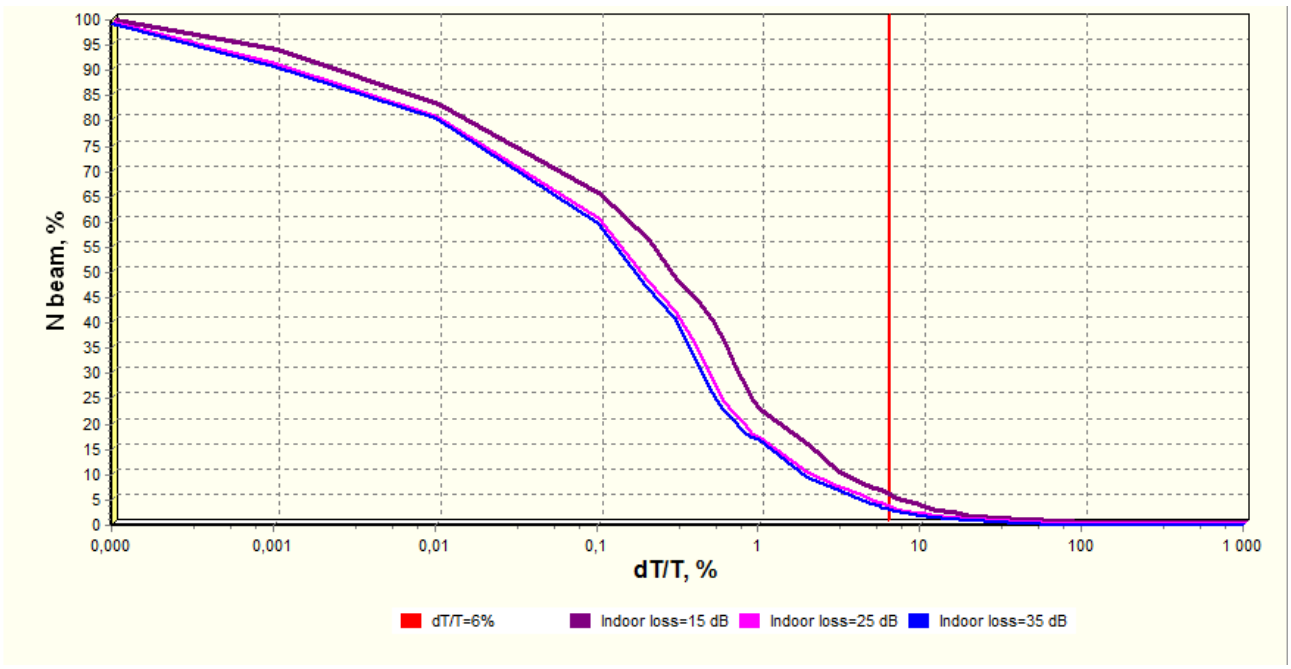

FIGURE 21

ΔT/T increase distribution for e.i.r.p. 15 dBm and dissemination 6% with beams filtered by gain and coverage footprint

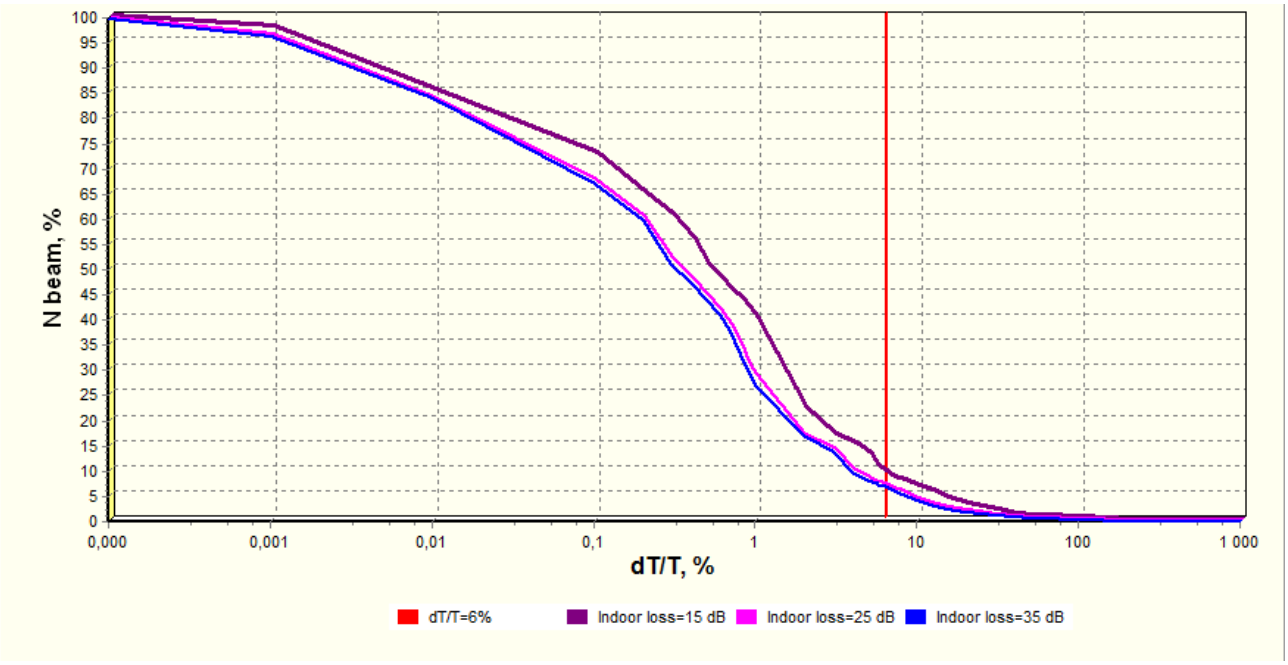

4.2 Impact on FSS NGSO networks

4.2.1 Assumptions

Unlike the GSO spacecraft rotating synchronously with the globe and for this reason having its position fixed relative to terrestrial points, the NGSO spacecraft is constantly moving relative to IMT transmitters deployed on the Earth's surface, and its service area is correspondingly moving along a flight trajectory (see Figs A3.1-A3.5, Appendix 3).

As a consequence, terrestrial points within the visibility of the NGSO SC are different at every instant of time hence the aggregate interference level at the SC receiver from IMT base stations changes during the flight of the SC. That is why the value of ΔT/T is not fixed and changes dynamically within twenty four hours. This results in the necessity of constant tracking of the NGSO SC relative to IMT base stations during its flight, for the purpose of building the function of ΔT/T versus time. A simulation increment from 10 to 100 seconds is chosen taking into account the dynamics of the NGSO SC angular displacement relative to terrestrial stations. Using this function, the percentage of time exceeding the specified ΔT/T value can be calculated averaged for the period of the flight simulation time of the NGSO SC. Parameters of the NGSO SC from section 3.3 show that all chosen SC have s GSO which makes it possible to limit the simulation period to twenty four hours because after that the SC flight trajectory regularly repeats.

Calculation of time exceeding the specified ΔT/T value allows using the criteria given in the Recommendation ITU-R S.1432-1, defining that the permissible long-term aggregate increase in noise temperature ΔT/T=6%, shall not be exceeded more than 20% of any month, and the short-term aggregate increase in noise temperature from IMT systems towards the NGSO SC receiver shall not exceed ΔT/T=57.5% for 0.03% of any month and ΔT/T=100% for 0.005% of any month (see Figure 3.3).

Analysis of interference impact of IMT transmitters on the GSO SC obtained in section 4.1.4 allow limiting IMT transmitter e.i.r.p. within 10-30 dBm for the NGSO simulation. All other IMT base station characteristics and factors taken the same.

4.2.2 Methodology

Calculation of the noise temperature increase ΔT/T as a result of interference from IMT systems to the NGSO SC is similar to the calculation methodology described for the GSO SC in section 4.1.2, and is performed using the equations (1) to (5). The only difference is that this calculation is repeated for every immediate point of the NGSO SC flight trajectory.

The calculation starts with the determination of immediate NGSO SC position using parameters of its orbit. For each city, according to its geographical coordinates, the following parameters are calculated: elevation angle towards the satellite, NGSO satellite receiving antenna gain G_{SAT} towards interfering IMT transmitter and signal propagation losses L_{fsl} and L_{atm}. The G_{SAT} value for NGSO spacecraft towards interfering IMT transmitter is determined according to the Recommendation ITU-R S.672, depending on the observation angle ψ from the SC towards the terrestrial IMT transmitter, $G_{SAT} = G(\psi)$:

$$G(\psi) = \begin{cases} G_m - 3(\psi/\psi_b)^{\alpha} & for \quad \psi_b \le \psi \le a\psi_b \\ G_m + L_N + 20\lg z & for \quad a\psi_b \le \psi \le 0.5b\psi_b \\ G_m + L_N & for \quad 0.5b\psi_b \le \psi \le b\psi_b \\ X - 25\lg\psi & for \quad b\psi_b \le \psi \le Y \\ L_F & for \quad Y < \psi \le 90^\circ \\ L_B & for \quad 90^\circ < \psi \le 180^\circ \end{cases};$$

where: ψ – angle between the direction of maximum SC antenna gain and the direction towards the terrestrial IMT transmitter (deg);

$$X = G_m + L_N + 25\lg(b\,\psi_b)$$

$$Y = b\,\psi_b\ 10^{0.04(G_m + L_N - L_F)}$$

b – 3 dB half-beamwidth in the given plain (3dB less than G_m), deg;

L_N – required level of the nearest side lobe relative to the maximum gain (L_N = -25 dB);

L_F – back lobe level (L_F =0 dB);

$L_B = 15 + L_N + 0.25 \cdot G_m + 5\lg z$ or 0 dB, whichever is higher, dB

α =2; a=2.58; b=6.32.

4.2.3 Example of calculations

The calculation methodology for the noise temperature increase ΔT/T from IMT system interference to the NGSO SC is similar to the calculation for the GSO SC in section 4.1.3.

4.2.4 Results

Calculations of the noise temperature increase ΔT/T at the NGSO SC receiver input with global deployment of advanced IMT systems were performed for all selected in Section 3.3 NGSO networks.

The performed studies show that variations of interference in time occurs only due to the changing number of interfering stations in the coverage area of the NGSO SC receiving antenna, which is determined by the satellite movement, and since this process is slow, short-term criteria of the exceeded $\Delta T/T$ ($\Delta T/T$=57.5% for 0.03% of any month and $\Delta T/T$=100% for 0.005% of any month) is always fulfilled and needn't be checked, because the dominant criterion is the long-term criterion, i.e. $\Delta T/T$=6% not exceeded 20% of the time. Taking this into account, the calculations for the NGSO SC based on the criterion of $\Delta T/T$=6% not exceeded 20% of any month are summarized in Tables 8 and 9.

TABLE 8

Percentage of time when ΔT/T=6% is not exceeded for NGSO spacecraft (IMT system e.i.r.p. 15 dBm)

Satellite	Beam	Satellite Maximum Receive Gain, (dBi)	Satellite Receiving System Noise Temperature (K)	Indoor-to-outdoor penetration losses								
				15 dB			25 dB			35 dB		
				Dissemination								
				1%	3%	6%	1%	3%	6%	1%	3%	6%
MOLNIA-1	R1	18	2500	0	0	0	0	0	0	0	0	0
MOLNIA-2	R1	17	3000	0	0	0	0	0	0	0	0	0
MOLNIA-3	R1	17,3	3000	0	0	0	0	0	0	0	0	0
USASAT-28C	OM1	3	630	0	0	0	0	0	0	0	0	0
OSAT	CRR	30	494	0	0	0	0	0	0	0	0	0
INSAT-NAV-A-GS	RTC	–3	1000	0	0	0	0	0	0	0	0	0
INSAT-NAVR-GS	RTC	–3	1000	0	0	0	0	0	0	0	0	0

TABLE 9

Percentage of time when ΔT/T=6% is not exceeded for NGSO spacecraft (IMT system e.i.r.p. 24 dBm)

Satellite	Beam	Satellite Maximum Receive Gain, (dBi)	Satellite Receiving System Noise Temperature (K)	Indoor-to-outdoor penetration losses								
				15 dB			25 dB			35 dB		
				Dissemination								
				1%	3%	6%	1%	3%	6%	1%	3%	6%
MOLNIA-1	R1	18	2500	0	0	0	0	0	0	0	0	0
MOLNIA-2	R1	17	3000	0	0	0	0	0	0	0	0	0
MOLNIA-3	R1	17,3	3000	0	0	0	0	0	0	0	0	0
USASAT-28C	OM1	3	630	0	0	0	0	0	0	0	0	0
OSAT	CRR	30	494	0	0	0	0	0	0	0	0	0
INSAT-NAV-A-GS	RTC	–3	1000	0	0	0	0	0	0	0	0	0
INSAT-NAVR-GS	RTC	–3	1000	0	0	0	0	0	0	0	0	0

5 Summary

The study considered the level of interference created by multiple IMT base stations on the Earth's surface towards the receiver of GSO and NGSO FSS space stations operating in the frequency band 5 925-6 425 MHz. Massive deployment of IMT base stations, serving small cells, has been used as the main assumption of the study, which corresponds to a large number of transmitters with omni antenna and relatively small e.i.r.p. The TDD frequency arrangement has been also assumed for this band, which permits modelling of the aggregate interference to FSS space stations, based only on IMT base station emissions. The density of such base stations has been associated with world population distribution between large cities. Both indoor and outdoor deployments have been studied.

Calculation results presented above have shown that the assumed IMT base station deployment in the 5 925-6 425 MHz frequency band could be implemented without creating significant interference to FSS space stations under specific conditions. Certain limitations on such usage for IMT stations should be enforced to facilitate sharing with FSS space stations:

– only indoor deployment;

– maximum e.i.r.p. not higher than 15 dBm/20 MHz (22 dBm per 100 MHz channel).

For 15 dBm e.i.r.p. per 20 MHz case for 95% of indoor small cells the coordination criteria $\Delta T/T=6\%$ is more easily fulfilled for 90-99% the considered satellite beams in the database depending on the assumptions. 90% corresponds to the most conservative and pessimistic assumptions and includes beams registered with high gain antennas in combination with global coverage. With other assumption only 1-2% of beams will be experiencing $\Delta T/T$ exceedance. In the limited number of cases when $\Delta T/T$ is not fulfilled the margin corresponds to few dBs. It should be noted that the $\Delta T/T=6\%$ is a coordination criteria and is very conservative thus the exceedance of this criteria for a few dBs is considered to be tolerable.

Thus aforementioned measures would facilitate sharing with both GSO and NGSO space stations operating within the 5 925-6 425 MHz frequency band.

APPENDIX 1 TO ANNEX 3

Population distribution

TABLE A1.1

Population of countries and the number of cities selected for modelling

No.	Country	Population	Number of selected cities	Date of the population census
1	Australia	23441000	70	January 15, 2013
2	Austria	8452835	10	January 1, 2012
3	Azerbaijan	9235100	20	January 1, 2012
4	Albania	2831741	5	October 1, 2011
5	Algeria	36485830	50	July 1, 2012
6	Angola	20162520	25	July 1, 2012
7	Andorra	78115	1	2011
8	Antigua and Barbuda	90510	1	July 1, 2012
9	Argentina	41281630	55	January 1, 2012
10	Armenia	3277500	10	September 1, 2011
11	Aruba	108587	1	July 1, 2012
12	Afghanistan	33397060	30	July 1, 2012
13	Bahamas	351275	15	July 1, 2012
14	Bangladesh	152518000	33	July 16, 2012
15	Barbados	274530	1	July 1, 2012
16	Bahrain	1234571	1	April 27, 2010
17	Belarus	9460000	20	November 1, 2012
18	Belize	322100	6	June 30, 2008
19	Belgium	11041270	10	January 1, 2012
20	Benin	9351838	10	July 1, 2012
21	Bermuda	65208	1	July 1, 2012
22	Burma	50020000	30	
23	Bulgaria	7364570	10	February 1, 2011
24	Bolivia	10248040	40	July 1, 2012
25	Bosnia and Herzegovina	3839737	5	June 30, 2011
26	Botswana	2053237	10	July 1, 2012
27	Brazil	197666000	150	January 15, 2013
28	Brunei	412892	1	July 1, 2012
29	Burkina Faso	17481980	20	July 1, 2012
30	Burundi	8749387	4	July 1, 2012
31	Bhutan	750443	4	July 1, 2012
32	Vanuatu	251674	3	July 1, 2012
33	Hungary	9962000	10	January 1, 2012
34	Venezuela	29491000	15	January 15, 2013
35	Virgin Islands (U.S.)	108590	1	July 1, 2012
36	East Timor	1066409	1	July 11, 2010
37	Vietnam	90549390	20	October 1, 2011
38	Gabon	1563873	10	July 1, 2012
39	Guyana	761510	3	end of 2006
40	Haiti	10255640	5	July 1, 2012
41	Gambia	1824777	5	July 1, 2012
42	Ghana	25545940	10	July 1, 2012
43	Guadeloupe	401554	1	January 1, 2009
44	Guatemala	15137570	10	July 1, 2012
45	Guiana (France)	232200	1	January 1, 2010
46	Guinea	10480710	8	July 1, 2012
47	Guinea-Bissau	1579632	3	July 1, 2012

No.	Country	Population	Number of selected cities	Date of the population census
48	Germany	81843810	100	January 1, 2012
49	Guernsey	61811	1	March 1, 2007
50	Gibraltar	29441	1	July 1, 2010
51	Honduras	7466000	5	July 1, 2011
52	Hong Kong	7136300	1	July 1, 2012
53	Grenada	105303	1	July 1, 2012
54	Greenland	57300	10	July 1, 2012
55	Greece	11290790	10	January 1, 2012
56	Georgia	4497600	5	January 1, 2012
57	Guam	184334	1	July 1, 2012
58	Denmark	5580516	5	January 1, 2012
59	Djibouti	922708	1	July 1, 2012
60	Dominica	67665	1	July 1, 2012
61	Dominican Republic	10183340	4	July 1, 2012
62	Egypt	83063000	10	January 15, 2013
63	Zambia	13883580	20	July 1, 2012
64	Zimbabwe	13013680	10	July 1, 2012
65	Yemen	25569260	4	July 1, 2012
66	Israel	7836000	5	December 31, 2011
67	India	1229583000	150	January 15, 2013
68	Indonesia	245641300	100	June 2011
69	Jordan	6390500	7	January 15, 2013
70	Iraq	33703070	15	July 1, 2012
71	Iran	77002700	50	December 23, 2012
72	Ireland	4581269	5	April 10, 2011
73	Iceland	317630	3	January 1, 2010
74	Spain	46163120	20	July 1, 2012
75	Italy	60820760	25	January 1, 2012
76	Cape Verde	505335	4	July 1, 2012
77	Kazakhstan	16856000	35	October 1, 2012
78	The Cayman Islands	57223	1	July 1, 2012
79	Cambodia	14478320	5	July 1, 2012
80	Cameroon	20468940	15	July 1, 2012
81	Canada	33673000	150	January 15, 2013
82	Qatar	1699435	1	April 21, 2010
83	Kenya	42749420	10	July 1, 2012
84	Cyprus	862011	3	January 1, 2012
85	Kiribati	102660	2	July 1, 2012
86	China	1355720000	250	January 15, 2013
87	Colombia	46868000	30	January 15, 2013
88	Comoros	753943	2	July 1, 2011
89	Congo, DR	69575390	25	July 1, 2012
90	Congo, Republic of	4233063	7	July 1, 2012
91	Korea, North	24553672	12	July 1, 2011
92	Korea, South	48580000	10	November 1, 2010
93	Costa Rica	4301712	9	June 3, 2011
94	Côte d'Ivoire	20594620	15	July 1, 2012
95	Cuba	11249270	10	July 1, 2012
96	Kuwait	2891553	1	July 1, 2012
97	Kyrgyzstan	5477600	9	January 1, 2011
98	Curacao (Netherlands)	149679	1	March 26, 2011
99	Laos	6348800	6	July 1, 2011
100	Latvia	2049500	3	February 1, 2012
101	Lesotho	2216850	2	July 1, 2012
102	Liberia	3476608	5	April 1, 2008
103	Lebanon	4291719	1	July 1, 2012

No.	Country	Population	Number of selected cities	Date of the population census
104	Libya	6469497	25	July 1, 2012
105	Lithuania	2988400	9	September 1, 2012
106	Liechtenstein	36476	1	December 31, 2011
107	Luxembourg	524853	1	January 1, 2012
108	Mauritius	1280294	1	July 1, 2010
109	Mauritania	3622961	5	July 1, 2012
110	Madagascar	21928520	20	July 1, 2012
111	Mayotte	217172	1	July 1, 2012
112	Macau	542200	1	December 31, 2009
113	Macedonia	2057284	5	December 31, 2010
114	Malawi	15882820	5	July 1, 2012
115	Malaysia	29562240	15	December 13, 2012
116	Mali	14517180	15	April 1, 2009
117	Maldives	324313	1	July 1, 2012
118	Malta	420085	1	January 1, 2012
119	Morocco	32783000	20	January 15, 2013
120	Martinique (France)	396404	1	January 1, 2009
121	Marshall Islands	55717	1	July 1, 2012
122	Mexico	114500000	50	December 12
123	Micronesia	112098	3	July 1, 2012
124	Mozambique	23700720	14	2012
125	Moldova	3559500	3	January 1, 2012
126	Monaco	35444	1	July 1, 2012
127	Mongolia	2736800	10	July 1, 2010
128	Namibia	2364433	15	July 1, 2012
129	Nepal	31011140	10	July 1, 2012
130	Niger	16644340	25	July 1, 2012
131	Nigeria	166629400	70	July 1, 2012
132	Netherlands	16804900	6	January 15, 2013
133	Nicaragua	5815524	8	July 1, 2010
134	New Zealand	4471500	15	January 15, 2013
135	New Caledonia	258735	5	July 1, 2012
136	Norway	5049100	20	January 15, 2013
137	UAE	4800250	3	June 10, 2011
138	Oman	2773479	7	December 12, 2010
139	Isle of Man	83739	1	July 1, 2012
140	Pakistan	177791000	25	January 15, 2013
141	Panama	3405813	5	May 16, 2010
142	Papua New Guinea	7170112	10	July 1, 2012
143	Paraguay	6337127	15	July 1, 2010
144	Peru	30135880	20	January 1, 2012
145	Poland	38208620	25	January 1, 2012
146	Portugal	10541840	10	January 1, 2012
147	Puerto Rico	3725789	1	April 1, 2010
148	Reunion (France)	816364	1	January 1, 2009
149	Russian Federation	143302400	300	November 1, 2012
150	Rwanda	10718380	1	July 31, 2011
151	Romania	21355850	20	January 1, 2012
152	Salvador	6264129	5	July 1, 2012
153	Samoa	184772	1	July 1, 2012
154	San Marino	31945	1	January 1, 2012
155	Sao Tome and Principe	171878	1	July 1, 2012
156	Saudi Arabia	28705130	25	July 1, 2012
157	Swaziland	1220408	4	July 1, 2012
158	Northern Mariana Islands	62152	1	July 1, 2012
159	Seychelles	87169	1	July 1, 2012

No.	Country	Population	Number of selected cities	Date of the population census
160	Gaza (PNA)	4168858	5	July 1, 2011
161	Senegal	13107950	15	July 1, 2012
163	Saint Vincent and the Grenadines	109367	1	July 1, 2012
164	St. Kitts and Nevis	53697	1	July 1, 2012
165	St. Lucia	177794	1	July 1, 2012
166	Serbia	9846582	10	July 1, 2012
167	Singapore	5183700	1	June 30, 2011
168	Syria	21117690	12	July 1, 2012
169	Slovakia	5404322	7	January 1, 2012
170	Slovenia	2062650	3	January 15, 2013
171	United Kingdom	62989550	40	January 1, 2012
172	U.S.	315071000	350	January 15, 2013
173	Solomon Islands	566481	8	July 1, 2012
174	Somalia	9797445	15	July 1, 2012
175	Sudan	30894000	20	April 22, 2008
176	Surinam	534175	3	July 1, 2012
177	Sierra Leone	6126450	3	July 1, 2012
178	Tajikistan	7800000	5	January 1, 2012
179	Taiwan	23282670	2	September 1, 2012
180	Thailand	65479450	10	September 1, 2010
181	Tanzania	47656370	30	July 1, 2012
182	Turks and Caicos	39761	1	July 1, 2012
183	Togo	5753324	10	November 6, 2010
184	Tonga	104891	4	July 1, 2012
185	Trinidad and Tobago	1317714	1	July 1, 2010
186	Tunisia	10673800	15	July 1, 2011
187	Turkmenistan	5169660	12	July 1, 2012
188	Turkey	74724270	50	December 31, 2011
189	Uganda	35620980	15	July 1, 2012
190	Uzbekistan	29874600	12	October 1, 2012
191	Ukraine	45560260	25	November 1, 2012
192	Uruguay	3203792	15	September 1, 2011
193	Faroe Islands	48660	1	January 1, 2010
194	Fiji	875822	1	July 1, 2012
195	Philippines	103775000	50	May 1, 2012
196	Finland	5426300	15	January 15, 2013
197	France	63468170	50	January 1, 2012
198	French Polynesia	276731	1	July 1, 2012
199	Croatia	4398150	5	January 1, 2012
200	Central African Republic	4575586	14	July 1, 2012
201	Chad	11274110	16	June 30, 2009
202	Montenegro	632796	1	July 1, 2012
203	Czech Republic	10507570	10	March 31, 2012
204	Chile	17516000	25	January 15, 2013
205	Switzerland	7952600	5	January 1, 2012
206	Sweden	9540065	25	September 30, 2012
207	Sri Lanka	21223550	10	July 1, 2012
208	Ecuador	14711000	16	January 15, 2013
209	Equatorial Guinea	740471	7	July 1, 2012
210	Eritrea	5580862	5	July 1, 2012
211	Estonia	1339662	10	January 1, 2012
212	Ethiopia	91195670	30	November 2012
213	South Sudan	8260490	1	April 22, 2008
214	Jamaica	2705800	1	December 31, 2010
215	Japan	127561000	100	July 1, 2012
	Total:	**6965239379**		

APPENDIX 2 TO ANNEX 3

FSS NGSO network characteristics

Figures A3.1-A3.5 show the NGSO satellite flight trajectories on the Earth surface with one instant coverage footprint.

FIGURE A3.1

Typical flight trajectory of MOLNIA-1, MOLNIA-2 and MOLNIA-3 spacecraft with one instant coverage footprint on the Earth surface

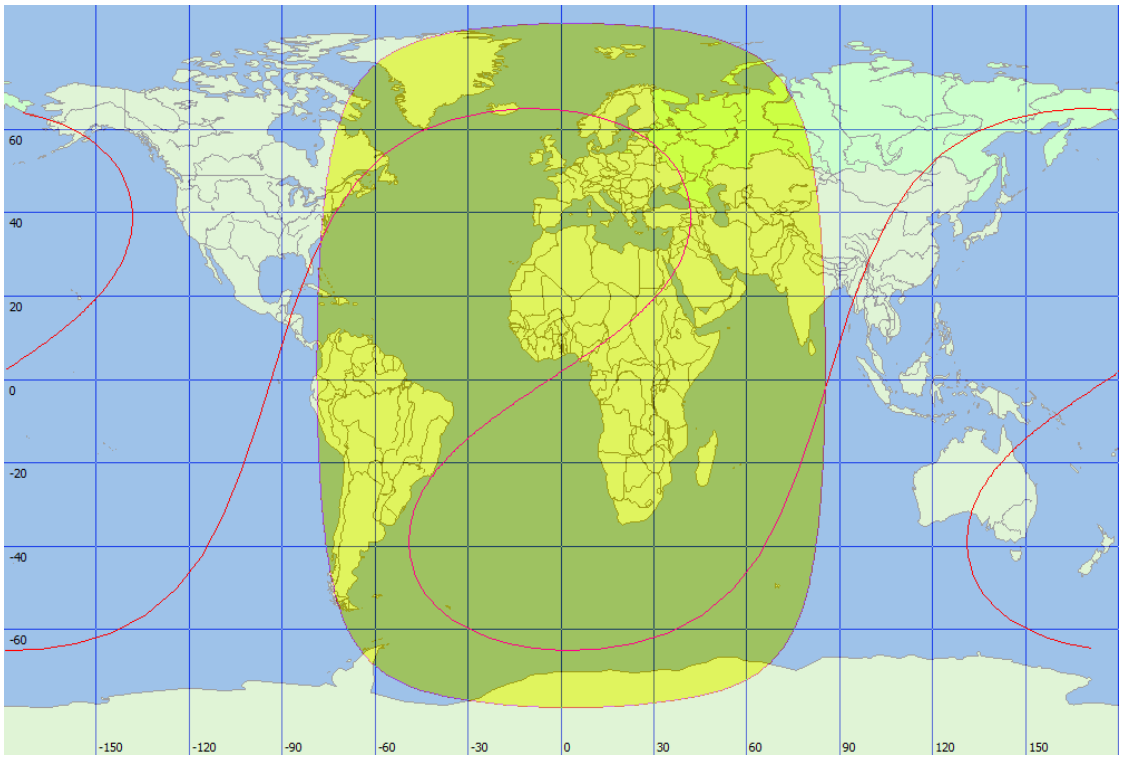

FIGURE A3.2

USASAT-28C spacecraft flight trajectory with one instant coverage footprint on the Earth surface

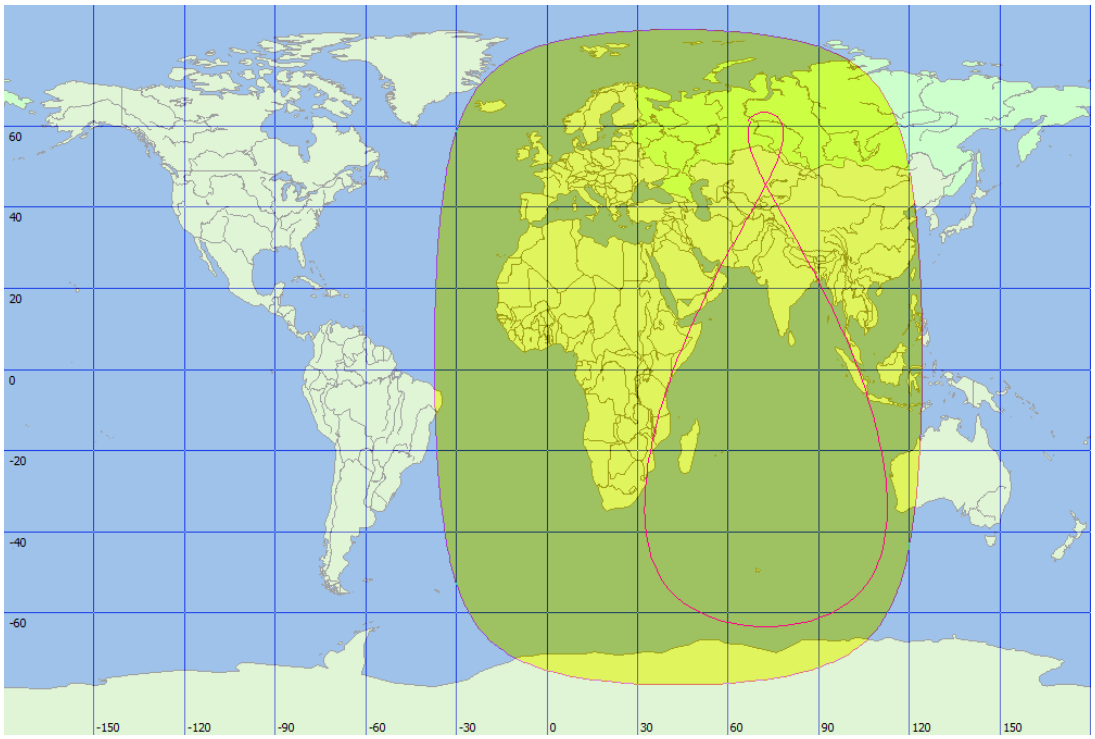

FIGURE A3.3

OSAT spacecraft flight trajectory with one instant coverage footprint on the Earth surface

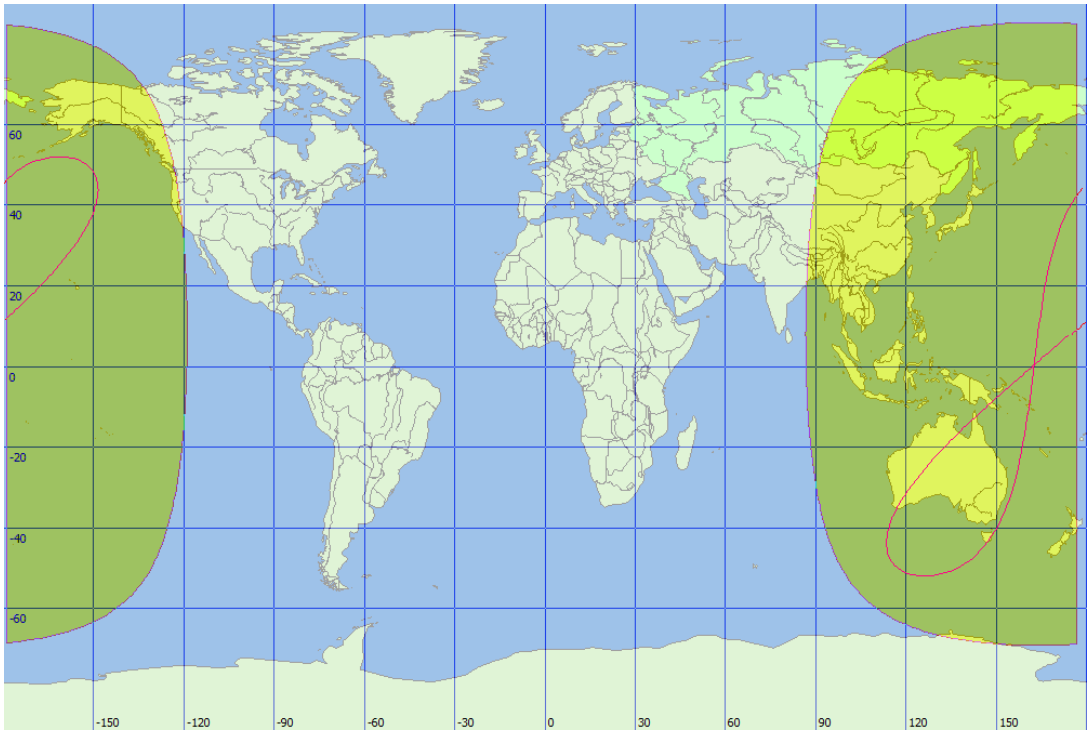

FIGURE A3.4

INSAT-NAV-A-GS spacecraft flight trajectory with one instant coverage footprint on the Earth surface

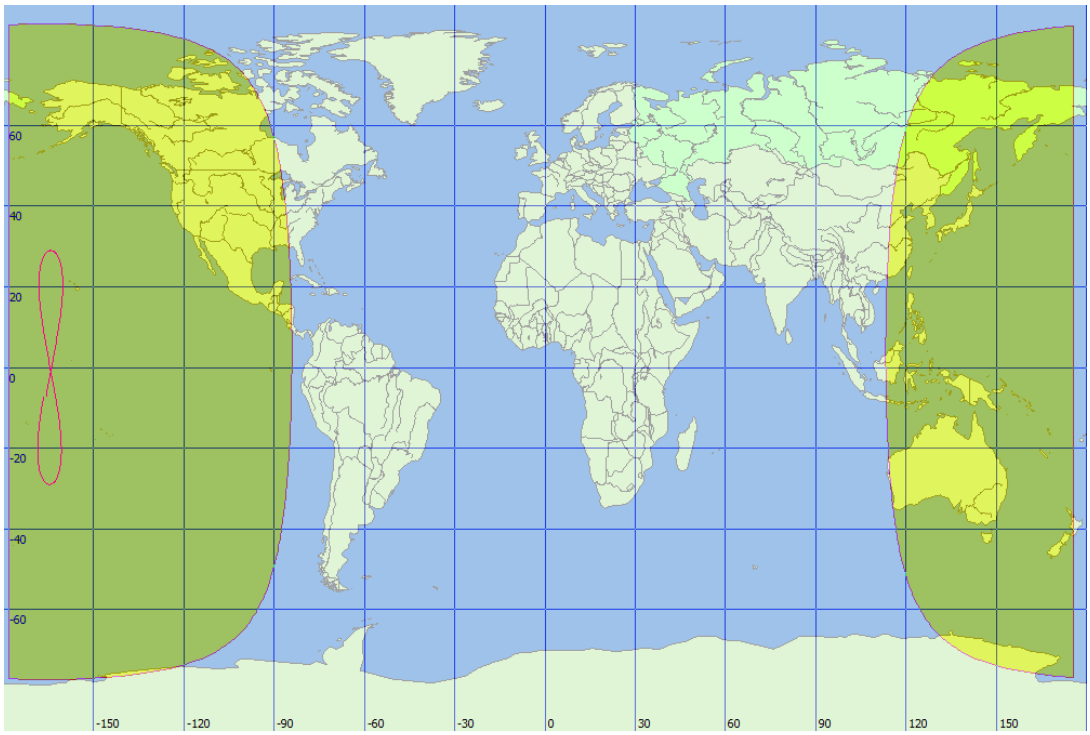

FIGURE A3.5

INSAT-NAVR-GS spacecraft flight trajectory with one instant coverage footprint on the Earth surface

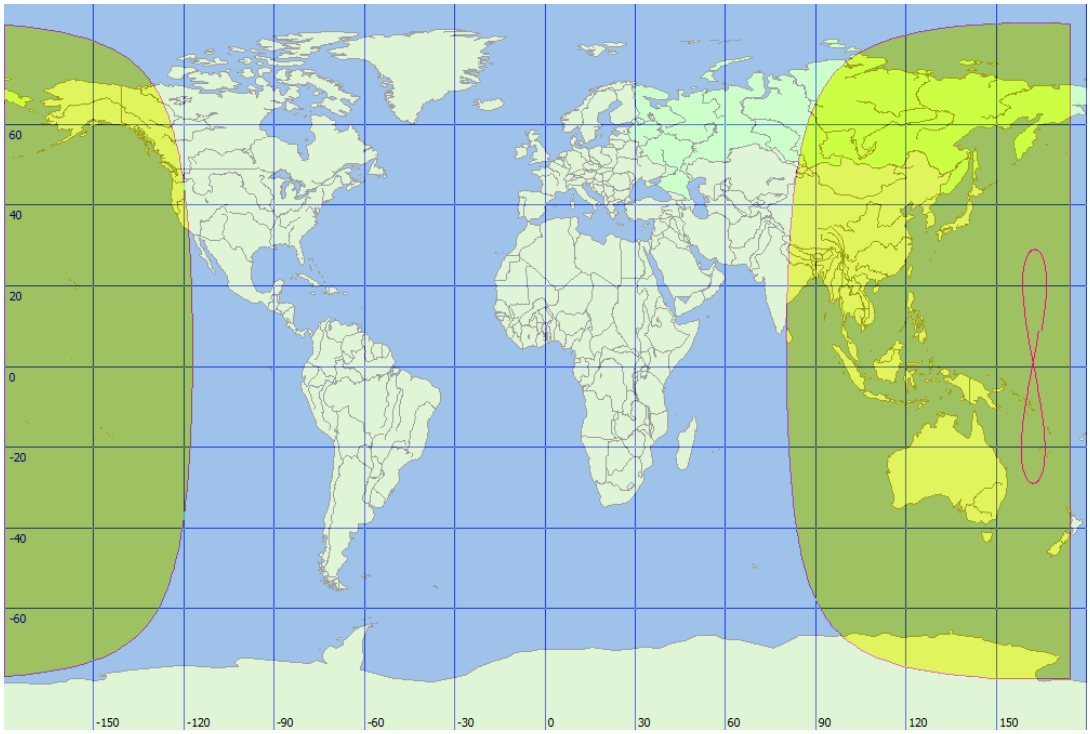

ANNEX 4

Sharing and compatibility between IMT systems and FSS receiving space stations in the 5 925-6 425 MHz frequency band

1 Introduction

The study in this annex examines the potential interference from IMT systems to space stations in FSS in the 5 925-6 425 MHz frequency band.

This part of the spectrum has been allocated to FSS networks on a primary basis, and it's extensively used by FSS Earth-to-space applications all over the world. Satellite operators rely on C-Band communication to support a variety of applications, including business communications, telemedicine, disaster recovery, VSAT Networks and Direct-to-Home broadcasting.

Nevertheless, the band 5 925-6 425 MHz has been identified as a possible candidate for IMT.

However, such an opportunity can only be realised if appropriate coexistence between IMT systems and FSS is duly safeguarded, requiring the definition of technical conditions in order to ensure the protection of the FSS services in the long term.

The study provides a calculation of the aggregate interference from the IMT stations and suggests the maximum power of the transmitters that would be required to protect FSS space stations. The results strongly depend on the adoption of the specific parameters for IMT density, building attenuation, propagation model and satellite characteristics (orbital position, footprints and transponder merit of factor G/T).

2 Technical characteristics

In addition to Report ITU-R M.2292-0 some technical and operational parameters of indoor IMT small cells are based on sharing studies between RLAN and EESS satellites in the band 5 350-5 470 MHz discussed under preparation to WRC-15 agenda item 1.1. While these parameters have been discussed and agreed in the context of sharing studies for the band 5 350-5 470 MHz, some of the assumptions are equally applicable to the band 5 925-6 425 MHz, including some parameters related to building penetration and propagation loss.

2.1 IMT system characteristics

The IMT station characteristics are based on Report ITU-R M.2292-0. The maximum e.i.r.p. is determined as an output of the study. The antennae were considered omnidirectional in both azimuth and elevation (0 dBi) and it is assumed that stations would be required to be limited to indoor-only operation, with small cells.

The IMT systems could operate with two modes, frequency division duplex (FDD) or TDD.

We assume that the system will operate in TDD mode, and hence base stations are assumed to transmit on all available frequencies.

The use of TDD means that user terminals will transmit on the same frequencies on the base stations. Considering that the small cells considered would use relatively low power, it is reasonable to assume that the user stations will transmit with a similar power, and hence we can consider as a worst case the base station transmitting continuously, without switching in the time with the subscribers.

The numbers of active IMT stations that contribute to the aggregate interference have a significant impact on the result of the calculations. Following the approach suggested by a study in Annex 3, the following factors were used:

– a predicted dissemination factor (K_{DISS}) expressed in % relative to population;

– an area activity factor (K_{ACTIVE}) of base stations simultaneously switched on in the reference band;

– a band usage factor ($K_{\Delta f}$): it's assumed that each single station will use 20 MHz channel over the proposed 500 MHz, therefore the expected $K_{\Delta f}$ is 4%, supposing that the IMT transmitters will be uniformly distributed over the entire available spectrum of 500 MHz.

In the analysis K_{DISS} is assumed to be 3%, 6% and 10%. Even if this factor is difficult to predict, the number of IMT stations used for small-cell is estimated to be around 90 million in 2016 (source: Informa Telecoms & Media), corresponding to around 1.5% of the world population. It's sensible to make conservative assumptions, as this market is expected to grow by over 100% per annum over the next years, in particular for small cells.

K_{ACTIVE} has been set to 20% and 50%: the first value (20%), used in Annex 3 is representative for a low traffic scenario with just one active station over five, and the second one (50%), is proposed to be considered as additional scenario.

2.2 Building attenuation

The study assumes that IMT base station deployment would be restricted to indoor use only, but to take into consideration for occasional outdoor use, 95% of the IMT stations have been modelled considering building attenuation, while the remaining 5% of the transmitters is assumed to be installed outdoor. If the percentage of outdoor users will be higher, the results will be worse: therefore an enforcement mechanism is necessary to limit IMT systems to indoor use only if a decision to allow IMT use in this band is based on this assumption.

Following the same assumptions as agreed for the band 5 350-5 470 MHz, the building attenuations have been modelled with a Gaussian distribution with a 17 dB mean and a 7 dB standard deviation (truncated at 1 dB). Generating a sequence of random independent Gaussian variables, N (17,7), one could see that the linear mean attenuation value is around 1/0.063, equivalent to 12 dB in a logarithmic scale.

2.3 Propagation model

The propagation model is based on free-space loss, with atmospheric absorption included following Recommendation ITU-R P.676-3.

In addition to the building attenuation discussed above, clutter loss is included to take account of additional losses due to ground clutter (trees, buildings, etc.) that may exist. Following the approach agreed for the band 5 350-5 470 MHz, an angular clutter loss model based on Recommendation ITU-R P.452 is used in conjunction with the antenna heights of transmitters. The antenna heights are randomly selected using a uniform probability distribution from a set of floors heights at 3 meter steps from 1.5 to 28.5 metres for the Urban Zone and from 1.5 to 4.5 metres for the Rural Zone.

The clutter loss model has been used in conjunction with data related to the percentage of the population living in urban and rural areas in each country. Information on the population living in "sub-urban" areas is not available and hence this area is not included in the model.

Table 1 summarizes the clutter loss obtained setting the frequency at 6 GHz and varying the height of the transmitter. Θ_{MAX} provides the angle from the IMT transmitter to the top of the clutter height; therefore if the spacecraft is at elevation angle below Θ_{MAX}, clutter losses have been added. If the spacecraft is above Θ_{MAX} of the respective clutter category, there is no loss (i.e. Clutter Loss Factor is 0 dB*).*

TABLE 1

	Θ max	**Clutter Loss Factor**
Rural 1.5m	1.40°	17.3 dB
Rural 4.5m	0°	00.0 dB
Urban 1.5m	42.80°	19.7 dB
Urban 4.5m	37.80°	19.6 dB
Urban 7.5m	32.00°	18.8 dB
Urban 10.5m	25.40°	15 dB
Urban 13.5m	18.00°	6.8 dB
Urban 16.5m	9.90°	1.3 dB
Urban > 16.5m	0°	0 dB

For each region, one could calculate the mean clutter loss, as a function of the elevation angle φ. It's worth noting that in the rural region the height of the IMT transmitter is 1.5 metres or 4.5 metres with 50% of probability each, while in the Urban region the height is 1.5 metres, 4.5 metres, 7.5 metres, 10.5 metres, 13.5 metres, 16.5 metres, 19.5 metres, 22.5 metres, 25.5 metres or 28.5 metres with 10% of probability each.

Therefore, fixed a region (urban or rural), the mean clutter loss can be calculated with the following formula:

$$Mean\ Clutter\ Loss(\varphi) = -10 \cdot \log\left(\sum_{h=1}^{H} P_h \cdot 10^{\frac{-CL_{h,\varphi}}{10}}\right)$$

where:

– φ is the elevation angle;

– H is the number of different options in the set of IMT heights (i.e. 2 for the rural area and 10 for the urban area);

– P_h is the probability to have a certain antenna height;

– $CL_{h,\varphi}$ is the clutter loss associated to the transmitter height and it depends on the elevation angle.

2.4 FSS GSO network characteristic

The satellite network is described by the following main parameters: the orbital position the receiving noise temperature, the peak gain and the specific gain over the considered cities.

The reference satellite is a typical spacecraft of the Inmarsat fleet, with a global C-band payload, mainly used for feeder links and telecommand. The satellite maximum receive gain is assumed to be 22 dBi and the satellite system noise temperature 500 K, equivalent to a G/T of around –5 dB/K on the beam peak. It's should be noted that Inmarsat footprints are global and therefore quite flat, with a gain range of about 4 dB from the peak to the edge. This antenna roll-off has been included in the model.

These characteristics are thought to be common in the FSS in this band. Some satellites using higher gain/regional beam antennas, which might lead to higher interference, have not been modelled here.

Additionally, since the aggregate interference strongly depends on the cities which are covered by the spacecraft footprint, the orbital position has been changed during the simulations and it was determined that the location 70°E was the worst case location, being the location where the satellite antenna beam is covering the most populated areas as China, India, Indonesia, Pakistan, Bangladesh and Russia.

3 Analysis

3.1 Methodology

The methodology used is similar to the one explained in Annex 3: the study is based on the estimation of the increment of the thermal noise into the wanted satellite receiver (ΔT), due to the aggregate interference created by the IMT stations simultaneously transmitting on the same band used by the earth-to-space FSS link. This amount of additional noise is then compared with that of the receiving wanted system (T), calculating the ratio ΔT/T, expressed in percentage (%).

Following the Recommendation ITU-R S.1432-1, the considered ΔT/T threshold for the maximum allowable aggregate interference originated by IMT systems is 6%.

For each city, the increase of temperature is computed as follows:

$$\Delta T\text{CITY} = \frac{e.i.r.p._{IMT} \cdot [G_{BA} \cdot P_{indoor} + (1 - P_{indoor})] \cdot G_{SAT,CITY} \cdot CL \cdot N_{IMT}}{\Delta f_{IMT} \cdot K \cdot 10^{\frac{L_{FSL}+L_{ATM}}{10}}}$$

where:

– $e.i.r.p._{IMT}$ is the equivalent isotropically radiated power of the IMT station, watt;

– $G_{SAT,CITY}$ is the gain of the satellite receiver in the direction of the considered city;

– CL is the clutter loss factor, in order to characterize the effect of ground clutter on the propagation path;

– N_{IMT} is the number of predicted IMT transmitters per each city:

$$N_{IMT} = M_{CITY} \cdot K_{DISS} \cdot K_{ACT} \cdot K_{\Delta f}$$

where

– M_{CITY} is the population of the city;

– Δf_{IMT} is the IMT signal channel bandwidth interfering on the wanted signal, Hz;

– G_{BA} is the building attenuation factor;

– K is the Boltzmann constant;

– L_{ATM} is the atmospheric loss (dB) computed using the Recommendation ITU-R P.676-3;

– L_{FSL} is the free-space loss (dB) computed according to the Recommendation ITU-R P.525-2.

For each city, the elevation, the gain of the satellite, the free-space loss and the atmospheric loss are calculated.

The population data have been extracted from the Wikipedia on-line database, which provides updated figures based on the most recent census. For the sake of simplicity, the whole population of each country has been thought to be concentrated in the capital city, except for those countries with very large territories. For the countries with largest areas – Russia, Canada, China, United States, Brazil, Australia, India and Argentina – a list of the cities with population over 1 million has been done and the total population of each country has been redistributed over these cities in a proportional way, so that the total population of the modelled cities is equal to the total population of the country.

In order to calculate the appropriate Clutter Loss factor, it's necessary to have for each country the percentages of the population living in urban areas. This data has been determined by the "World Resources Institute" and is available on-line at the following address:

http://www.theguardian.com/news/datablog/2009/aug/18/percentage-population-living-cities

A summarizing table (Table 2) of the used data is reported here below:

TABLE 2

Country	City	Population M_{CITY}	Urban population in 2015	Rural population in 2015	Site Latitude ϑ_T	Site Longitude λ_T
American Samoa	Pago Pago	55128	94.1	5.9	14.28°S	170.70°W
Antigua and Barbuda	St John's	81799	44.7	55.3	17.10°N	61.85°W
Argentina	Buenos Aires	22436134	91.6	8.4	34.60°S	58.45°W
Argentina	Córdoba	10090174	91.6	8.4	31.42°S	64.17°W
Argentina	Rosario	9134108	91.6	8.4	32.95°S	60.67°W
Australia	Sydney	7393567	89.9	10.1	33.87°S	151.22°E
Australia	Melbourne	6726748	89.9	10.1	37.82°S	144.97°E
Australia	Brisbane	3469044	89.9	10.1	27.47°S	153.03°E
Australia	Perth	3005956	89.9	10.1	31.93°S	115.83°E
Australia	Adelaide	2023205	89.9	10.1	34.93°S	138.60°E
Bahamas	Nassau	353658	92.2	7.8	25.08°N	77.35°W
Bahrain	Al Manamah	1234571	98.2	1.8	26.22°N	50.58°E
Bangladesh	Dhaka	152518016	29.9	70.1	23.72°N	90.42°E
Barbados	Bridgetown	277821	58.8	41.2	13.10°N	59.62°W
Belarus	Minsk	9460000	76.7	23.3	53.90°N	27.57°E
Belgium	Brussels	11041266	97.5	2.5	50.83°N	04.33°E
Belize	Belmopan	334297	51.2	48.8	17.25°N	88.77°W
Benin	Cotonou	9351838	44.6	55.4	06.35°N	02.43°E
Bermuda	Hamilton	64806	100	0	32.29°N	64.79°W

Bhutan	Thimphu	750443	14.8	85.2	27.47°N	89.65°E
Bolivia	La Paz	10461053	68.8	31.2	16.50°S	68.15°W
Bosnia	Bosna-sarai	3839737	51.8	48.2	43.83°N	18.42°E
Botswana	Gaborone	2053237	64.6	35.4	24.67°S	25.92°E
Brazil	São Paulo	53491810	88.2	11.8	23.53°S	46.62°W
Brazil	Rio de Janeiro	30080006	88.2	11.8	22.90°S	43.25°W
Brazil	Salvador	12733173	88.2	11.8	12.98°S	38.52°W
Brazil	Brasília	12192549	88.2	11.8	15.78°S	47.92°W
Brazil	Fortaleza	12139473	88.2	11.8	03.72°S	38.50°W
Brazil	Belo Horizonte	11300482	88.2	11.8	19.92°S	43.93°W
Brazil	Manaus	8574987	88.2	11.8	03.13°S	60.02°W
Brazil	Curitiba	8310348	88.2	11.8	25.42°S	49.25°W
Brazil	Recife	7311515	88.2	11.8	08.05°S	34.90°W
Brazil	Porto Alegre	6707374	88.2	11.8	30.07°S	51.18°W
Brazil	Belém	6622182	88.2	11.8	01.45°S	48.48°W
Brazil	Goiânia	6193371	88.2	11.8	16.67°S	49.27°W
Brazil	Guarulhos	5815007	88.2	11.8	23.47°S	46.53°W
Brazil	Campinas	5142537	88.2	11.8	22.90°S	47.08°W
Brazil	São Gonçalo	4833932	88.2	11.8	22.85°S	43.07°W
Brazil	São Luís	4814024	88.2	11.8	02.52°S	44.27°W
Brazil	Maceió	4769934	88.2	11.8	09.67°S	35.72°W
Brunei	Bandar Seri Begawan	412892	77.6	22.4	04.88°N	114.93°E
Bulgaria	Sofia	7364570	72.8	27.2	42.68°N	23.32°E
Burkina Faso	Ouagadouga	17481984	22.8	77.2	12.37°N	01.52°W
Burma	Dagon	50020000	37.4	62.6	16.80°N	96.15°E
Burundi	Cibitoke	8749387	13.5	86.5	02.88°S	29.12°E
Cambodia	Phnom Penh	14478320	26.1	73.9	11.55°N	104.92°E
Cameroon	Douala	20468944	62.7	37.3	04.05°N	09.70°E
Canada	Toronto	12802999	81.4	18.6	45.42°N	75.70°W
Canada	Montreal (Laval)	8769646	81.4	18.6	43.65°N	79.38°W
Canada	Vancouver (Surrey)	5304889	81.4	18.6	45.52°N	73.57°W
Canada	Ottawa - Gatineau	2835119	81.4	18.6	49.27°N	123.12°W
Canada	Calgary	2785850	81.4	18.6	45.42°N	75.70°W
Canada	Edmonton	2659794	81.4	18.6	51.05°N	114.08°W
Cape Verte	Praia	429474	64.3	35.7	14.92°N	23.52°W
Central African Republic	Bangui	4575586	40.4	59.6	53.55°N	113.47°W
Chad	Tandjile	11274106	30.5	69.5	09.68°N	16.72°E
Chile	Santiago	17402630	90.1	9.9	33.45°S	70.67°W
China	Guangzhou	143687218	49.2	50.8	23.12°N	113.30°E

China	Shanghai	90717675	49.2	50.8	33.27°N	114.25°E
China	Beijing	64181225	49.2	50.8	39.92°N	116.38°E
China	Shantou	37728300	49.2	50.8	23.43°N	116.70°E
China	Tianjin	33383192	49.2	50.8	39.13°N	117.20°E
China	Chengdu	29874582	49.2	50.8	30.75°N	104.07°E
China	Hangzhou	26459400	49.2	50.8	30.30°N	120.18°E
China	Wuhan	23671379	49.2	50.8	39.53°N	106.92°E
China	Xi'an	23252472	49.2	50.8	34.25°N	108.83°E
China	Nanjing	23245410	49.2	50.8	31.98°N	118.85°E
China	Shenyang	22649611	49.2	50.8	33.78°N	120.25°E
China	Chongqing	21984729	49.2	50.8	29.57°N	106.45°E
China	Quanzhou	19692951	49.2	50.8	24.95°N	118.58°E
China	Wenzhou	18988316	49.2	50.8	27.95°N	120.63°E
China	Qingdao	18699282	49.2	50.8	36.08°N	120.35°E
China	Harbin	17134682	49.2	50.8	45.75°N	126.62°E
China	Xiamen	16591892	49.2	50.8	24.53°N	118.10°E
China	Zhengzhou	15789442	49.2	50.8	34.70°N	113.68°E
China	Jinan	14065335	49.2	50.8	36.58°N	117.00°E
China	Nanchang	13325921	49.2	50.8	28.67°N	115.97°E
China	Changsha	13214599	49.2	50.8	28.20°N	113.03°E
China	Taiyuan	13177385	49.2	50.8	37.83°N	112.62°E
China	Shijiazhuang	12960421	49.2	50.8	38.00°N	114.50°E
China	Dalian	11950429	49.2	50.8	38.92°N	121.65°E
China	Kunming	11624375	49.2	50.8	25.13°N	102.72°E
China	Wuxi	11491017	49.2	50.8	31.53°N	120.30°E
China	Changchun	11451429	49.2	50.8	43.85°N	125.33°E
China	Ningbo	11326479	49.2	50.8	29.92°N	121.47°E
China	Zibo	11304430	49.2	50.8	36.80°N	118.07°E
China	Hefei	10873883	49.2	50.8	31.78°N	117.25°E
China	Changzhou	10674291	49.2	50.8	31.77°N	119.93°E
China	Taizhou	10605364	49.2	50.8	32.48°N	119.92°E
China	Tangshan	10338944	49.2	50.8	39.58°N	118.15°E
China	Nantong	10318679	49.2	50.8	32.00°N	120.87°E
China	Nanning	10307410	49.2	50.8	22.83°N	108.30°E
China	Guiyang	9852316	49.2	50.8	26.63°N	106.72°E
China	Ürümqi	9695167	49.2	50.8	43.80°N	87.58°E
China	Fuzhou	9477980	49.2	50.8	27.97°N	116.33°E
China	Huai'an	8542617	49.2	50.8	33.50°N	119.13°E
China	Xuzhou	8509029	49.2	50.8	34.20°N	117.22°E
China	Linyi	8434854	49.2	50.8	37.18°N	116.85°E
China	Lanzhou	8084915	49.2	50.8	36.05°N	103.68°E
China	Yangzhou	7782432	49.2	50.8	32.33°N	119.42°E
China	Anshan	7261461	49.2	50.8	41.13°N	122.98°E

China	Haikou	6637684	49.2	50.8	20.08°N	110.33°E
China	Yiwu	6612417	49.2	50.8	29.32°N	120.07°E
China	Baotou	6601374	49.2	50.8	40.63°N	110.00°E
China	Liuzhou	6484444	49.2	50.8	24.37°N	109.33°E
China	Anyang	6474096	49.2	50.8	36.02°N	114.42°E
China	Hohhot	6425482	49.2	50.8	40.85°N	111.63°E
China	Jilin City	6409357	49.2	50.8	43.85°N	126.55°E
China	Putian	6337984	49.2	50.8	25.53°N	119.02°E
China	Xiangtan	6083332	49.2	50.8	27.90°N	112.92°E
China	Yantai	6068086	49.2	50.8	37.47°N	121.40°E
China	Luoyang	6023570	49.2	50.8	34.68°N	112.42°E
China	Huainan	5954081	49.2	50.8	32.53°N	116.98°E
China	Nanyang	5877123	49.2	50.8	32.93°N	112.53°E
China	Baoding	5805166	49.2	50.8	38.78°N	115.50°E
China	Nanchong	5747975	49.2	50.8	30.78°N	106.05°E
China	Fuyang	5738331	49.2	50.8	32.78°N	115.77°E
China	Tai'an	5629832	49.2	50.8	41.40°N	122.45°E
China	Suzhou	5344827	49.2	50.8	31.27°N	120.62°E
China	Lu'an	5334128	49.2	50.8	31.73°N	116.50°E
China	Datong	5284467	49.2	50.8	40.15°N	113.28°E
China	Zhanjiang	5230180	49.2	50.8	21.22°N	110.38°E
China	Tengzhou	5202282	49.2	50.8	35.08°N	117.15°E
China	Huangshi	5195752	49.2	50.8	30.20°N	115.00°E
China	Jiangyin	5173506	49.2	50.8	31.92°N	120.28°E
China	Weifang	4935956	49.2	50.8	36.72°N	119.10°E
China	Yinchuan	4908548	49.2	50.8	38.47°N	106.32°E
China	Changshu	4898661	49.2	50.8	31.63°N	120.73°E
China	Zhuhai	4865887	49.2	50.8	29.73°N	113.12°E
China	Dengzhou	4762280	49.2	50.8	37.73°N	120.75°E
China	Cixi	4743861	49.2	50.8	30.17°N	121.23°E
China	Changde	4731381	49.2	50.8	29.07°N	111.70°E
China	Pizhou	4729759	49.2	50.8	34.34°N	118.01°E
China	Zhangzhou	4713861	49.2	50.8	24.63°N	117.65°E
China	Datong	4695743	49.2	50.8	40.15°N	113.28°E
China	Baoji	4664122	49.2	50.8	34.43°N	107.20°E
China	Suqian	4663745	49.2	50.8	33.92°N	118.22°E
China	Daqing	4591023	49.2	50.8	46.67°N	125.00°E
China	Bozhou	4572104	49.2	50.8	33.87°N	115.75°E
China	Handan	4552651	49.2	50.8	36.58°N	114.47°E
China	Panjin	4517143	49.2	50.8	41.12°N	122.05°E
China	Wenling	4433796	49.2	50.8	28.38°N	121.37°E
China	Ma'anshan	4432181	49.2	50.8	31.63°N	118.50°E
China	Zigong	4418427	49.2	50.8	29.33°N	104.80°E

China	Mianyang	4396592	49.2	50.8	31.38°N	104.82°E
China	Yingkou	4384226	49.2	50.8	40.67°N	122.20°E
China	Yichang	4379785	49.2	50.8	30.70°N	111.37°E
China	Heze	4368594	49.2	50.8	35.23°N	115.47°E
China	Chifeng	4325858	49.2	50.8	42.27°N	118.95°E
China	Guilin	4302969	49.2	50.8	25.35°N	110.25°E
China	Xiangyang	4200013	49.2	50.8	34.43°N	108.67°E
China	Rugao	4110267	49.2	50.8	32.40°N	120.57°E
China	Xuchang	4105038	49.2	50.8	34.00°N	113.97°E
China	Wuhu	4102069	49.2	50.8	31.30°N	118.45°E
China	Neijiang	4058458	49.2	50.8	29.63°N	104.97°E
China	Zhangjiagang	4049761	49.2	50.8	37.53°N	108.75°E
China	Yixing	4007791	49.2	50.8	31.35°N	119.80°E
China	Fuqing	4005722	49.2	50.8	25.78°N	119.40°E
China	Zhaoqing	3998789	49.2	50.8	23.07°N	112.47°E
China	Xinyang	3989895	49.2	50.8	32.08°N	114.12°E
China	Liaocheng	3989379	49.2	50.8	36.45°N	115.97°E
China	Maoming	3950176	49.2	50.8	21.68°N	110.87°E
China	Panzhihua	3938449	49.2	50.8	26.58°N	101.71°E
China	Jiaxing	3898873	49.2	50.8	30.73°N	120.77°E
China	Haicheng	3896632	49.2	50.8	40.85°N	122.72°E
China	Zhenjiang	3894007	49.2	50.8	32.05°N	119.43°E
China	Xining	3887208	49.2	50.8	36.62°N	101.77°E
China	Tianshui	3883542	49.2	50.8	34.58°N	105.72°E
China	Taixing	3867449	49.2	50.8	32.17°N	120.00°E
China	Huazhou	3824175	49.2	50.8	21.63°N	110.58°E
China	Qujing	3801247	49.2	50.8	25.52°N	103.75°E
China	Dingzhou	3779763	49.2	50.8	38.52°N	114.98°E
China	Zhuji	3756141	49.2	50.8	29.72°N	120.22°E
China	Xingtai	3747379	49.2	50.8	37.00°N	114.50°E
China	Jingzhou	3743768	49.2	50.8	30.35°N	112.17°E
China	Shouguang	3696128	49.2	50.8	36.88°N	118.73°E
China	Yuzhou	3671536	49.2	50.8	29.57°N	106.45°E
China	Bazhong	3655222	49.2	50.8	31.90°N	106.70°E
China	Zoucheng	3622491	49.2	50.8	35.40°N	116.97°E
China	Jining	3617949	49.2	50.8	41.03°N	113.12°E
China	Huaibei	3611530	49.2	50.8	33.93°N	116.80°E
China	Zunyi	3552711	49.2	50.8	27.67°N	106.93°E
China	Guigang	3523963	49.2	50.8	26.63°N	106.72°E
China	Zhucheng	3523551	49.2	50.8	35.97°N	119.47°E
China	Jinhua	3494680	49.2	50.8	29.15°N	119.63°E
China	Hengyang	3488893	49.2	50.8	26.93°N	112.58°E
China	Zhangqiu	3452185	49.2	50.8	36.73°N	117.55°E

China	Zhuzhou	3423551	49.2	50.8	27.87°N	113.20°E
China	Lianyungang	3405573	49.2	50.8	34.63°N	119.45°E
China	Ezhou	3360625	49.2	50.8	30.40°N	114.88°E
China	Pingdingshan	3354137	49.2	50.8	33.68°N	113.45°E
China	Qinhuangdao	3340172	49.2	50.8	40.00°N	119.53°E
China	Linhai	3337350	49.2	50.8	51.60°N	124.37°E
China	Wuwei	3277321	49.2	50.8	31.28°N	117.90°E
China	Hezhou	3261766	49.2	50.8	24.42°N	111.55°E
China	Zaoyang	3259304	49.2	50.8	32.13°N	112.75°E
China	Xiangcheng	3255687	49.2	50.8	33.85°N	113.48°E
Colombia	Bogota	47072915	75.7	24.3	04.60°N	74.00°W
Comoro Islands	Moroni	753943	44	56	11.68°S	43.27°E
Cook Islands	Avarua	10900	76.7	23.3	21.22°S	159.81°W
Costa Rica	San Jose	4586353	66.9	33.1	09.93°N	74.10°W
Cote-d'Ivoire	Abidjan	20594616	49.8	50.2	05.32°N	04.03°W
Croatia	Zagreb	4398150	59.5	40.5	45.80°N	16.00°E
Cuba	Havana	11167325	74.7	25.3	23.13°N	82.37°W
Cyprus	Lemesos	862011	71.5	28.5	34.67°N	33.03°E
Czech Republic	Praha	10507566	74	26	50.08°N	14.43°E
Denmark	Copenhagen	5580516	86.9	13.1	55.67°N	12.58°E
Djibouti	Jibuti	922708	89.6	10.4	11.58°N	43.13°E
Dominica	Roseau	72660	76.4	23.6	15.30°N	61.40°W
Dominican Republic	Santo Domingo	9445281	73.6	26.4	18.47°N	69.90°W
DRC	Kinshasa	69575392	38.6	61.4	04.33°S	15.31°E
East Timor	Dili	1066409	31.2	68.8	08.56°S	125.57°E
Ecuador	Quito	15223680	67.6	32.4	00.22°S	78.50°W
Egypt	Al Qahirah	83063000	45.4	54.6	30.05°N	31.25°E
El Salvador	San Salvador	6134000	63.2	36.8	13.70°N	89.20°W
Equatorial Guinea	Bata	740471	41.1	58.9	01.85°N	09.75°E
Eritrea	Asmara	5580862	24.3	75.7	15.32°N	38.95°E
Estonia	Tallinn	1339662	70.1	29.9	59.42°N	24.75°E
Ethiopia	Addis Abeba	91195672	19.1	80.9	09.02°N	38.77°E
Fiji	Suva	874742	56.1	43.9	18.13°S	178.45°E
Finland	Helsinki	5426300	62.7	37.3	60.17°N	24.97°E
France	Paris	63468168	79	21	48.87°N	02.33°E
French Polynesia	Papete	268270	52.3	47.7	17.65°S	149.44°W
Gabon	Libreville	1563873	87.7	12.3	00.38°N	09.45°E
Gambia	Banjul	1782893	61.8	38.2	13.45°N	16.58°W
Georgia	Tbilisi	4497600	53.8	46.2	41.71°N	44.80°E
Germany	Berlin	81843808	76.3	23.7	52.52°N	13.37°E

Ghana	Accra	25545940	55.1	44.9	05.55°N	00.22°W
Gibraltar	Gibraltar	29441	100	0	36.03°N	05.60°E
Greece	Athens	11290785	61	39	37.98°N	23.73°E
Greenland	Nuuk	56370	85.5	14.5	64.16°N	51.71°W
Grenada	St George's	109590	32.2	67.8	12.05°N	61.75°W
Guam	Hagatha	184334	95.3	4.7	13.47°N	144.75°E
Guatemala	Guatemala C.	15438384	52	48	14.63°N	90.52°W
Guernsey	St.Peter Port	61811	31.5	68.5	49.47°N	02.54°W
Guinea	Conakry	10057975	38.1	61.9	09.52°N	13.72°W
Guinea-Bissau	Bissau	1533964	31.1	68.9	11.85°N	15.58°W
Guyana	George Town	739903	29.4	70.6	06.80°N	58.17°W
Haiti	Port-Au-Prince	9719932	45.5	54.5	18.53°N	72.33°W
Honduras	Tegucigalpa	8249574	51.4	48.6	14.10°N	87.22°W
Hong Kong	Hong Kong	7136300	100	0	22.29°N	114.16°E
Hungary	Budapest	9962000	70.3	29.7	47.50°N	19.08°E
Iceland	Reykjavik	307261	93.6	6.4	64.15°N	21.95°W
India	Mumbai	126501820	32	68	18.97°N	72.83°E
India	Delhi	111593306	32	68	28.67°N	77.22°E
India	Chennai	91046895	32	68	13.08°N	80.28°E
India	Bangalore	85419326	32	68	12.98°N	77.58°E
India	Hyderabad	69036924	32	68	17.38°N	78.47°E
India	Ahmedabad	56472503	32	68	23.03°N	72.62°E
India	Kolkata	45484270	32	68	22.53°N	88.37°E
India	Surat	45234104	32	68	21.17°N	72.83°E
India	Pune	31583072	32	68	18.53°N	73.87°E
India	Jaipur	31156470	32	68	26.92°N	75.82°E
India	Lucknow	28543508	32	68	26.85°N	80.92°E
India	Kanpur	28051123	32	68	26.47°N	80.35°E
India	Nagpur	24385256	32	68	21.15°N	79.10°E
India	Indore	19876142	32	68	22.72°N	75.83°E
India	Thane	18439042	32	68	19.20°N	72.97°E
India	Bhopal	18203606	32	68	23.27°N	77.40°E
India	Visakhapatnam	17541335	32	68	17.70°N	83.30°E
India	Pimpri-Chinchwad	17531593	32	68	18.50°N	73.75°E
India	Patna	17063650	32	68	25.60°N	85.12°E
India	Vadodara	16896410	32	68	22.30°N	73.20°E
India	Ghaziabad	16585844	32	68	28.67°N	77.43°E
India	Ludhiana	16360890	32	68	30.90°N	75.85°E
India	Agra	15962116	32	68	27.18°N	78.02°E
India	Nashik	15074375	32	68	20.08°N	73.80°E
India	Faridabad	14239845	32	68	28.42°N	77.31°E
India	Meerut	13270384	32	68	28.98°N	77.70°E

India	Rajkot	13047073	32	68	22.30°N	70.78°E
India	Kalyan-Dombivali	12635343	32	68	19.25°N	73.15°E
India	Vasai-Virar	12380402	32	68	19.47°N	72.80°E
India	Solapur	12195066	32	68	17.68°N	75.92°E
India	Varanasi	12183550	32	68	25.33°N	83.00°E
India	Srinagar	12092078	32	68	34.08°N	74.82°E
India	Aurangabad	11874504	32	68	19.88°N	75.33°E
India	Dhanbad	11775470	32	68	23.80°N	86.45°E
India	Amritsar	11483506	32	68	31.58°N	74.88°E
India	Navi Mumbai	11348838	32	68	19.01°N	73.01°E
India	Allahabad	11324680	32	68	25.45°N	81.85°E
India	Ranchi	10882132	32	68	23.35°N	85.33°E
India	Howrah	10869166	32	68	22.59°N	88.31°E
India	Coimbatore	10760551	32	68	11.00°N	76.97°E
India	Jabalpur	10688463	32	68	23.17°N	79.95°E
India	Gwalior	10680038	32	68	26.22°N	78.17°E
India	Vijayawada	10626664	32	68	16.52°N	80.62°E
India	Jodhpur	10481473	32	68	26.28°N	73.03°E
India	Madurai	10308799	32	68	09.93°N	78.12°E
India	Raipur	10239883	32	68	21.23°N	81.63°E
India	Kota	10151463	32	68	25.27°N	75.92°E
Indonesia	Medan	245641328	58.5	41.5	03.58°N	98.67°E
Iran	Tehran	77002704	71.9	28.1	35.67°N	51.43°E
Iraq	Baghdad	33703068	66.9	33.1	33.35°N	44.38°E
Ireland	Dublin	4234925	63.8	36.2	53.33°N	06.25°W
Isle of Man	Doolish	83739	52.8	47.2	54.15°N	04.50°W
Israel	Jerusalem	7836000	91.9	8.1	31.77°N	35.23°E
Italy	Rome	60820764	69.5	30.5	41.90°N	12.48°E
Jamaica	Kingston	2889187	56.7	43.3	18.00°N	76.83°W
Japan	Tokyo	127561000	68.2	31.8	35.67°N	139.77°E
Jordan	Amman	6390500	85.3	14.7	31.95°N	35.93°E
Kiribati	South Tarawa	103500	55.4	44.6	01.33°N	172.98°E
Laos	Nakhon Viangchan	6348800	24.9	75.1	17.97°N	102.60°E
Latvia	Riga	2049500	68.9	31.1	56.95°N	24.10°E
Lebanon	Beirut	4291719	87.9	12.1	33.88°N	35.50°E
Lesoto	Maseru	2216850	22	78	29.47°S	27.48°E
Liberia	Monrovia	3476608	64.8	35.2	06.32°N	10.80°W
Libya	Tripoli	6469497	87.4	12.6	32.90°N	13.18°E
Liechtenstein	Vaduz	36476	14.7	85.3	47.13°N	09.50°E
Lithuania	Vilnius	2988400	66.8	33.2	54.68°N	25.32°E
Luxemburg	Luxemburg	524853	82.1	17.9	49.75°N	06.08°E

Marshall Islands	Majuro	68000	69.3	30.7	07.09°N	171.38°E
Mauritania	Nouakchott	3129486	43.1	56.9	18.12°N	15.98°W
Mexico	Mexico City	118395054	78.7	21.3	19.40°N	99.15°W
Montenegro	Podgorica	632796	55.1	44.9	42.44°N	19.27°E
Namibia	Windhoek	2364433	41.1	58.9	22.57°S	17.10°E
Nauru	Yaren	9378	100	0	00.53°S	166.93°E
Nepal	Katmandu	31011136	20.9	79.1	27.72°N	85.32°E
New Caledonia	Nourrea	256000	67.4	32.6	22.28°S	166.46°E
New Zealand	Wellington	4468200	87.4	12.6	41.30°S	174.80°E
Nicaragua	Managua	6071045	63	37	12.15°N	86.28°W
Niger	Niamey	16644339	19.3	80.7	13.52°N	02.12°E
Nigeria	Lagos	166629376	55.9	44.1	06.45°N	03.38°E
Niue	Alofi	1398	43.2	56.8	19.05°S	169.87°W
North Korea	Pyongyang	24760000	65.5	34.5	38.42°N	127.28°E
N.Mariana I.	Saipan	62152	95.9	4.1	15.19°N	145.75°E
Norway	Oslo	5049100	78.6	21.4	59.92°N	10.75°E
Pakistan	Karachi	177791008	39.6	60.4	24.87°N	67.05°E
Palau	Ngerulmud	20956	70.9	29.1	07.50°N	134.57°E
Panama	Panama City	3661868	77.9	22.1	08.97°N	79.52°W
P.N. Guinea	Port Moresby	7170112	15	85	09.50°S	147.12°E
Paraguay	Asuncion	6800000	64.4	35.6	25.27°S	57.67°W
Peru	Lima	30475144	74.9	25.1	12.05°S	77.05°W
Philippines	Manila	103775000	69.6	30.4	14.58°N	121.00°E
Poland	Warsaw	38208616	64	36	52.25°N	21.00°E
Portugal	Lisbon	10409995	63.6	36.4	38.72°N	09.13°W
Puerto Rico	San Juan	3725789	99.3	0.7	18.46°N	66.10°W
Qatar	Doha	1699435	96.2	3.8	25.28°N	51.53°E
Reunion	Saint-Denis	816364	95	5	20.88°S	55.45°E
Romania	Bucuresti	21355848	56.1	43.9	44.43°N	26.10°E
Russian Federation	Moscow	58504188	72.6	27.4	55.75°N	37.58°E
Russian Federation	Saint Petersburg	24636407	72.6	27.4	59.92°N	30.25°E
Russian Federation	Novosibirsk	7488042	72.6	27.4	55.03°N	82.92°E
Russian Federation	Yekaterinburg	6860027	72.6	27.4	56.85°N	60.60°E
Russian Federation	Nizhny Novgorod	6354362	72.6	27.4	57.63°N	45.08°E
Russian Federation	Samara	5918824	72.6	27.4	53.20°N	50.15°E
Russian Federation	Omsk	5863314	72.6	27.4	55.00°N	73.40°E

Russian Federation	Kazan	5810345	72.6	27.4	55.75°N	49.13°E
Russian Federation	Chelyabinsk	5742905	72.6	27.4	55.17°N	61.40°E
Russian Federation	Rostov-on-Don	5537521	72.6	27.4	47.23°N	39.70°E
Russian Federation	Ufa	5397535	72.6	27.4	54.73°N	55.93°E
Russian Federation	Volgograd	5188930	72.6	27.4	48.73°N	44.42°E
Rwanda	Kigali	10718379	28.7	71.3	01.95°S	30.07°E
Saint Kitts and Navis	Besseterre	51300	33.5	66.5	17.30°N	62.72°W
Saint Lucia	Castries	173765	50	50	14.02°N	61.00°W
Saint Vincent and the Grenadines	Kingstown	103000	50	50	13.15°N	61.23°W
Samoa	Apia	194320	24.9	75.1	13.64°S	172.41°W
San Marino	San Marino	31945	99.3	0.7	43.92°N	12.47°E
Sao Tome and Principe	Sao Tome	171878	65.8	34.2	00.33°N	06.73°E
Saudi Arabia	Riyadh	28705132	83.2	16.8	24.72°N	46.72°E
Senegal	Dakar	13711597	44.7	55.3	14.67°N	17.43°W
Serbia	Kosovo	9846582	55.1	44.9	42.67°N	21.17°E
Seychelles	Victoria	87169	58.2	41.8	04.63°S	55.45°E
Sierra Leone	Freetown	6440053	48.2	51.8	08.50°N	13.25°W
Singapore	Singapore	5183700	100	0	01.30°N	103.87°E
Slovakia	Bratislava	5404322	58	42	48.15°N	17.12°E
Slovenia	Ljubljana	2062650	53.3	46.7	46.03°N	14.50°E
Solomon Islands	Honiara	523000	20.5	79.5	09.40°S	159.90°E
Somali	Mogadishu	9797445	40.1	59.9	02.05°N	45.37°E
South Africa	Pretoria	51770560	64.1	35.9	25.75°S	28.17°E
South Korea	Seoul	48580000	83.1	16.9	37.57°N	127.00°E
South Sudan	Djuba	8260490	49.4	50.6	04.85°N	31.60°E
Spain	Madrid	46163116	78.3	21.7	40.40°N	03.68°W
Sri Lanka	Colombo	21223550	15.7	84.3	06.93°N	79.85°E
Sudan	Umm Durman	30894000	49.4	50.6	15.63°N	32.50°E
Suriname	Paramaribo	566846	77.4	22.6	05.83°N	55.17°W
Swaziland	Manzini	1220408	27.5	72.5	26.48°S	31.37°E
Sweden	Stockholm	9540065	85.1	14.9	59.33°N	18.05°E
Switzerland	Geneve	7952600	78.7	21.3	46.17°N	06.17°E
Syria	Aleppo	21117690	53.4	46.6	36.21°N	37.15°E
The Gaza Strip	Khan Yunis	4168858	72.9	27.1	31.35°N	34.30°E
Netherlands	Amsterdam	16804900	84.9	15.1	52.37°N	04.90°E

The Republic of Congo	Brazzaville	4233063	64.2	35.8	04.26°S	15.28°E
Tonga	Nuku'alofa	103036	27.4	72.6	21.18°S	175.18°W
Trinidad and Tobago	Port of Spain	1346350	15.8	84.2	10.65°N	61.52°W
UAE	Dubayy	4800250	77.4	22.6	25.30°N	55.30°E
Uganda	Kampala	35620976	14.5	85.5	00.32°N	32.58°E
Ukraine	Kiev	45560256	70.2	29.8	50.43°N	30.52°E
United Kingdom	London	62989552	90.6	9.4	51.50°N	00.17°W
United States	New York	109957572	83.7	16.3	40.66°N	73.94°W
United States	Los Angeles	50882767	83.7	16.3	34.02°N	118.41°W
United States	Chicago	35807823	83.7	16.3	41.84°N	87.68°W
United States	Houston	28500332	83.7	16.3	29.78°N	95.39°W
United States	Philadelphia	20412293	83.7	16.3	40.01°N	75.13°W
United States	Phoenix	19635994	83.7	16.3	33.57°N	112.09°W
United States	San Antonio	18240549	83.7	16.3	29.47°N	98.53°W
United States	San Diego	17652254	83.7	16.3	32.82°N	117.14°W
United States	Dallas	16370411	83.7	16.3	32.78°N	96.80°W
Uruguay	Montevideo	3324460	93.1	6.9	34.88°S	56.18°W
Uzbekistan	Tashkent	29874600	38	62	41.33°N	69.30°E
Vanuatu	Port Vila	224564	28.1	71.9	17.76°S	168.31°E
Vatican City	Vatican City	900	100	0	41.90°N	12.48°E
Venezuela	Caracas	28946101	95.9	4.1	10.50°N	66.93°W
Vietnam	Ho Chi Minh C.	90549392	31.6	68.4	10.75°N	106.67°E
Western Sahara	Laayoun	513000	92.4	7.6	27.15°N	13.20°W
Yemen	Sanaa	25569264	31.9	68.1	15.38°N	44.20°E
Zambia	Lusaka	13883577	37	63	15.41°S	28.30°E
Zimbabwe	Harare	13013678	40.9	59.1	17.82°S	31.06°E
Afghanistan	Kabul	33397058	27	73	34.52°N	69.20°E
Albania	Tirana	2831741	52.8	47.2	41.33°N	19.83°E
Algeria	Algiers	36485828	69.3	30.7	36.78°N	03.05°E
Andorra	Andorra La Vella	78115	87.8	12.2	42.52°N	01.52°E
Angola	Luanda	20162516	59.7	40.3	08.80°S	13.23°E
Armenia	Yerevan	3277500	64.1	35.9	40.18°N	44.50°E
Austria	Wien	8452835	67.7	32.3	48.20°N	16.37°E
Azerbaijan	Baku	9235100	52.8	47.2	40.38°N	49.85°E
Kenia	Nairobi	42749416	24.1	75.9	01.28°S	36.82°E
Kirgizstan	Bishkek	5477600	38.1	61.9	42.90°N	74.60°E
Kuwait	Al Kuwait	2891553	98.5	1.5	29.33°N	47.98°E
Kazakhstan	Almaty	16856000	60.3	39.7	43.25°N	76.95°E
Madagaskar	Antananarivo	21928518	30.1	69.9	18.92°S	47.50°E
Maldives	Male	324313	34.8	65.2	04.17°N	73.51°E

Mozambique	Maputo	23700716	42.4	57.6	25.97°S	32.57°E
Macao	Macau	542200	100	0	22.20°N	113.55°E
Macedonia	Skopje	2057284	75.1	24.9	42.00°N	21.48°E
Malawi	Lilongwe	15882815	22.1	77.9	13.98°S	33.78°E
Malaysia	Kuala Lumpur	29562236	75.4	24.6	03.17°N	101.70°E
Mali	Bamako	14517176	36.5	63.5	12.63°N	08.00°W
Malta	Birkirkara	420085	97.2	2.8	35.91°N	14.46°E
Marocco	Casablanca	32783000	65	35	33.60°N	07.62°W
Mauritius	Port Louis	1280294	44.1	55.9	20.17°S	57.50°E
Mayotte	Mamoudzou	217172	100	0	12.78°S	45.23°E
Moldova	Chisinau	3559500	50	50	46.98°N	28.87°E
Monaco	Monaco	35444	100	0	43.73°N	07.42°E
Mongolia	Da Huryee	2736800	58.8	41.2	47.92°N	106.92°E
Oman	As Sib	2773479	72.3	27.7	23.67°N	58.20°E
Taiwan	Taipei	23282670	49.2	50.8	25.05°N	121.50°E
Thailand	Bangkok	65479452	36.2	63.8	13.75°N	100.52°E
Tunisia	Tunes	10673800	69.1	30.9	36.80°N	10.18°E
Turkey	Constantinople	74724272	71.9	28.1	41.02°N	28.97°E
Turkmenistan	Asgabat	5169660	50.8	49.2	37.95°N	58.38°E
Tajikistan	Djuschambe	7800000	24.6	75.4	38.58°N	68.80°E
Tanzania	Dar Es Salaam	47656368	28.9	71.1	06.80°S	39.28°E
Togo	Lome	5753324	47.4	52.6	06.13°N	01.22°E

3.2 Results

Figure 2 shows the behaviour of the relative increase of the noise temperature with the increase of e.i.r.p. for three different dissemination factors (K_{DISS}): 3% (blue line), 6% (green line) and 10% (black line). The ΔT/T threshold (displayed in red) has been set at 6%, based on Appendix **S8** of if the ITU Radio Regulations and consistent with the interference criterion in Recommendation ITU-R S.1432-1. The activity factor is 20%, meaning that only one IMT over five is active. It can be noted that a maximum e.i.r.p. of 12 dBm is required to meet the criterion in the three cases.

FIGURE 2

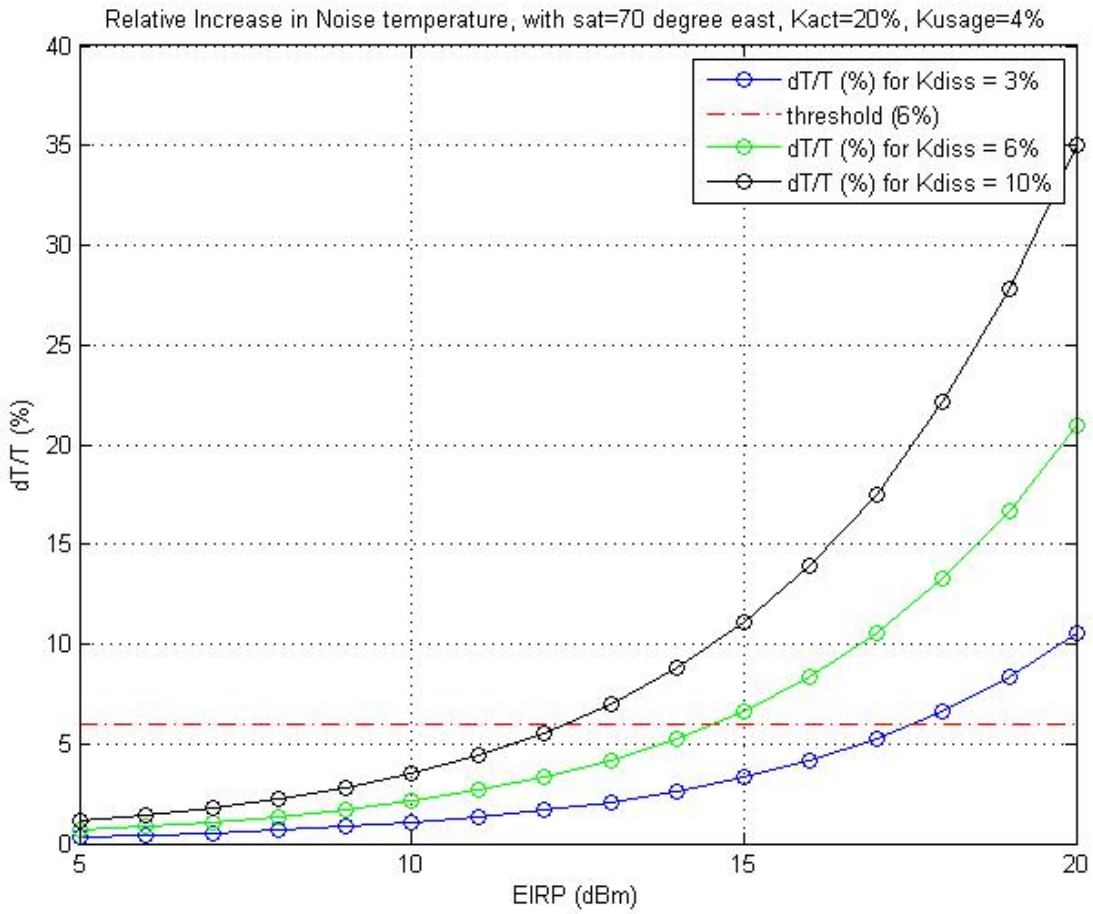

Figure 3 shows the relative increase in Noise Temperature using more conservative assumptions in regards to the active IMT stations: the activity factor in the graph below is 50%, i.e. one active IMT base station in every two deployed. It can be noted that a maximum e.i.r.p. of 8 dBm is required to meet the criterion in the three cases.

FIGURE 3

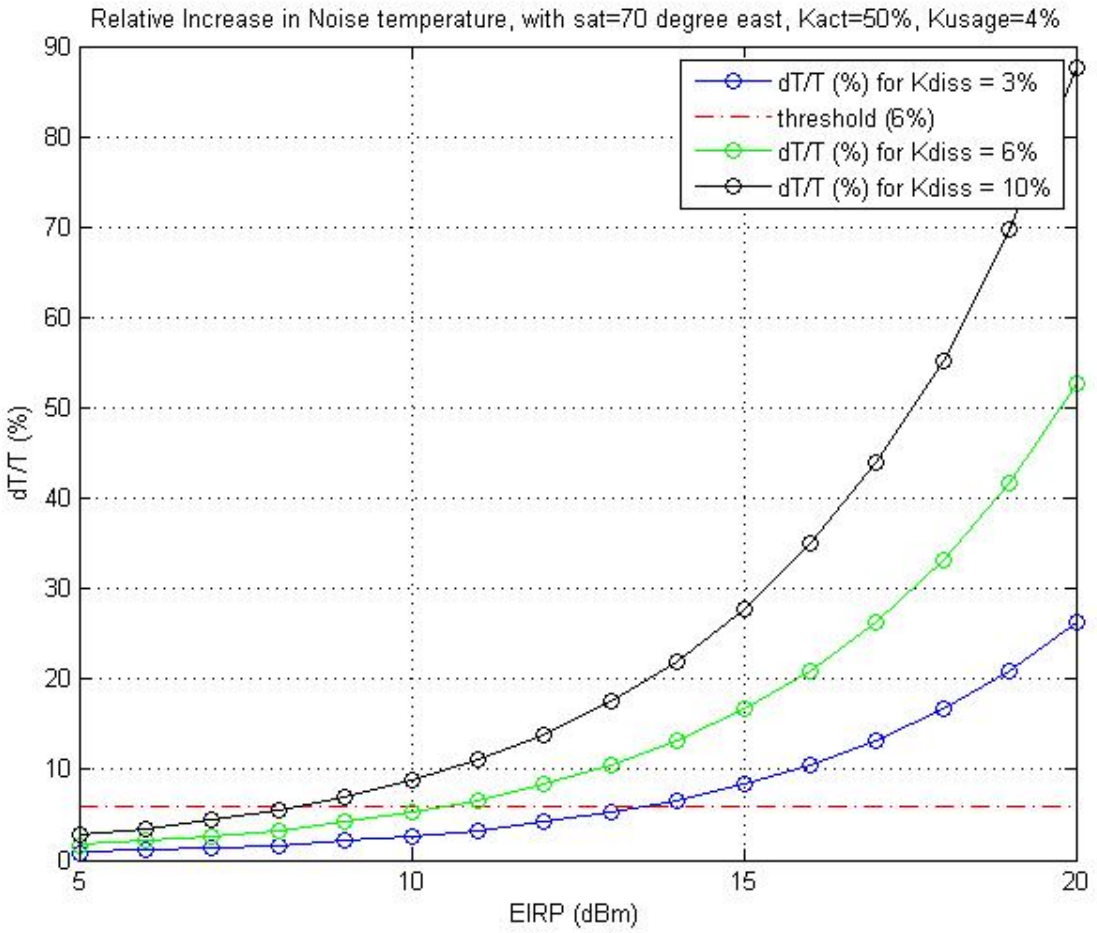

4 Conclusions

The results of the study suggest the maximum power of the IMT transmitters that can be deployed without harmfully affecting the operation of the FSS networks.

It can be seen that the assumption of several hypotheses (such as the spacecraft orbital position, the IMT stations dissemination, the activity of the IMT transmitters) have a significant impact on the analysis outcome. These factors are difficult to predict but it would be sensible to make conservative assumptions in this regard (i.e. high values for dissemination and activity), since if interference above the criterion were to occur, it would not practically be possible for an administration to take action to reduce interference. We have tentatively used the following assumptions:

– a dissemination factor (K_{DISS}) of 6% of the population;

– an area activity factor (K_{ACTIVE}) of 50% of base stations simultaneously switched on in the reference band;

Further study would be required to validate these and other assumptions, including the assumption that IMT stations are almost exclusively deployed indoors, before any decision is taken to allow IMT use of the band under study. The above calculations have been produced for a generic FSS network, using the coverage of Inmarsat-3 satellites (Global C-Band), considered being located at different orbital positions. These FSS characteristics are quite typical of FSS networks which use a

"global" beam. Some FSS networks use smaller, regional beams which have a higher gain, but over a reduced area. Such networks have not been modelled here, but might lead to worse results.

Significant increase of Noise Temperature is shown even considering 95% of indoor base stations: assuming that each single base station will use only one 20 MHz channel over the proposed 500 MHz (therefore usage factor estimated at 4%) and an activity factor of 50%, this study suggests limiting the mean e.i.r.p. emitted by each IMT transmitter at 10 dBm for a dissemination factors of 6%.

Based on this study, if this band were to be used for IMT system, the e.i.r.p. should be limited to a maximum value of 10 dBm and devices would need to be limited to indoor only operation.
The limitation may be placed on the e.i.r.p in the total bandwidth of the emission, rather than on the power spectral density, on the assumption that a use of emissions with a narrow bandwidth (that would leave to higher e.i.r.p spectral density) is balanced by a lower probability of the emission coinciding with the FSS receiver bandwidth (i.e. a lower band usage factor).
It has to be noted that these values have been estimated basing the calculation on the hypothesis that the IMT transmitters will use frequencies uniformly distributed over the entire available spectrum of 500 MHz. If a smaller bandwidth were to be made available for IMT devices, this would increase the band usage factor, leading to increased interference to the FSS in that part of the band in which IMT devices operate, and increased interference to FSS space stations operating in that part of the band.